



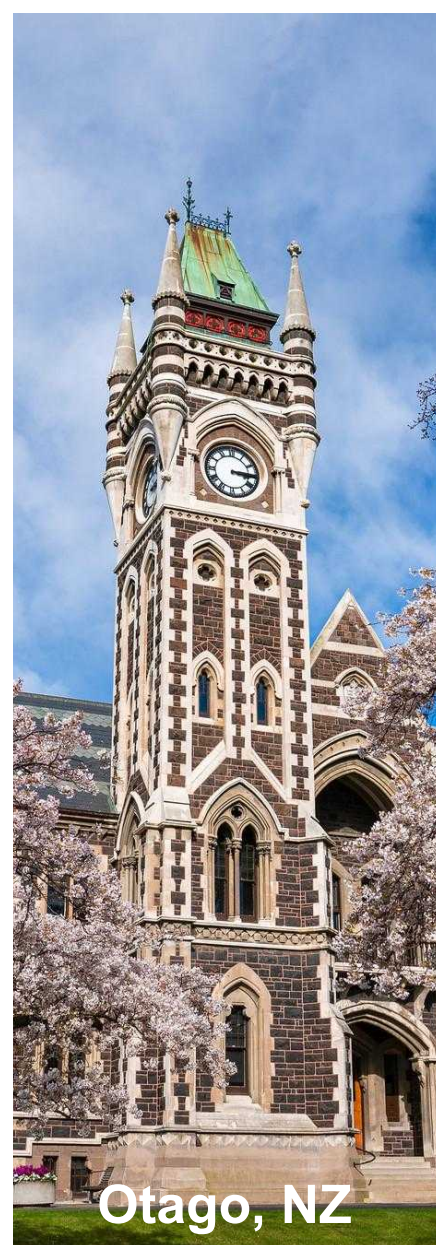
**PSI**

Center for Scientific Computing,  
Theory and Data

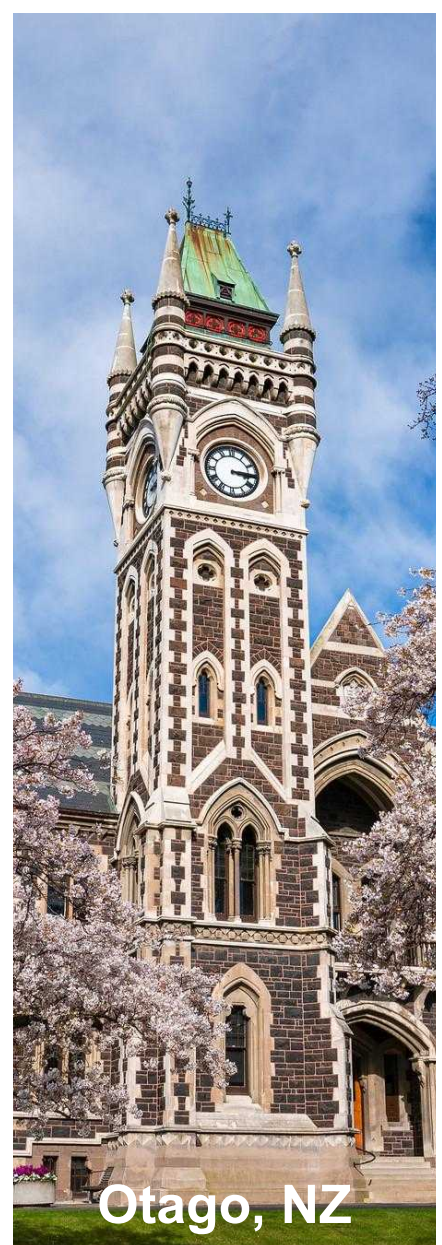
# Correcting the failures of DFT Koopmans functionals, DFT+*U*, and more

Edward Linscott

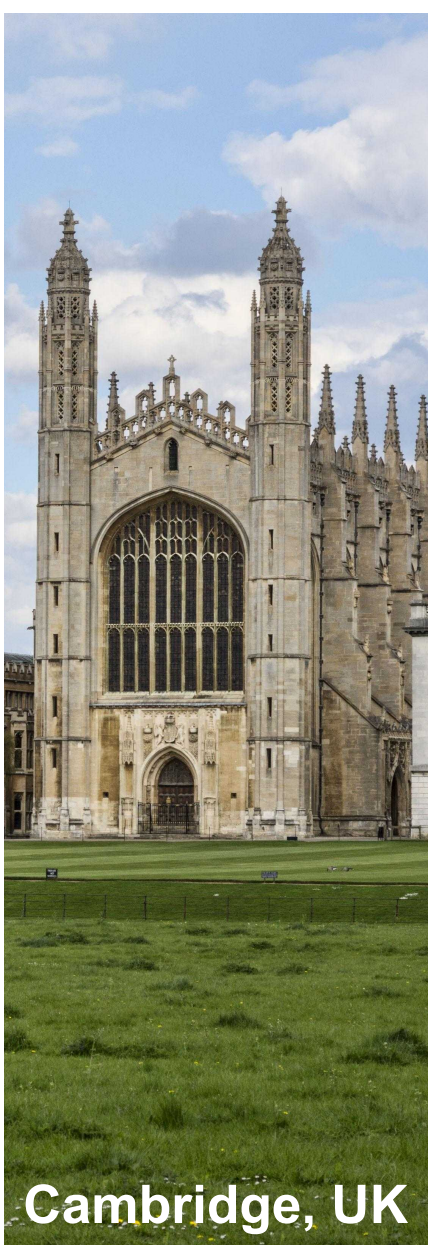
PsiQuantum, 30 October 2025



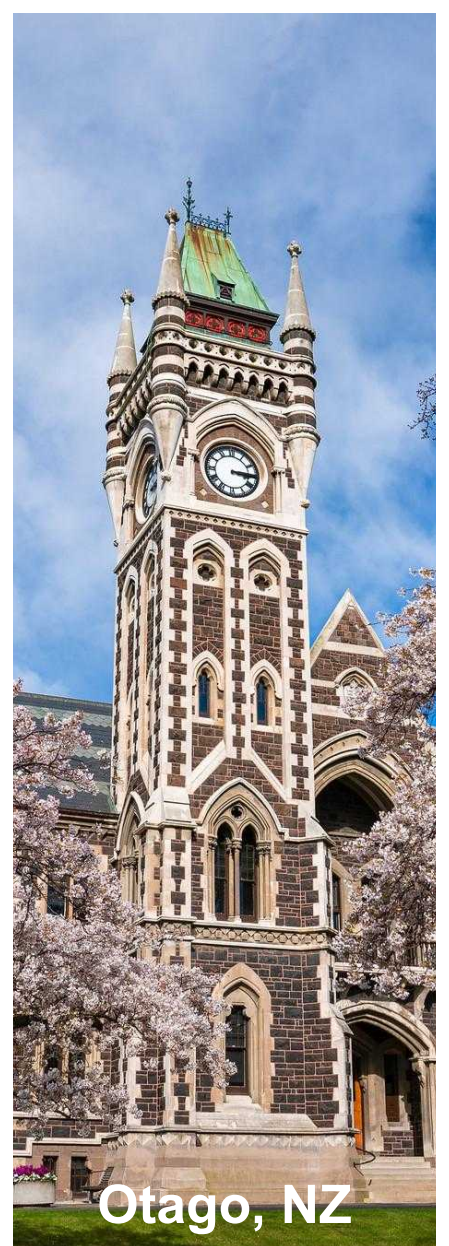
Otago, NZ



Otago, NZ



Cambridge, UK



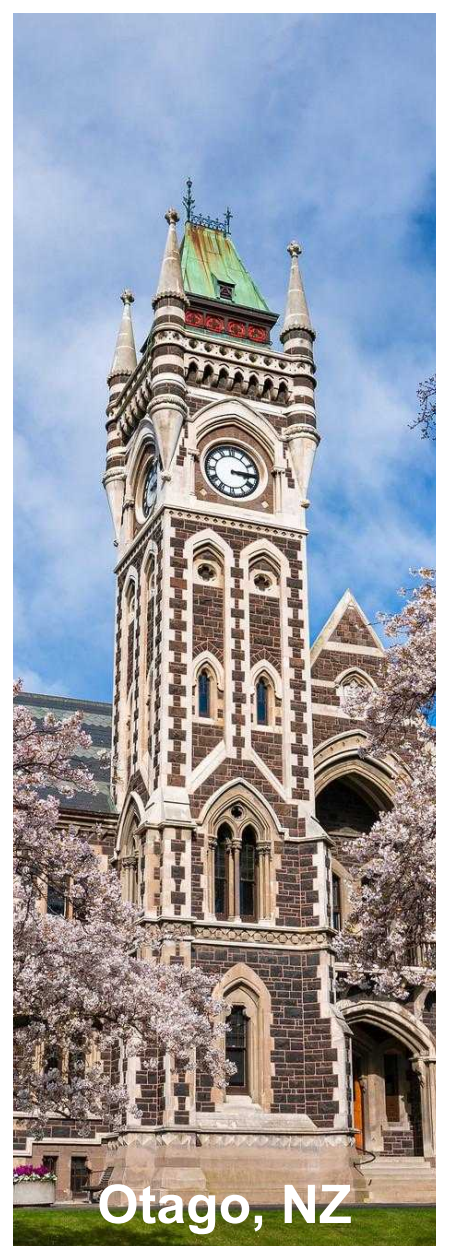
Otago, NZ



Cambridge, UK



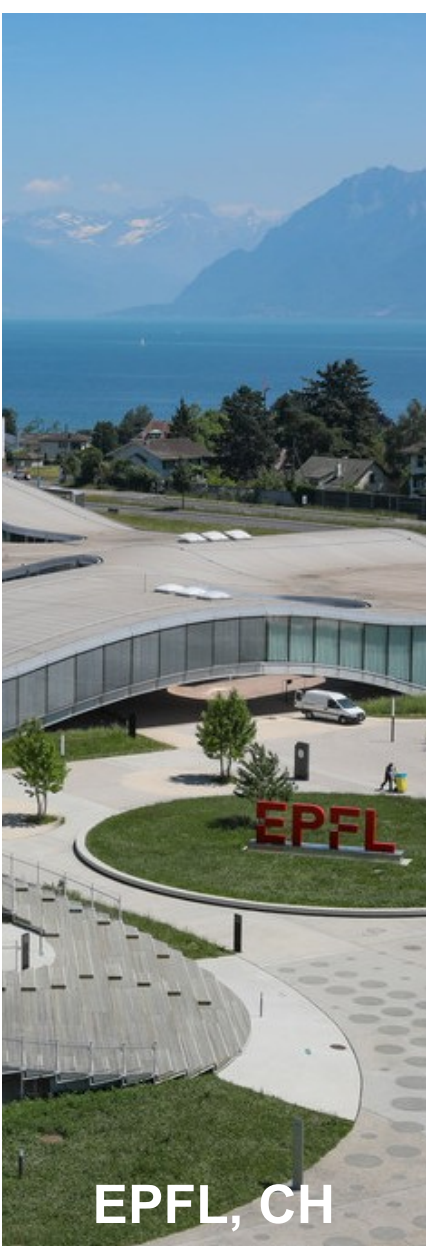
EPFL, CH



Otago, NZ



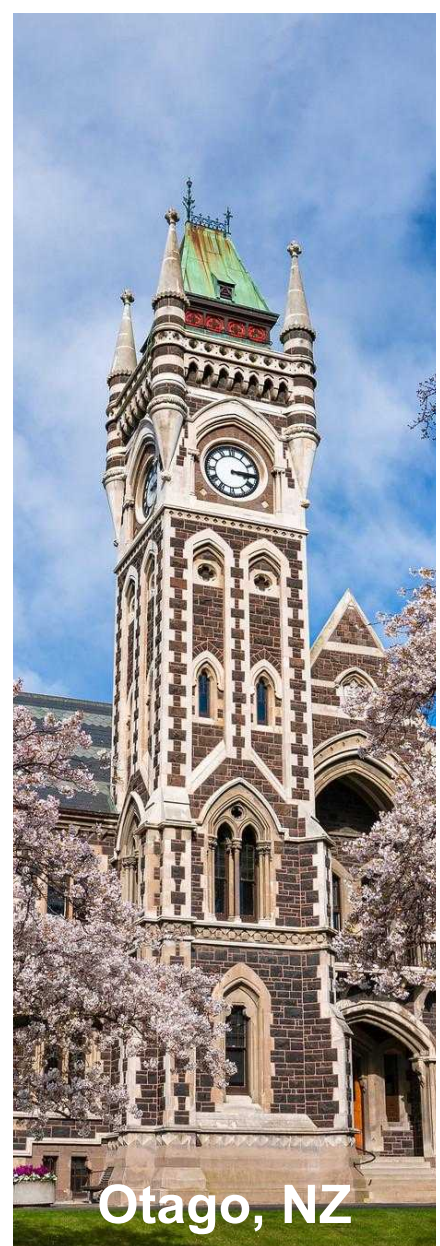
Cambridge, UK



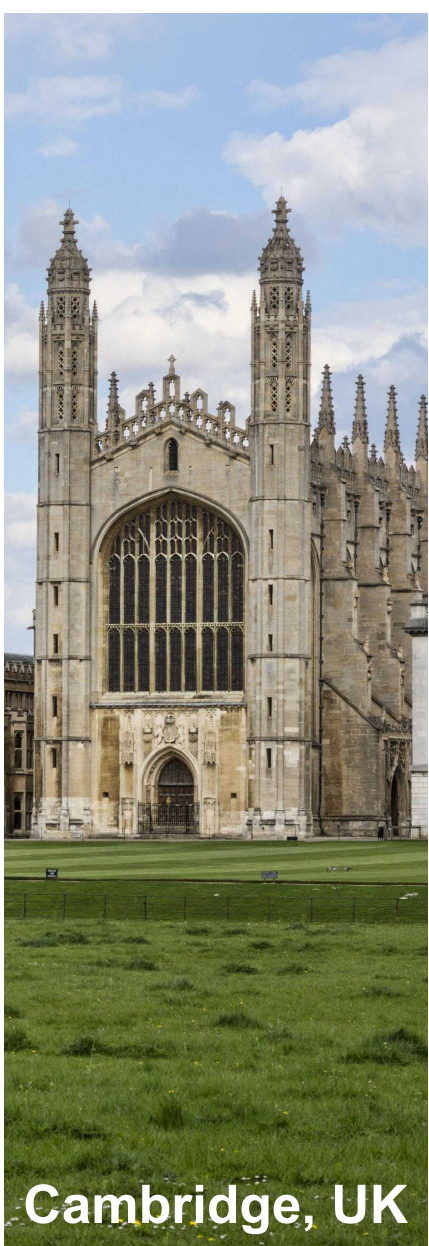
EPFL, CH



PSI, CH



Otago, NZ



Cambridge, UK



EPFL, CH



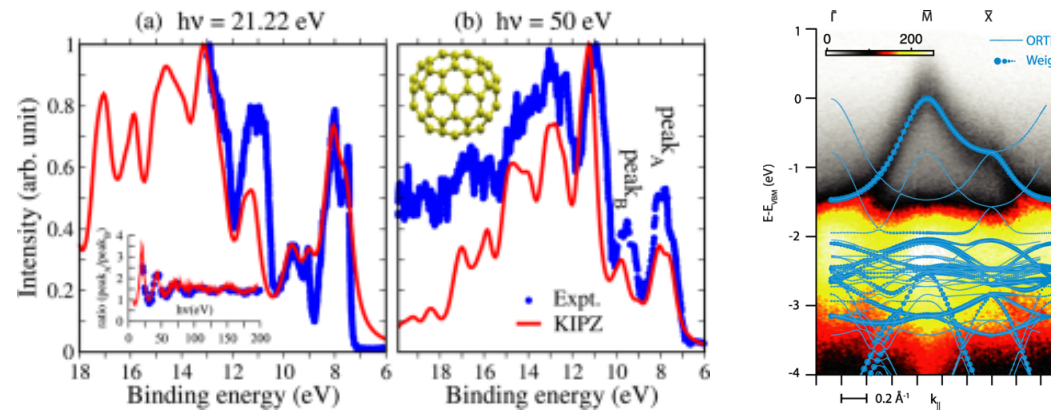
PSI, CH



... PsiQuantum  
AU?

# Predicting electronic excitations

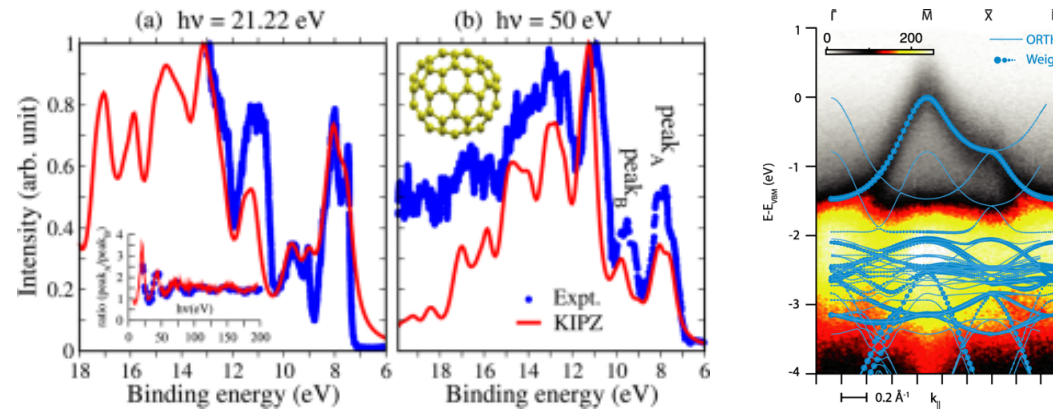
Spectral properties are fundamental to understanding molecules and materials...



<sup>1</sup>N. L. Nguyen *et al.* *Phys. Rev. Lett.* 114, 166405 (2015), M. Puppin *et al.* *Phys. Rev. Lett.* 124, 206402 (2020)

# Predicting electronic excitations

Spectral properties are fundamental to understanding molecules and materials...

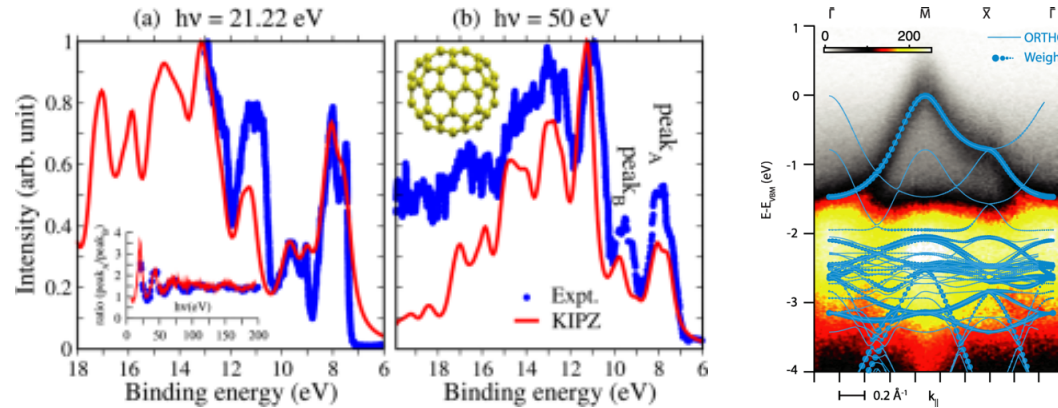


... but how can we routinely compute them?

<sup>1</sup>N. L. Nguyen *et al.* *Phys. Rev. Lett.* 114, 166405 (2015), M. Puppin *et al.* *Phys. Rev. Lett.* 124, 206402 (2020)

# Predicting electronic excitations

Spectral properties are fundamental to understanding molecules and materials...



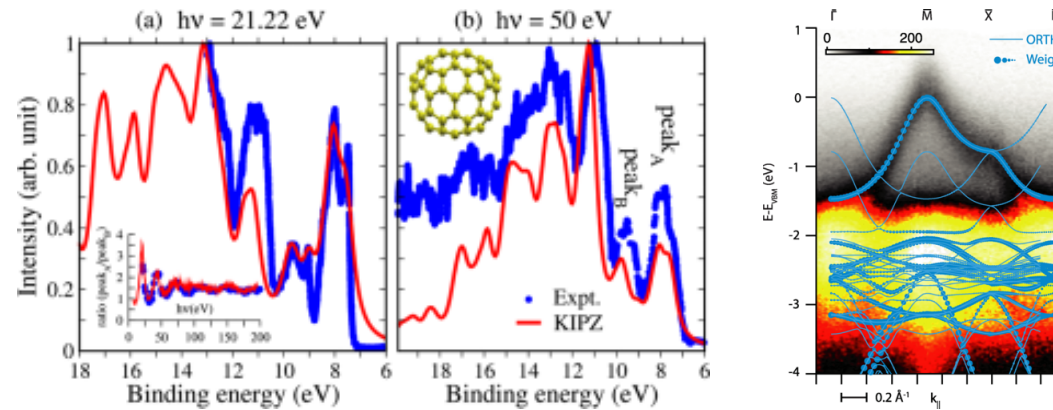
... but how can we routinely compute them?

- quantum chemistry: gold standard, but scales prohibitively (for now...)
- GW: accurate but expensive, often ill-behaved, diagrammatic
- DFT: plagued by intrinsic errors

<sup>1</sup>N. L. Nguyen *et al.* *Phys. Rev. Lett.* 114, 166405 (2015), M. Puppin *et al.* *Phys. Rev. Lett.* 124, 206402 (2020)

# Predicting electronic excitations

Spectral properties are fundamental to understanding molecules and materials...



... but how can we routinely compute them?

- quantum chemistry: gold standard, but scales prohibitively (for now...)
- GW: accurate but expensive, often ill-behaved, diagrammatic
- DFT: plagued by intrinsic errors

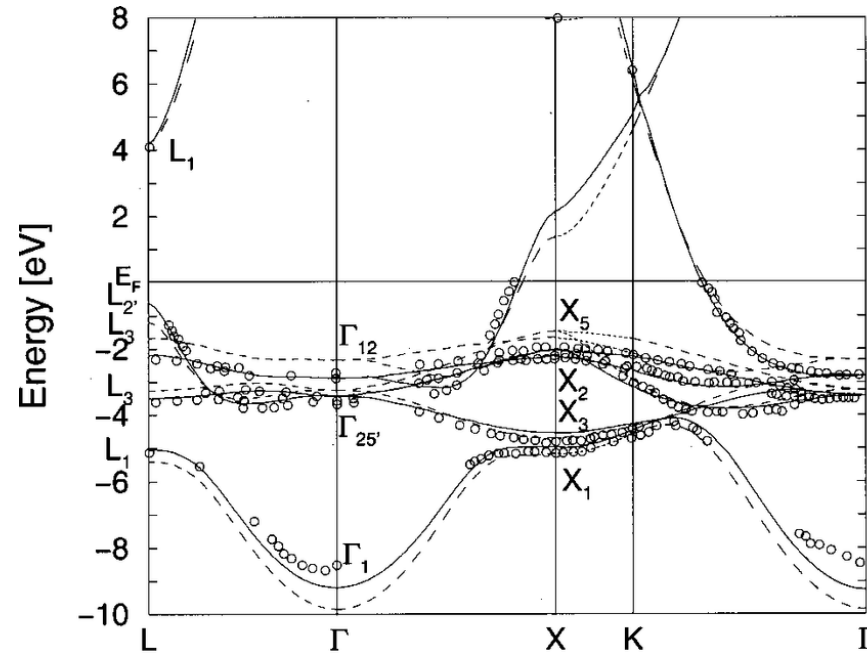
## My work: understanding and correcting these intrinsic errors

<sup>1</sup>N. L. Nguyen *et al.* *Phys. Rev. Lett.* 114, 166405 (2015), M. Puppin *et al.* *Phys. Rev. Lett.* 124, 206402 (2020)

# The failures of DFT

# Learning nothing from Icarus

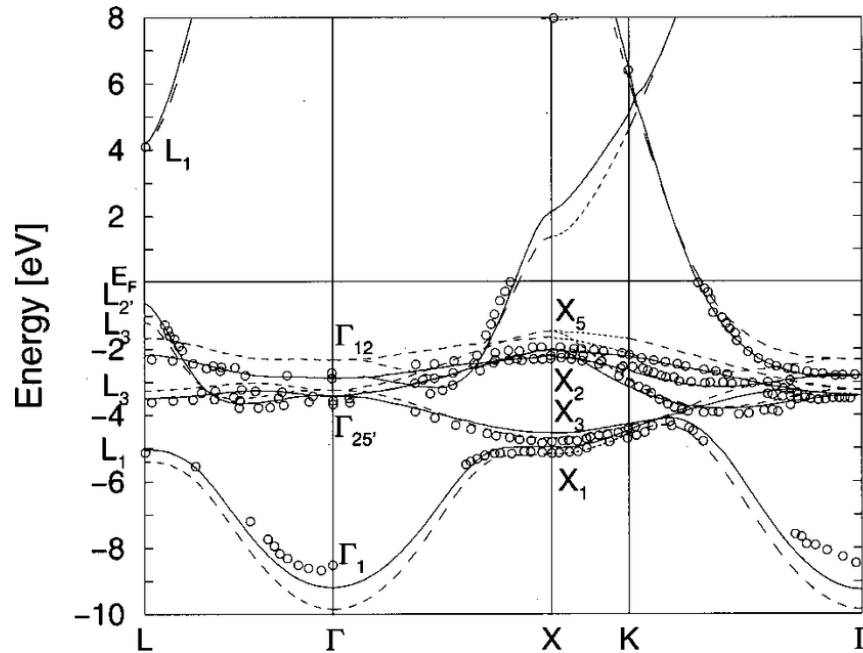
From the auxiliary, non-interacting system:



<sup>1</sup>G. Onida *et al.* Rev. Mod. Phys. 74, 601 (2002)

# Learning nothing from Icarus

From the auxiliary, non-interacting system:



... the temptation is too much!

<sup>1</sup>G. Onida *et al.* Rev. Mod. Phys. 74, 601 (2002)

# Learning nothing from Icarus

But single-particle excitation energies can be related to total energy differences

$$-\varepsilon_{\text{HOMO}} = I = E(N-1) - E(N)$$

... and even to the long-range decay of the density

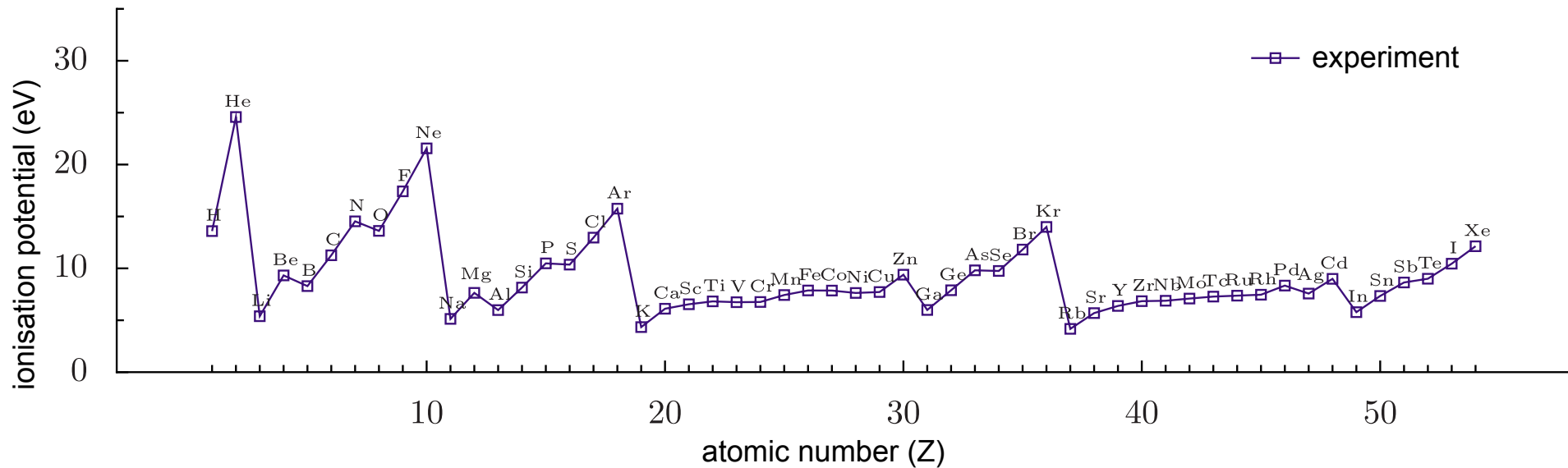
<sup>1</sup>I. Dabo *et al.* *Phys. Rev. B* 82, 115121 (2010)

# Learning nothing from Icarus

But single-particle excitation energies can be related to total energy differences

$$-\varepsilon_{\text{HOMO}} = I = E(N-1) - E(N)$$

... and even to the long-range decay of the density



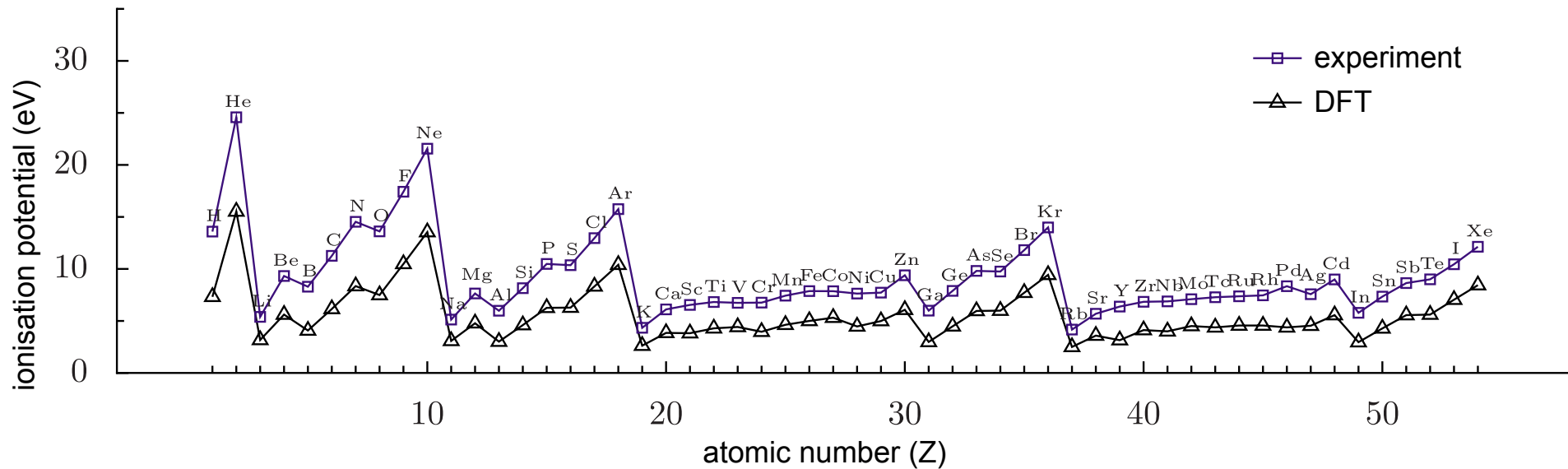
<sup>1</sup>I. Dabo *et al.* Phys. Rev. B 82, 115121 (2010)

# Learning nothing from Icarus

But single-particle excitation energies can be related to total energy differences

$$-\varepsilon_{\text{HOMO}} = I = E(N-1) - E(N)$$

... and even to the long-range decay of the density



<sup>1</sup>I. Dabo *et al.* Phys. Rev. B 82, 115121 (2010)

# What's going wrong?

$$\varepsilon_i \stackrel{?}{=} \begin{cases} E(N) - E_i(N-1) & \text{if } i \in \text{occ} \\ E_i(N+1) - E(N) & \text{if } i \in \text{emp} \end{cases}$$

# What's going wrong?

$$\varepsilon_i \stackrel{?}{=} \begin{cases} E(N) - E_i(N-1) & \text{if } i \in \text{occ} \\ E_i(N+1) - E(N) & \text{if } i \in \text{emp} \end{cases}$$

*cf.* Janak's theorem:

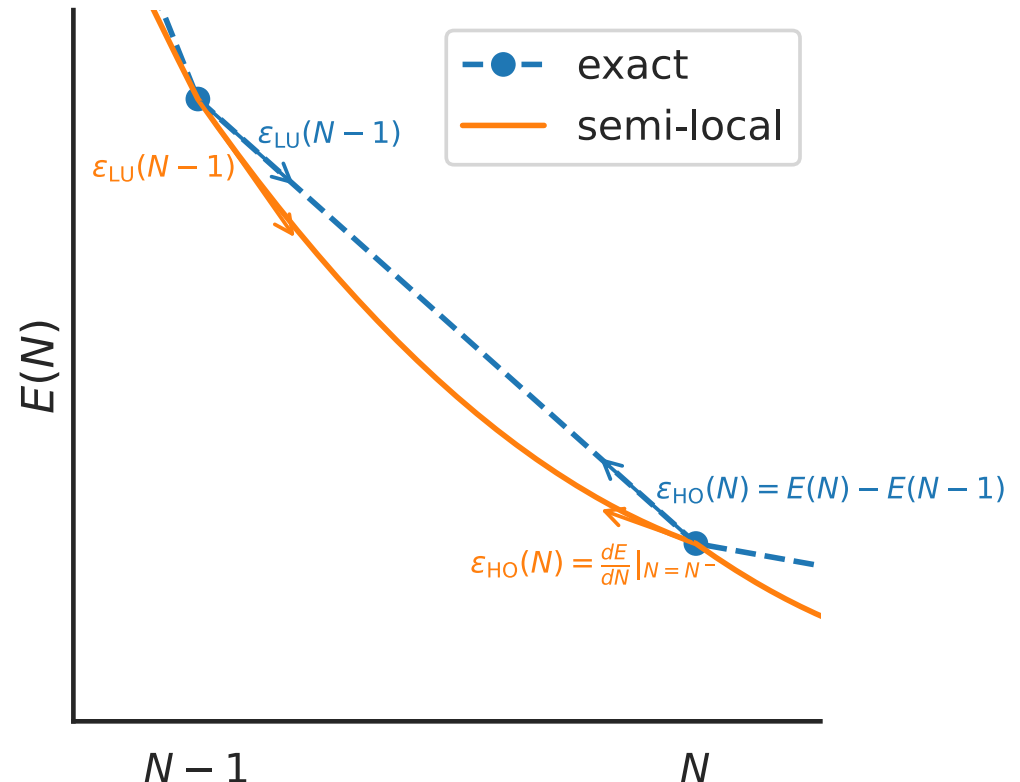
$$\varepsilon_i^{\text{DFT}} = \frac{dE^{\text{DFT}}}{df_i}$$

# What's going wrong?

$$\varepsilon_i \stackrel{?}{=} \begin{cases} E(N) - E_i(N-1) & \text{if } i \in \text{occ} \\ E_i(N+1) - E(N) & \text{if } i \in \text{emp} \end{cases}$$

cf. Janak's theorem:

$$\varepsilon_i^{\text{DFT}} = \frac{dE^{\text{DFT}}}{df_i}$$



# Aside: piecewise linearity

# Aside: piecewise linearity

<sup>1</sup>J. P. Perdew *et al.* *Phys. Rev. Lett.* 49, 1691–1694 (1982)

<sup>2</sup>W. Yang *et al.* *Phys. Rev. Lett.* 84, 5172–5175 (2000)

<sup>3</sup>A. C. Burgess *et al.* *J. Chem. Phys.* 159, 211102 (2023)

<sup>4</sup>A. C. Burgess *et al.* *Phys. Rev. Lett.* 133, 26404 (2024)

# Aside: piecewise linearity

- Perdew, Parr, Levy, and Balduz<sup>1</sup> showed that the exact total energy is piecewise linear in electron number (using ensembles)

<sup>1</sup>J. P. Perdew *et al.* *Phys. Rev. Lett.* 49, 1691–1694 (1982)

<sup>2</sup>W. Yang *et al.* *Phys. Rev. Lett.* 84, 5172–5175 (2000)

<sup>3</sup>A. C. Burgess *et al.* *J. Chem. Phys.* 159, 211102 (2023)

<sup>4</sup>A. C. Burgess *et al.* *Phys. Rev. Lett.* 133, 26404 (2024)

# Aside: piecewise linearity

- Perdew, Parr, Levy, and Balduz<sup>1</sup> showed that the exact total energy is piecewise linear in electron number (using ensembles)
- Yang, Zhang, and Ayers<sup>2</sup> provided an alternative proof without invoking ensembles

<sup>1</sup>J. P. Perdew *et al.* *Phys. Rev. Lett.* 49, 1691–1694 (1982)

<sup>2</sup>W. Yang *et al.* *Phys. Rev. Lett.* 84, 5172–5175 (2000)

<sup>3</sup>A. C. Burgess *et al.* *J. Chem. Phys.* 159, 211102 (2023)

<sup>4</sup>A. C. Burgess *et al.* *Phys. Rev. Lett.* 133, 26404 (2024)

# Aside: piecewise linearity

- Perdew, Parr, Levy, and Balduz<sup>1</sup> showed that the exact total energy is piecewise linear in electron number (using ensembles)
- Yang, Zhang, and Ayers<sup>2</sup> provided an alternative proof without invoking ensembles
- We showed<sup>3</sup> that the “convexity condition” follows *i.e.* for all DFTs that are
  - exact for all  $\nu$ -representable densities
  - size-consistent
  - translationally invariant

then

$$2E(N) \leq E(N + 1) + E(N - 1)$$

- ... and that similar reasoning applies to total energy as a function of total magnetisation<sup>4</sup>

<sup>1</sup>J. P. Perdew *et al.* *Phys. Rev. Lett.* 49, 1691–1694 (1982)

<sup>2</sup>W. Yang *et al.* *Phys. Rev. Lett.* 84, 5172–5175 (2000)

<sup>3</sup>A. C. Burgess *et al.* *J. Chem. Phys.* 159, 211102 (2023)

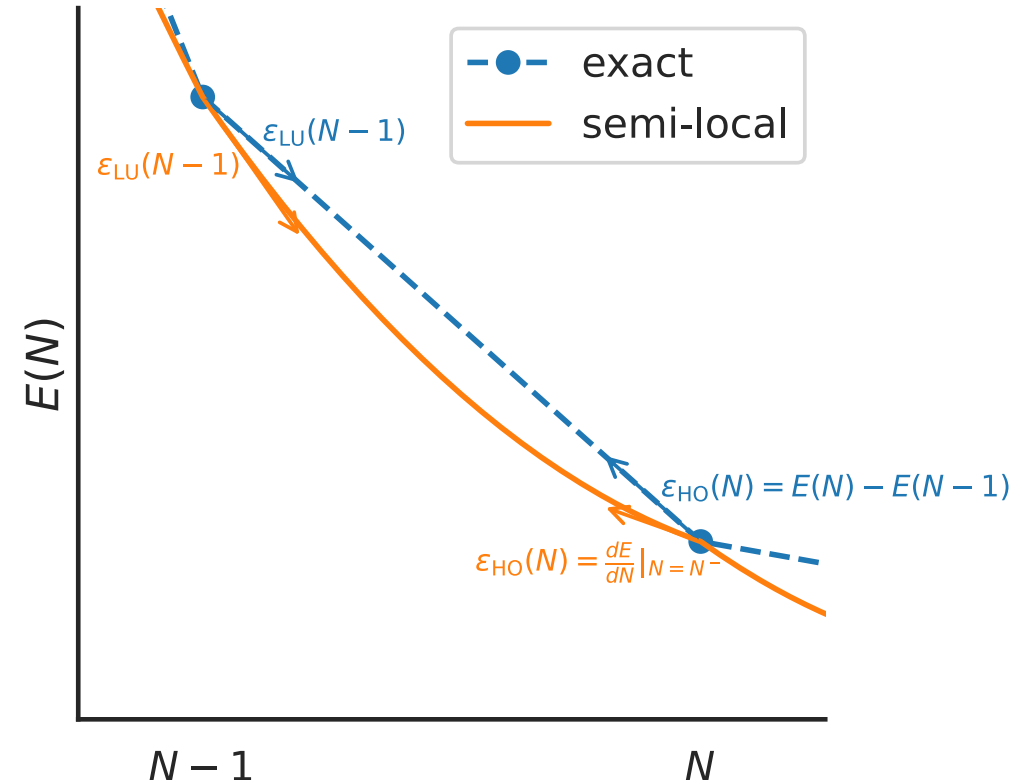
<sup>4</sup>A. C. Burgess *et al.* *Phys. Rev. Lett.* 133, 26404 (2024)

**Core idea: enforce piecewise linearity**

# Imposing generalised piecewise linearity

$$E^{\text{KI}}[\rho, \{\rho_i\}] = E^{\text{DFT}}[\rho]$$

$$+ \sum_i \left( - \int_0^{f_i} \langle \varphi_i | \hat{h}^{\text{DFT}}(f) | \varphi_i \rangle df + f_i \int_0^1 \langle \varphi_i | \hat{h}^{\text{DFT}}(f) | \varphi_i \rangle df \right)$$

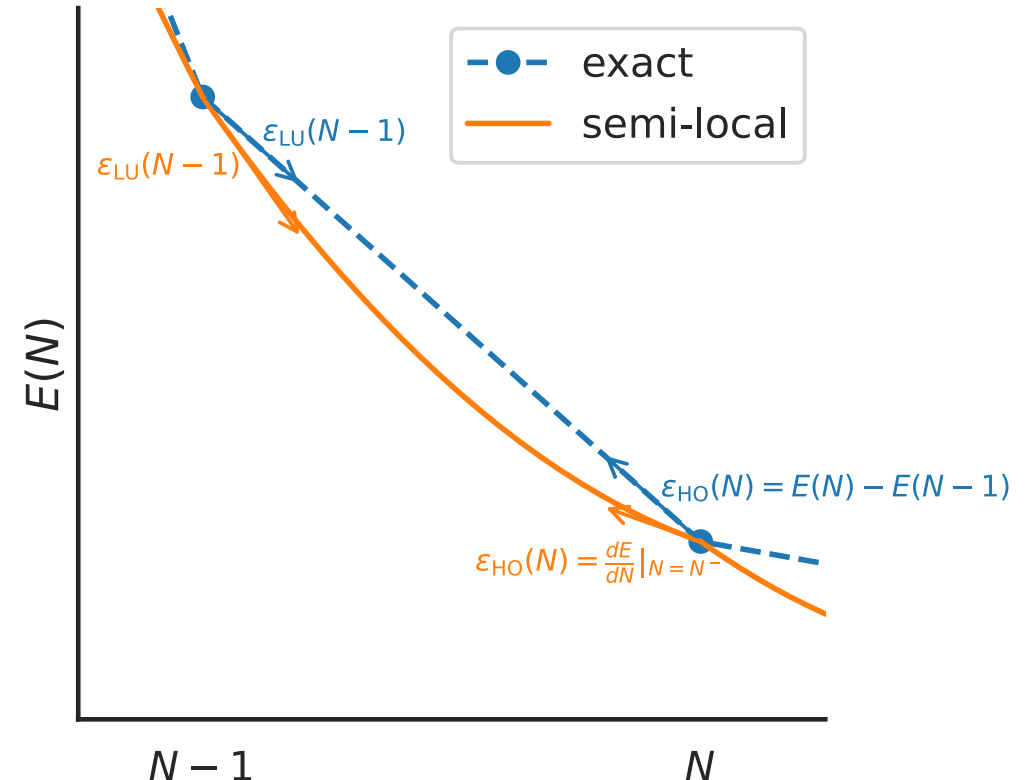


# Imposing generalised piecewise linearity

$$E^{\text{KI}}[\rho, \{\rho_i\}] = E^{\text{DFT}}[\rho]$$

$$+ \sum_i \left( - \int_0^{f_i} \langle \varphi_i | \hat{h}^{\text{DFT}}(f) | \varphi_i \rangle df + f_i \int_0^1 \langle \varphi_i | \hat{h}^{\text{DFT}}(f) | \varphi_i \rangle df \right)$$

removes dependence on  $f_i$



# Imposing generalised piecewise linearity

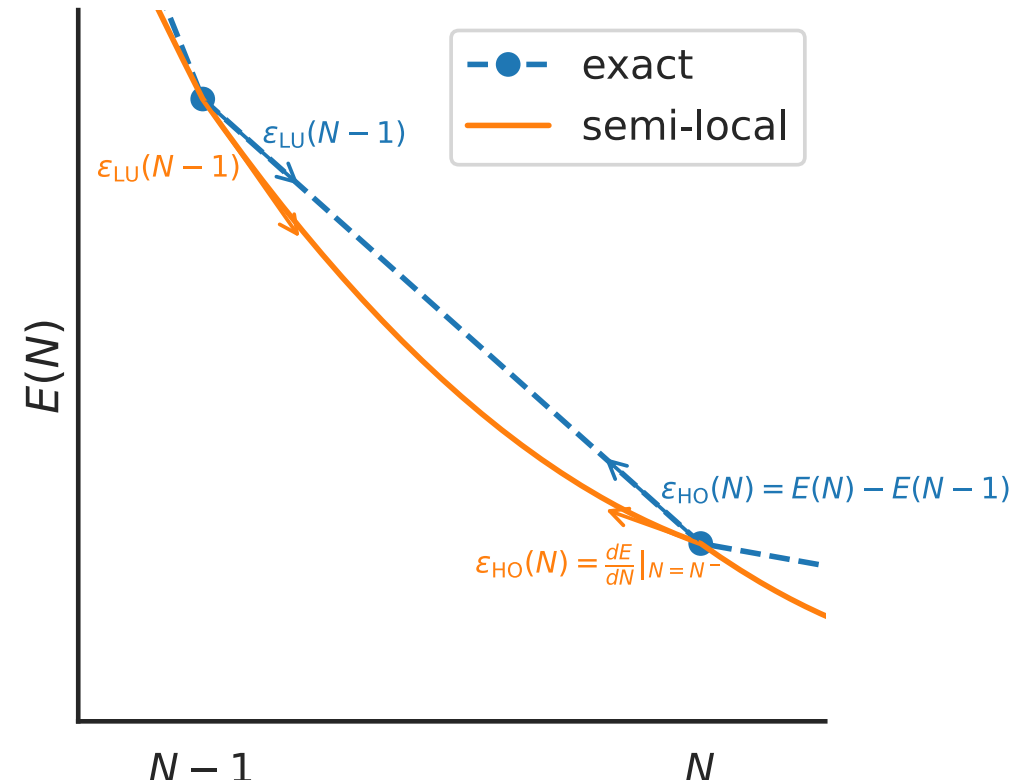
$$E^{\text{KI}}[\rho, \{\rho_i\}] = E^{\text{DFT}}[\rho]$$

$$+ \sum_i \left( - \int_0^{f_i} \langle \varphi_i | \hat{h}^{\text{DFT}}(f) | \varphi_i \rangle df \right)$$

$$+ f_i \int_0^1 \langle \varphi_i | \hat{h}^{\text{DFT}}(f) | \varphi_i \rangle df \right)$$

removes dependence on  $f_i$

restores linear dependence on  $f_i$

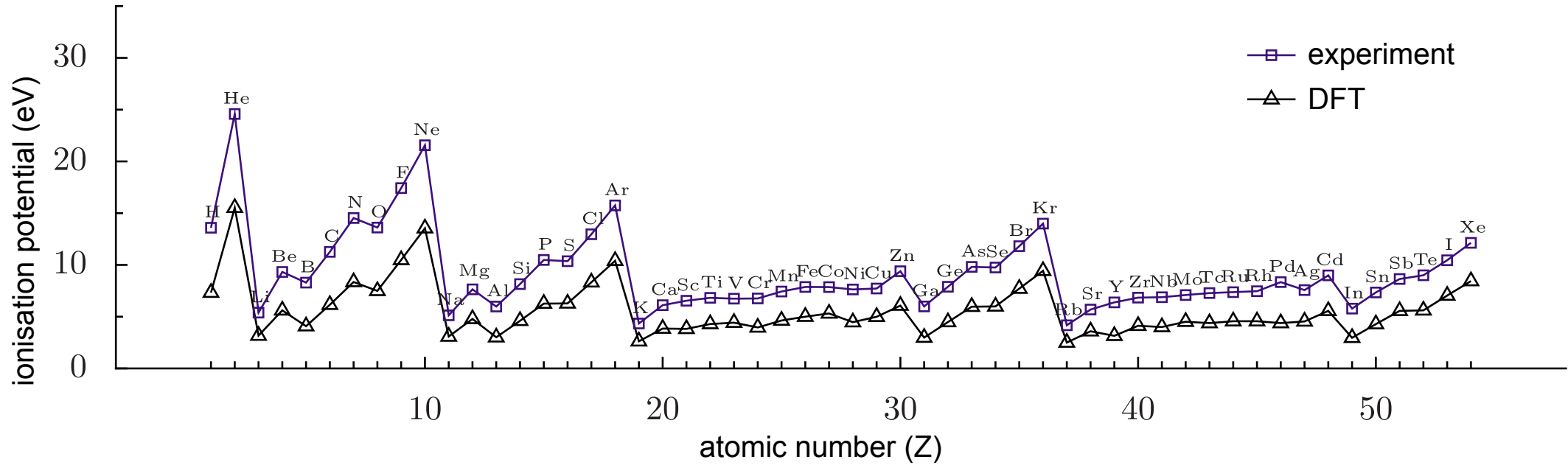


# Details for the experts

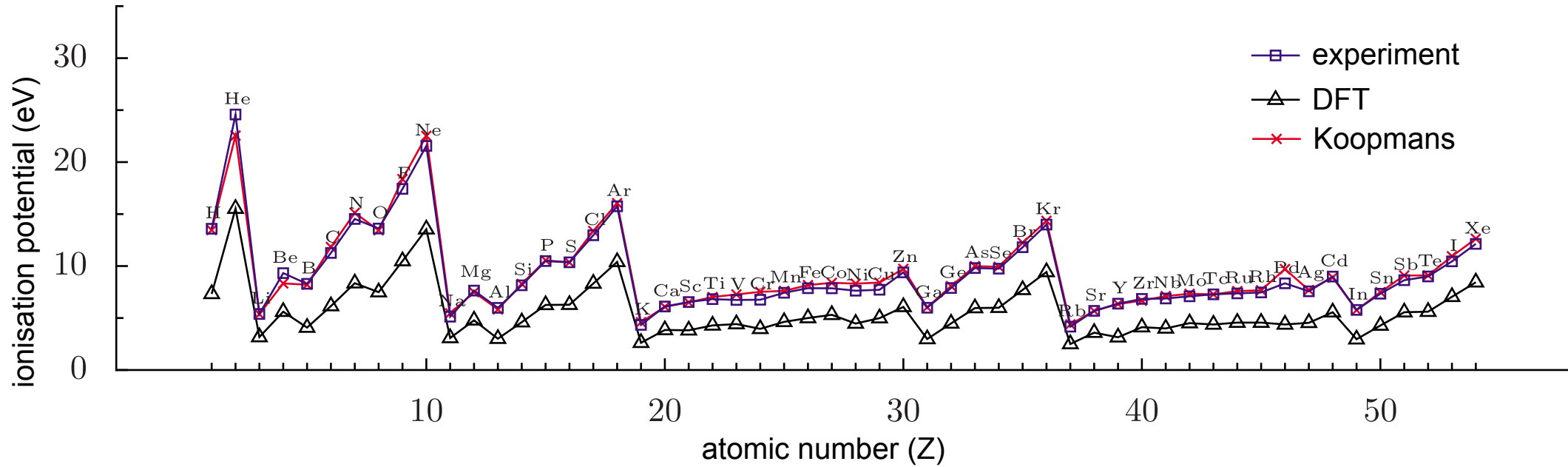
$$E_{\alpha}^{\text{KI}}[\rho, \{\rho_i\}] = E^{\text{DFT}}[\rho] + \sum_i \alpha_i \left\{ - (E^{\text{DFT}}[\rho] - E^{\text{DFT}}[\rho - \rho_i]) \right. \\ \left. + f_i (E^{\text{DFT}}[\rho - \rho_i + n_i] - E^{\text{DFT}}[\rho - \rho_i]) \right\}$$

- orbital-density-dependence
- screening parameters
- total energy at integer occupations unchanged!

# Results



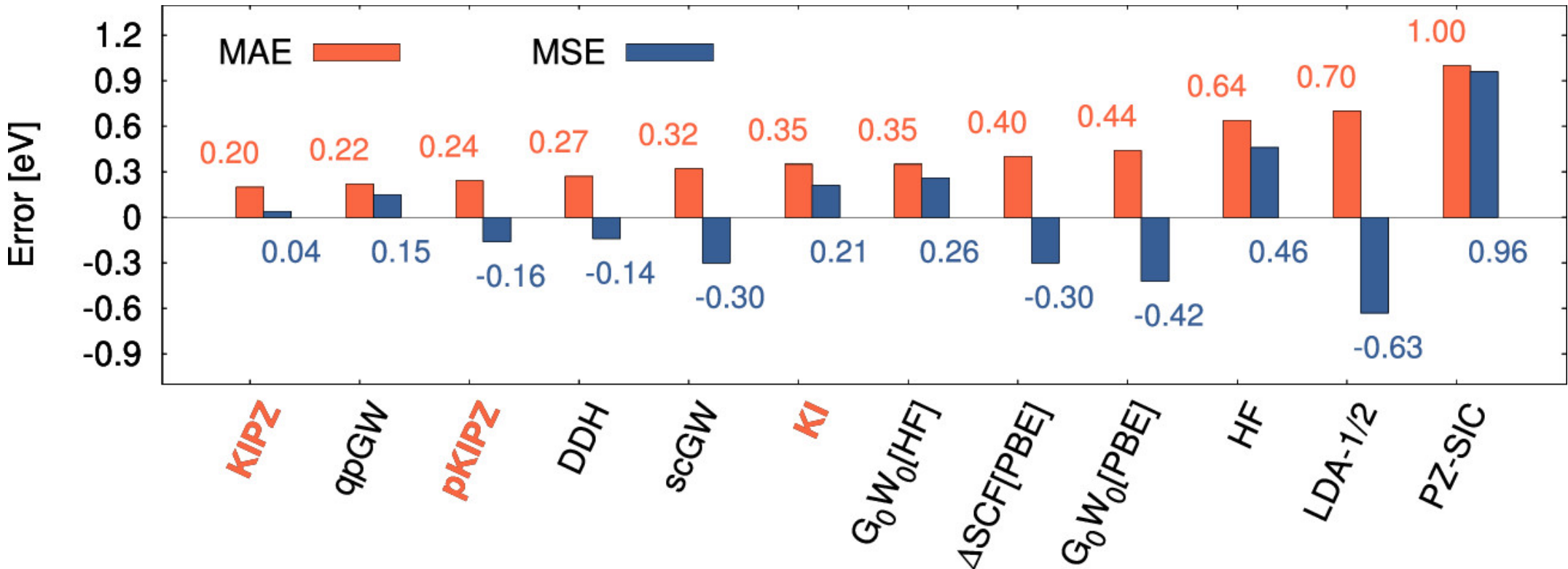
<sup>1</sup>I. Dabo *et al.* Phys. Rev. B 82, 115121 (2010)



<sup>1</sup>I. Dabo *et al.* Phys. Rev. B 82, 115121 (2010)

# Molecules

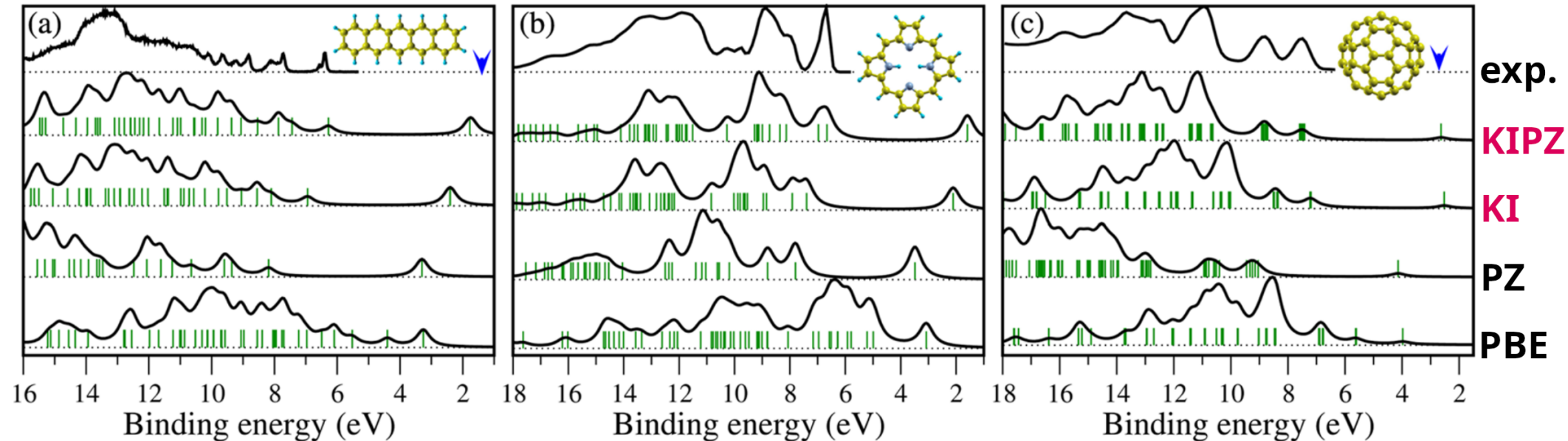
## Ionisation potentials<sup>1</sup>



<sup>1</sup>N. Colonna et al. J. Chem. Theory Comput. 15, 1905 (2019)

# Molecules

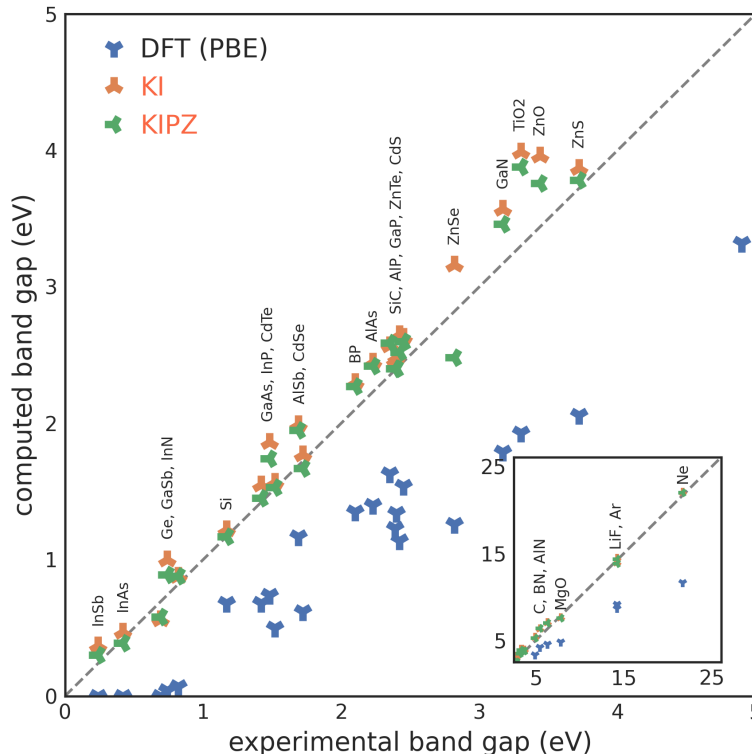
## UV photoemission spectra<sup>1</sup>



<sup>1</sup>N. L. Nguyen *et al.* Phys. Rev. Lett. 114, 166405 (2015)

# Materials

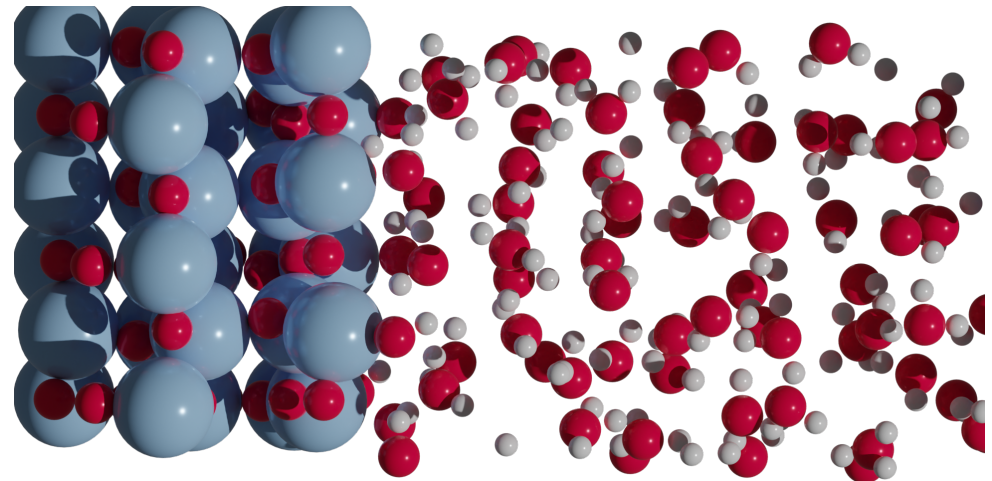
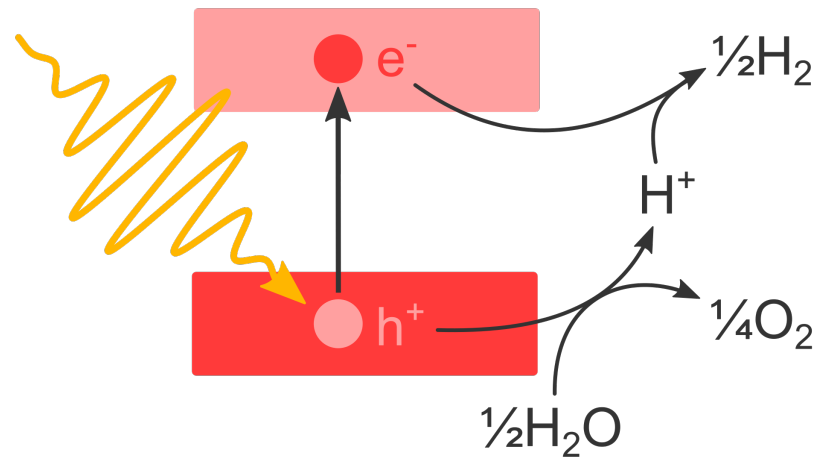
## Prototypical semiconductors and insulators<sup>1</sup>



	PBE	$G_0W_0$	KI	KIPZ	$QSG\tilde{W}$
$E_{\text{gap}}$	2.54	0.56	<b>0.27</b>	<b>0.22</b>	0.18
IP	1.09	0.39	<b>0.19</b>	<b>0.21</b>	0.49

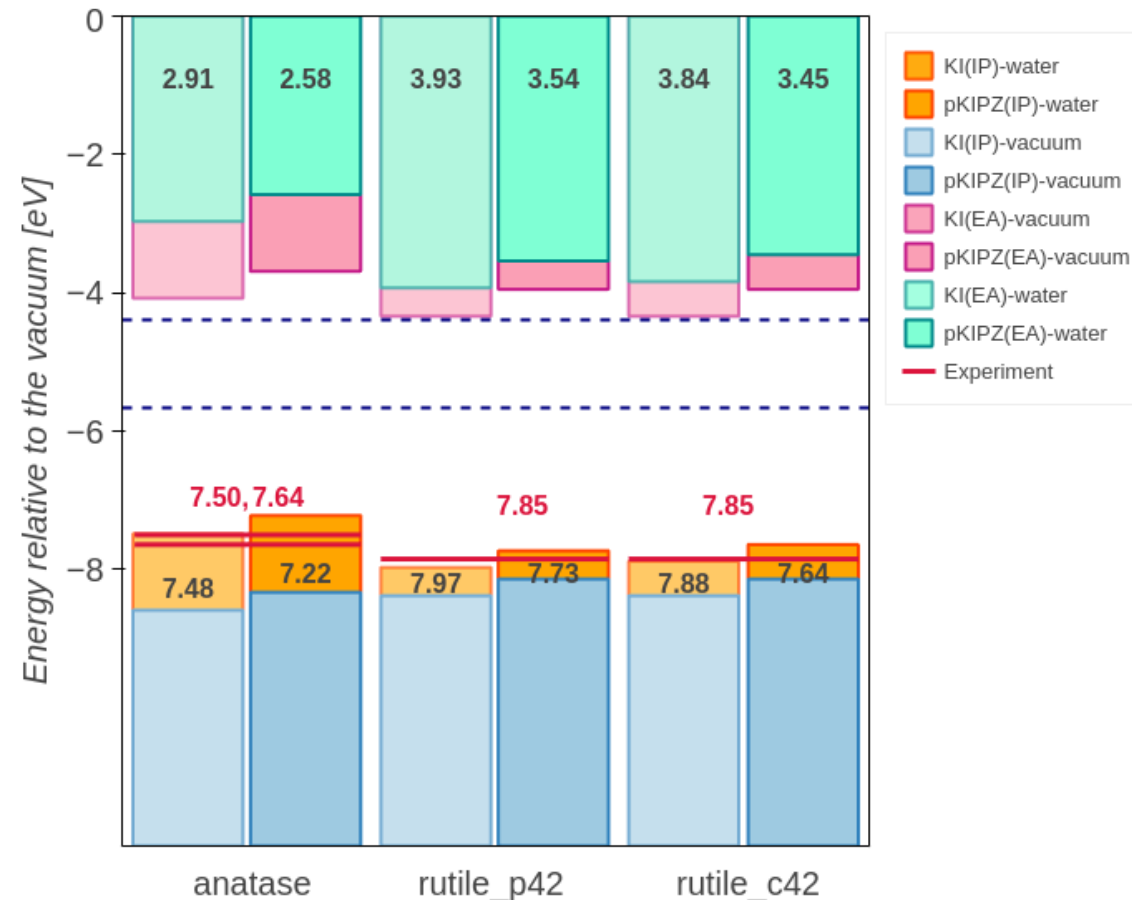
<sup>1</sup>N. L. Nguyen *et al.* Phys. Rev. X 8, 21051 (2018)

# Photocatalysis



<sup>1</sup>M. Stojkovic *et al.* (2024) doi:10.48550/arXiv.2412.17488

# Photocatalysis



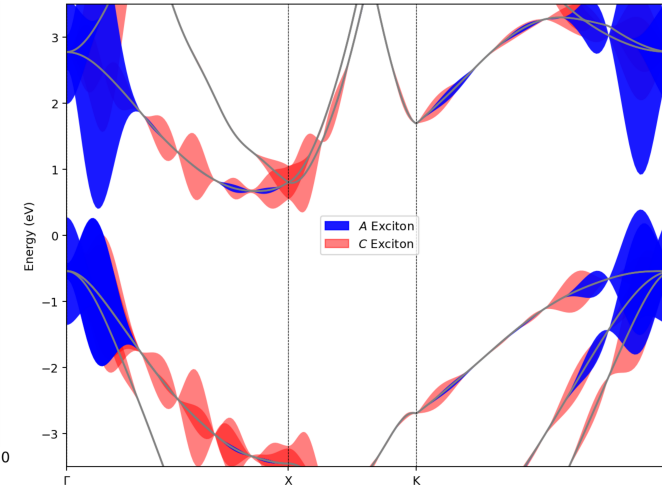
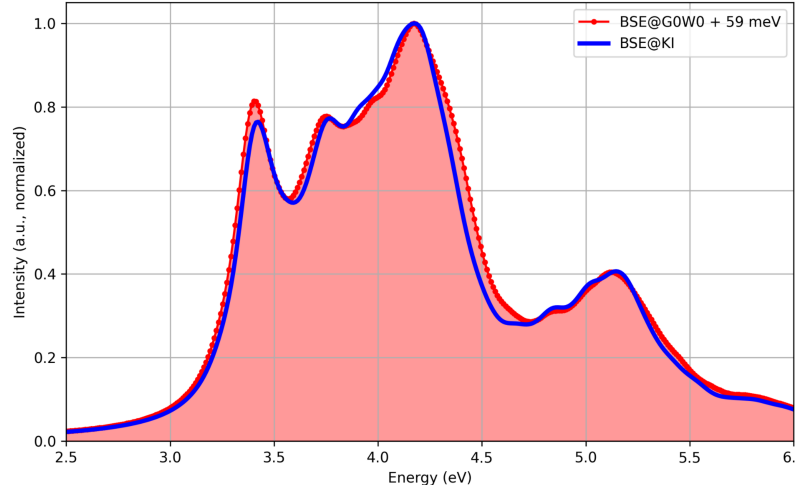
<sup>1</sup>M. Stojkovic *et al.* (2024) doi:10.48550/arXiv.2412.17488

# Optical spectra

Solve the BSE, using Koopmans eigenvalues in lieu of GW

# Optical spectra

Solve the BSE, using Koopmans eigenvalues in lieu of GW



silicon

indirect gap

direct gap

first excitonic peak

excitonic binding  
energy

**qKI+BSE**

1.12

3.31

3.42

0.09

**G<sub>0</sub>W<sub>0</sub>+BSE**

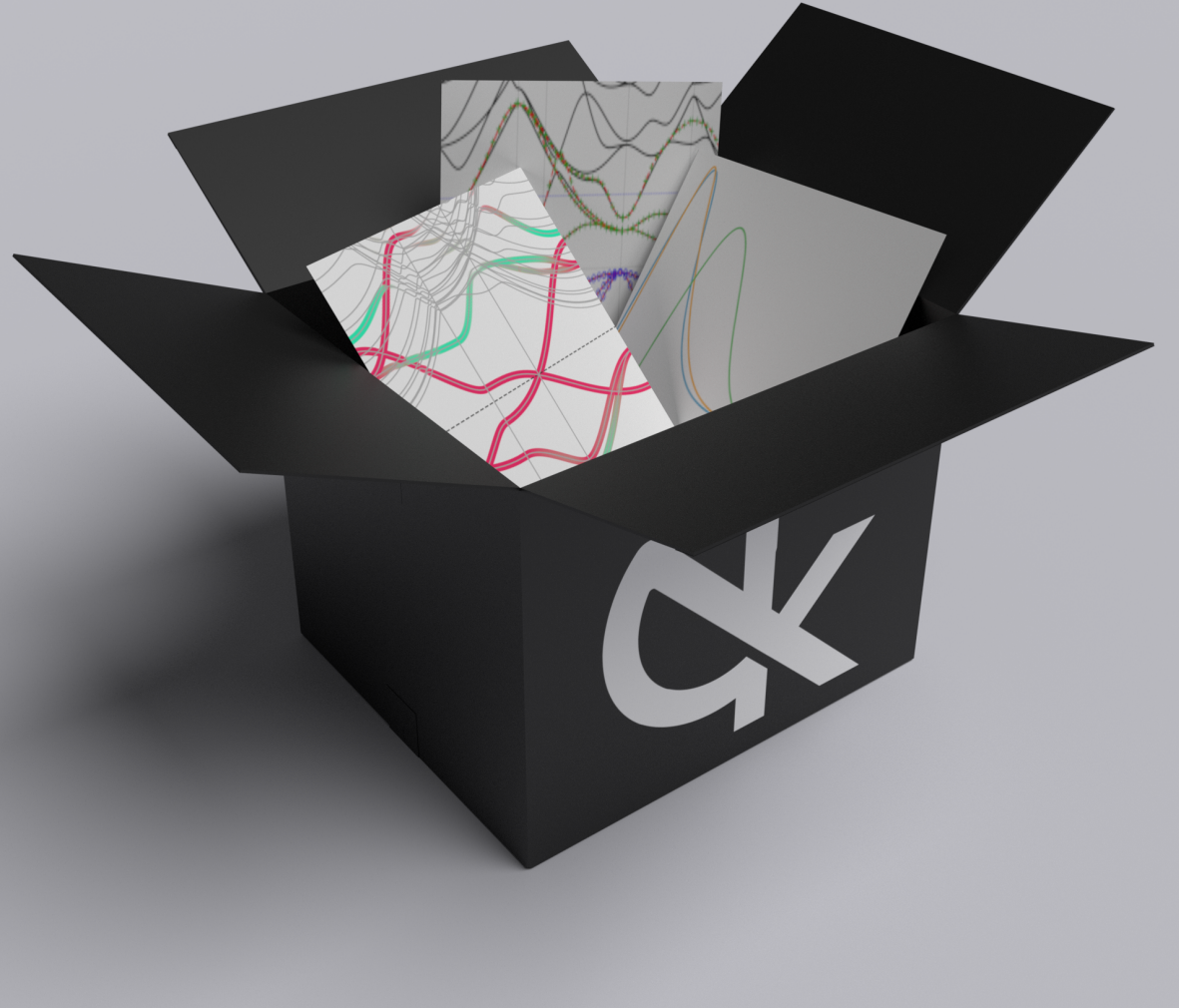
1.17

3.25

3.34

0.09

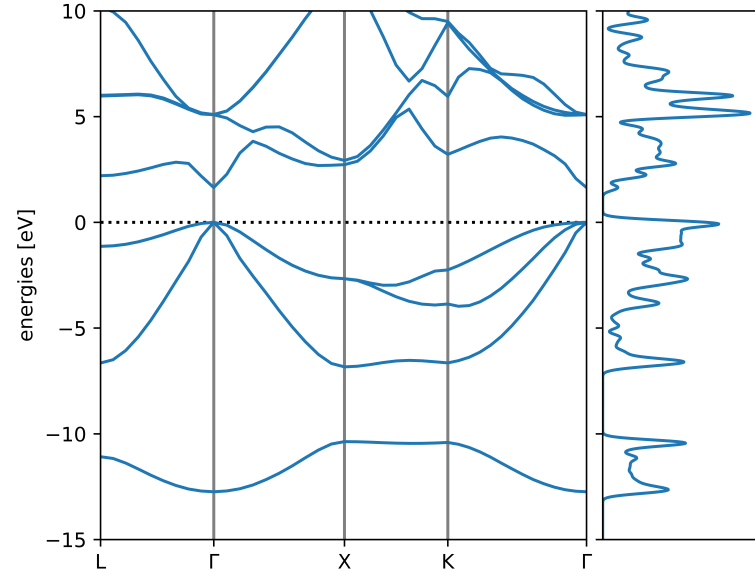
koopmans



Our goal:

1. accurate
2. robust
3. minimal input
4. fast

```
{
  "workflow": {
    "functional": "ki",
    "method": "dfpt",
    "init_orbitals": "mlwfs",
    "pseudo_library": "PseudoDojo/0.4/LDA/SR/standard/upf",
    "block_wannierization_threshold": 5.0,
    "orbital_groups_spread_tol": 0.05
  },
  "atoms": {
    "cell_parameters": {
      "periodic": true,
      "ibrav": 2,
      "celldms": {"l": 10.68374}
    },
    "atomic_positions": {
      "units": "crystal",
      "positions": [[{"Ga": 0.0, 0.0, 0.0}, {"As": 0.25, 0.25, 0.25}]]
    }
  },
  "kpoints": {
    "grid": [6, 6, 6]
  },
  "calculator_parameters": {
    "ecutwfc": 60.0,
    "w90": {
      "dis_proj_max": 0.8,
      "auto_projections": true
    },
    "ui": {
      "smooth_int_factor": 2
    }
  }
}
```



	LDA	HSE	$GW_0$	scG $\tilde{W}$	KI	exp
$E_{\text{gap}}$	0.26	1.28	1.55	1.62	<b>1.54</b>	1.55
$\langle \varepsilon_d \rangle$	-14.9	-15.6	-17.3	-17.6	<b>-17.9</b>	-18.9
$\Delta$	12.8	13.9			<b>12.7</b>	13.1



- used by a Fortune Global 500 company
- two schools (online and then in Pavia, IT)

See [koopmans-functionals.org](http://koopmans-functionals.org)

<sup>1</sup>E. B. Linscott *et al.* *J. Chem. Theory Comput.* 19, 7097 (2023)

# An alternative approach: DFT + $U$

$$E_{\text{DFT}+U} = E_{\text{DFT}} + \sum_{I\sigma} \frac{U^I}{2} \text{Tr}[n^{I\sigma}(1 - n^{I\sigma})]$$

<sup>1</sup>E. B. Linscott *et al.* *Phys. Rev. B* 98, 235157 (2018)

$$E_{\text{DFT}+U} = E_{\text{DFT}} + \sum_{I\sigma} \frac{U^I}{2} \text{Tr}[n^{I\sigma}(1 - n^{I\sigma})]$$

site and spin indices

<sup>1</sup>E. B. Linscott *et al.* *Phys. Rev. B* 98, 235157 (2018)

$$E_{\text{DFT}+U} = E_{\text{DFT}} + \sum_{I\sigma} \frac{U^I}{2} \text{Tr}[\mathbf{n}^{I\sigma} (1 - \mathbf{n}^{I\sigma})]$$

site and spin indices  
 local occupation matrix

<sup>1</sup>E. B. Linscott *et al.* *Phys. Rev. B* 98, 235157 (2018)

$$E_{\text{DFT}+U} = E_{\text{DFT}} + \sum_{I\sigma} \frac{U^I}{2} \text{Tr}[\mathbf{n}^{I\sigma} (1 - \mathbf{n}^{I\sigma})]$$

site and spin indices local occupation matrix

$$n_{mm'}^{I\sigma} = \langle \varphi_m^I | \hat{\rho}^\sigma | \varphi_{m'}^I \rangle = \sum_i \langle \varphi_m^I | \psi_i \rangle f_i \langle \psi_i | \varphi_{m'}^I \rangle$$

<sup>1</sup>E. B. Linscott *et al.* *Phys. Rev. B* 98, 235157 (2018)

Hubbard parameter

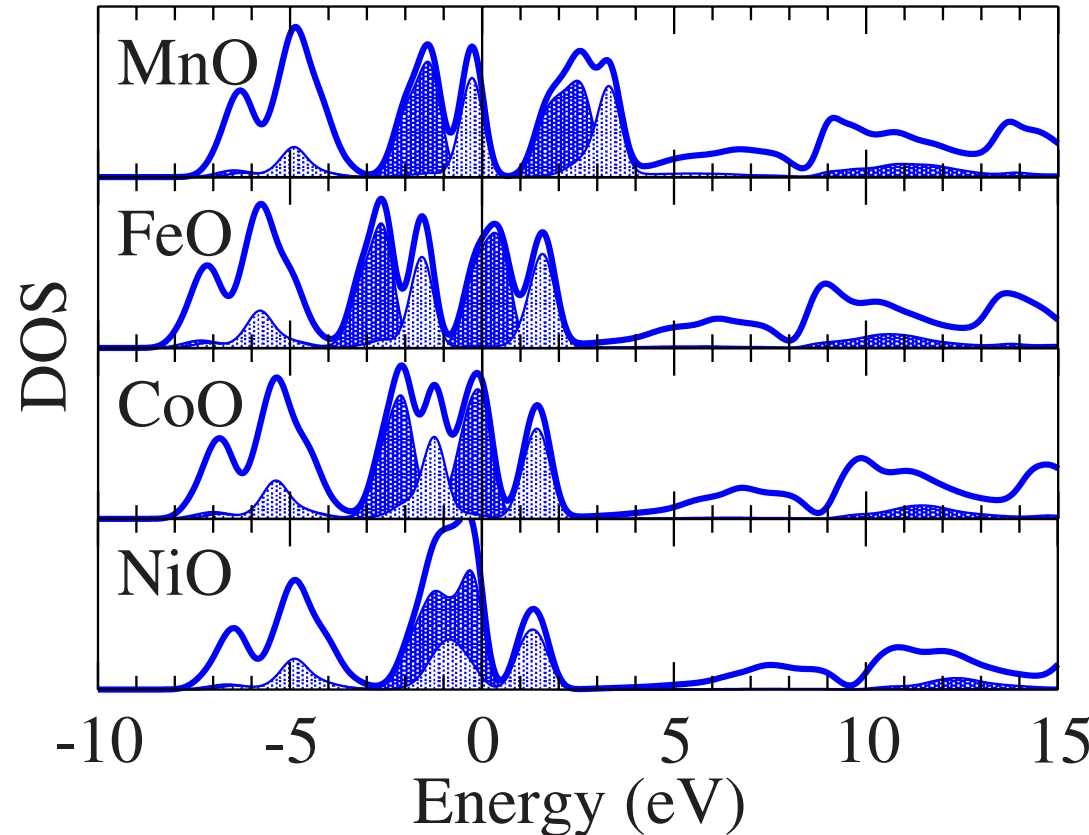
$$E_{\text{DFT}+U} = E_{\text{DFT}} + \sum_{I\sigma} \frac{U^I}{2} \text{Tr}[\mathbf{n}^{I\sigma} (1 - \mathbf{n}^{I\sigma})]$$

site and spin indices      local occupation matrix

$$n_{mm'}^{I\sigma} = \langle \varphi_m^I | \hat{\rho}^\sigma | \varphi_{m'}^I \rangle = \sum_i \langle \varphi_m^I | \psi_i \rangle f_i \langle \psi_i | \varphi_{m'}^I \rangle$$

<sup>1</sup>E. B. Linscott *et al.* *Phys. Rev. B* 98, 235157 (2018)

# The historical derivation of DFT+ $U$ (+ $J$ )



<sup>1</sup>C. Rödl *et al.* Phys. Rev. B 79, 235114 (2009)

# The historical derivation of DFT+U(+J)

Let a correlated subspace be defined by a set of basis orbitals (known as *Hubbard projectors*). Within this subspace, the operator associated with electron-electron interactions is

$$\hat{U} = \sum_{mnm'n'} \sum_{\sigma\sigma'} U_{mnm'n'} \hat{c}_{m\sigma}^\dagger \hat{c}_{n\sigma'}^\dagger \hat{c}_{m'\sigma'} \hat{c}_{n'\sigma}, \quad (1)$$

where  $(m, n, m', n')$  are Hubbard projector labels and  $\{\sigma\}$  are spin indices, and  $\hat{c}_{m\sigma}^\dagger$  are the associated creation operators. One can show that

$$\begin{aligned} E_{\text{Hub}} = \langle \hat{U} \rangle &= \frac{1}{2} \sum_{\substack{mnm'n'\sigma \\ m \neq n, m' \neq n'}} (U_{mnm'n'} - U_{mnn'm'}) \langle n', \sigma; m', \sigma | \hat{\rho}_2 | n, \sigma; m, \sigma \rangle \\ &\quad + \frac{1}{2} \sum_{mnm'n'\sigma} U_{mnm'n'} \langle n', \sigma; m', -\sigma | \hat{\rho}_2 | n, -\sigma; m, \sigma \rangle - U_{mnn'm'} \langle n', -\sigma; m', \sigma | \hat{\rho}_2 | n, -\sigma; m, \sigma \rangle \end{aligned} \quad (2)$$

## Hartree-Fock approximation

where  $\hat{\rho}_2$  is the two-body density matrix. Adopting the ansatz that the many-body wavefunction is a Slater determinant of single-particle states, the two-body density matrices  $\hat{\rho}_2$  can be decomposed as determinants of single-body density.<sup>1</sup> In this case

$$E_{\text{Hub}} = \frac{1}{2} \sum_{\substack{mnm'n'\sigma \\ m \neq n, m' \neq n'}} (U_{mnn'm'} - U_{mnm'n'}) n_{mm'}^\sigma n_{nn'}^\sigma + \frac{1}{2} \sum_{mnm'n'\sigma} U_{mnm'n'} n_{mn}^\sigma n_{nm}^{-\sigma}, \quad (3)$$

where  $n_{mm'}^\sigma = \langle m | \hat{\rho}^\sigma | m' \rangle$ . At this stage the only approximation that has been introduced is the assertion that the state corresponds to a Slater determinant. If  $U_{mnm'n'}$  is obtained using the unscreened Coulomb potential, then Equation 3 is equivalent to a Hartree-Fock treatment of the system.

## two-site terms only

Now, all but two-site terms are ignored. Due to the symmetries of  $U_{mnm'n'}$ , this leaves only two types of terms:  $U_{mnnm}$  and  $U_{mnmm}$ . These are then averaged over the Hubbard projectors to yield two scalars:

$$U = \frac{1}{(2l+1)^2} \sum_{mn} U_{mnnm}; J = \frac{1}{(2l+1)^2} \sum_{mn} U_{mnmm}. \quad (4)$$

Using these average values in place of the tensorial terms simplifies Equation 3 to

<sup>1</sup>R. G. Parr *et al.* (Oxford University Press, Oxford, 1989).

average a rank-2 tensor

# The historical derivation of DFT+ $U(+J)$

$$E_{\text{Hub}} = \frac{1}{2} \sum_{mn\sigma} U(n_{mm}^\sigma n_{nn}^\sigma - n_{mn}^\sigma n_{nm}^\sigma + n_{mm}^\sigma n_{nn}^{-\sigma}) + \frac{1}{2} \sum_{mn\sigma} J(n_{mn}^\sigma n_{nm}^\sigma - n_{mm}^\sigma n_{nn}^\sigma + n_{mn}^\sigma n_{nm}^{-\sigma}) = \sum_\sigma \frac{U}{2} ((n^\sigma)^2 + n^\sigma n^{-\sigma} - \text{Tr}(n^\sigma n^\sigma)) + \frac{J}{2} (\text{Tr}(n^\sigma n^\sigma + n^\sigma n^{-\sigma}) - (n^\sigma)^2) \quad (5)$$

where  $n^\sigma = \text{Tr}(n^\sigma)$ . If at this stage Equation 5 was to be incorporated directly into the DFT formalism, interactions associated with the subsystems that are already being handled by the conventional exchange-correlation functional would be double-counted. To avoid this, the **fully localised limit**<sup>1</sup> is considered, where all correlated subspaces have integer occupancy. In this approximation

adopt some double-counting term

$$\text{Tr}(n^\sigma n^\sigma) \rightarrow n^\sigma; \text{Tr}(n^\sigma n^{-\sigma}) \rightarrow n^{\sigma_{\min}}, \quad (6)$$

where  $\sigma_{\min}$  denotes the minority spin. Thus in the fully localised limit, the double counting term becomes

$$E_{\text{DC}} = \frac{U}{2} n(n-1) - \frac{J}{2} \sum_\sigma n^{\sigma(n^\sigma-1)} + J n^{\sigma_{\min}} \quad (7)$$

where  $n = \sum_\sigma n^\sigma$ . Hence

$$E_{\text{Hub}} - E_{\text{DC}} = \sum_{I\sigma} \frac{U^I - J^I}{2} \text{Tr}(n^{I\sigma}(1 - n^{I\sigma})) + \sum_{I\sigma} \frac{J^I}{2} (\text{Tr}(n^{I\sigma} n^{I-\sigma}) - 2\delta_{\sigma\sigma_{\min}} n^{I\sigma}). \quad (8)$$

Note that the entire expression has now been generalised to allow for the possibility of multiple sites (labelled with the index  $I$ ), to each of which a correction term is applied. As a final approximation, **terms arising from interaction between opposite spin (those contained in the second sum) are neglected**. This leaves

neglect  $J$

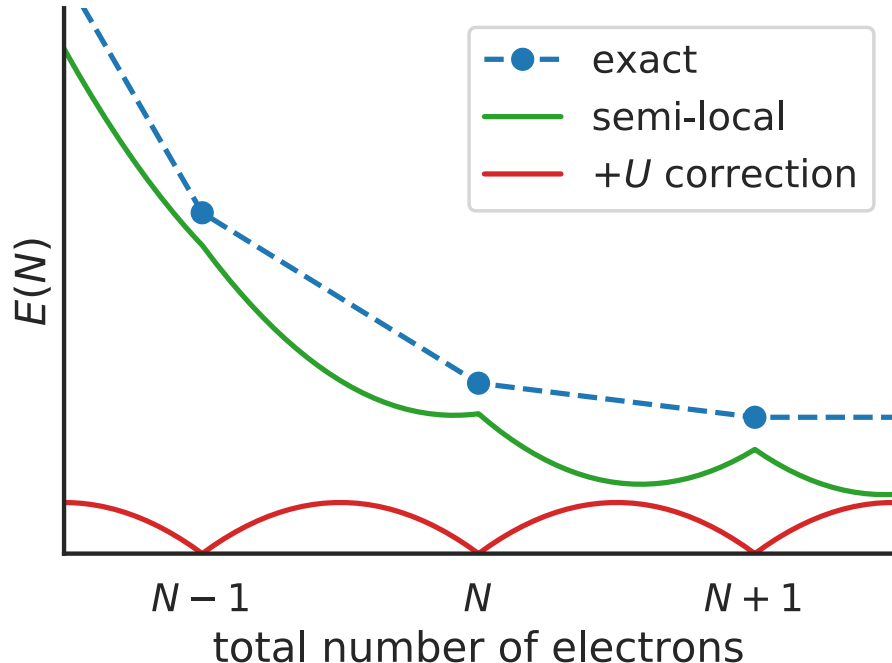
$$E_U = E_{\text{Hub}} - E_{\text{DC}} = \sum_{I\sigma} \frac{U_{\text{eff}}^I}{2} \text{Tr}(n^{I\sigma}(1 - n^{I\sigma})), \quad (9)$$

where the on-site Coulomb repulsion parameter  $U^I$  has been effectively reduced by  $J^I$  to  $U_{\text{eff}}^I$ . The DFT+ $U$  correction to the KS potential is given by

$$\hat{V}_U = \sum_{I\sigma mn} U^I |m\rangle \left( \frac{1}{2} - n_{mn}^{I\sigma} \right) \langle n|. \quad (10)$$

<sup>1</sup>A. G. Petukhov *et al.* *Phys. Rev. B* 67, 153106 (2003)

# The modern interpretation

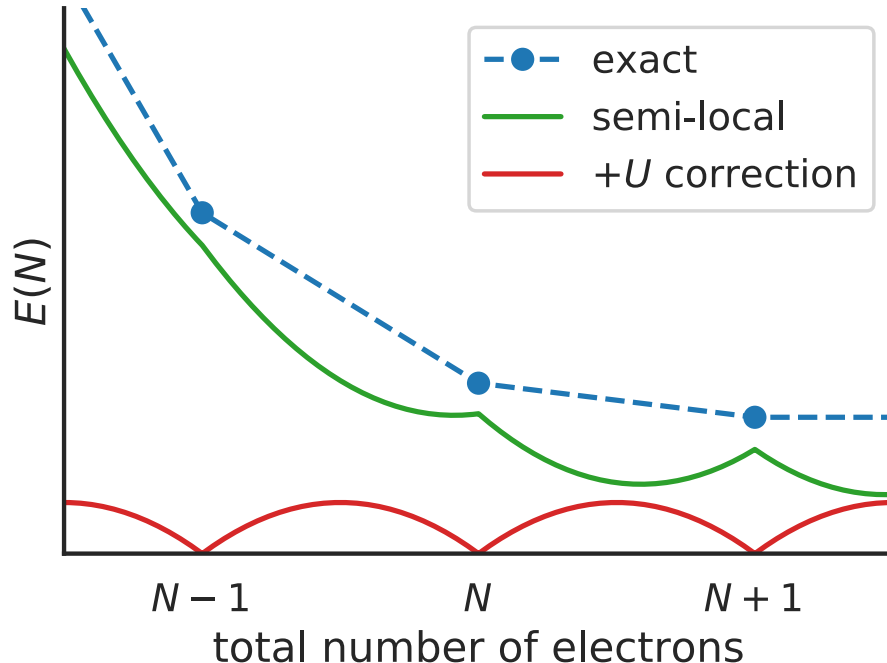


In a basis such that  $n_{ij}^{I\sigma} = \lambda_i^{I\sigma} \delta_{ij}$ ,

$$E_U = \sum_{I\sigma} \frac{U^I}{2} \sum_i \lambda_i^{I\sigma} (1 - \lambda_i^{I\sigma})$$

<sup>1</sup>M. Cococcioni *et al.* Phys. Rev. B 71, 35105 (2005)

# The modern interpretation



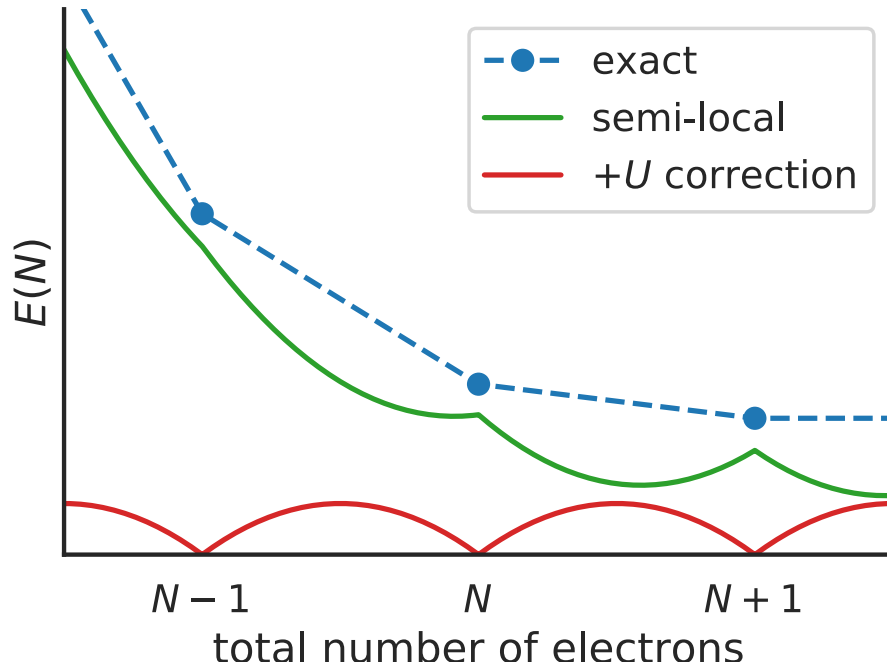
In a basis such that  $n_{ij}^{I\sigma} = \lambda_i^{I\sigma} \delta_{ij}$ ,

$$E_U = \sum_{I\sigma} \frac{U^I}{2} \sum_i \lambda_i^{I\sigma} (1 - \lambda_i^{I\sigma})$$

$U$  can be measured by linear response<sup>1</sup>

<sup>1</sup>M. Cococcioni *et al.* Phys. Rev. B 71, 35105 (2005)

# The modern interpretation



In a basis such that  $n_{ij}^{I\sigma} = \lambda_i^{I\sigma} \delta_{ij}$ ,

$$E_U = \sum_{I\sigma} \frac{U^I}{2} \sum_i \lambda_i^{I\sigma} (1 - \lambda_i^{I\sigma})$$

$U$  can be measured by linear response<sup>1</sup> –  
**critical for predictive calculations**

<sup>1</sup>M. Cococcioni *et al.* Phys. Rev. B 71, 35105 (2005)

$$E_{\text{DFT}+U} = E_{\text{DFT}} + \sum_{I\sigma} \frac{U^I}{2} \text{Tr}[\mathbf{n}^{I\sigma}(1 - \mathbf{n}^{I\sigma})] \quad U^I = [\chi_0^{-1} - \chi^{-1}]_{II}$$

<sup>1</sup>E. B. Linscott *et al.* *Phys. Rev. B* 98, 235157 (2018)

$$E_{\text{DFT}+U} = E_{\text{DFT}} + \sum_{I\sigma} \frac{U^I}{2} \text{Tr}[\mathbf{n}^{I\sigma} (1 - \mathbf{n}^{I\sigma})]$$

$$U^I = [\chi_0^{-1} - \chi^{-1}]_{II}$$

functional treats spin channels  
separately

<sup>1</sup>E. B. Linscott *et al.* *Phys. Rev. B* 98, 235157 (2018)

$$E_{\text{DFT+}U} = E_{\text{DFT}} + \sum_{I\sigma} \frac{U^I}{2} \text{Tr}[\mathbf{n}^{I\sigma} (1 - \mathbf{n}^{I\sigma})]$$

$$U^I = [\chi_0^{-1} - \chi^{-1}]_{II}$$

functional treats spin channels  
separately

LR treats them together

<sup>1</sup>E. B. Linscott *et al.* *Phys. Rev. B* 98, 235157 (2018)

## Role of spin in the calculation of Hubbard $U$ and Hund's $J$ parameters from first principles

Edward B. Linscott,<sup>1,\*</sup> Daniel J. Cole,<sup>2</sup> Michael C. Payne,<sup>1</sup> and David D. O'Regan<sup>3,†</sup>

<sup>1</sup>*Cavendish Laboratory, University of Cambridge, J. J. Thomson Avenue, Cambridge CB3 0HE, United Kingdom*

<sup>2</sup>*School of Natural and Environmental Sciences, Newcastle University, Newcastle upon Tyne NE1 7RU, United Kingdom*

<sup>3</sup>*School of Physics, CRANN and AMBER, Trinity College Dublin, Dublin 2, Ireland*



(Received 25 February 2018; revised manuscript received 19 November 2018; published 26 December 2018)

The density functional theory (DFT) +  $U$  method is a pragmatic and effective approach for calculating the ground-state properties of strongly correlated systems, and linear-response calculations are widely used to determine the requisite Hubbard parameters from first principles. We provide a detailed treatment of spin within the linear-response framework, demonstrating that the conventional Hubbard  $U$  formula, unlike the conventional DFT +  $U$  corrective functional, incorporates interactions that are off-diagonal in the spin indices and places greater weight on one spin channel over the other. We construct alternative definitions for Hubbard and Hund's parameters that are consistent with the contemporary DFT +  $U$  functional, expanding upon the minimum-tracking linear-response method. This approach allows Hund's  $J$  and spin-dependent  $U$  parameters to be calculated with the same ease as for the standard Hubbard  $U$ . Our methods accurately reproduce the

# Spin-resolved linear response

conventional

→

spin-resolved

# Spin-resolved linear response

conventional

→

spin-resolved

$$\chi_{IJ} = \frac{dn^I}{dv^J}$$

# Spin-resolved linear response

conventional

→

spin-resolved

$$\chi_{IJ} = \frac{dn^I}{dv^J}$$

→

$$\chi_{IJ}^{\sigma\sigma'} = \frac{dn^{I\sigma}}{dv^{J\sigma'}}$$

# Spin-resolved linear response

conventional

→

spin-resolved

$$\chi_{IJ} = \frac{dn^I}{dv^J}$$

→

$$\chi_{IJ}^{\sigma\sigma'} = \frac{dn^{I\sigma}}{dv^{J\sigma'}}$$

$$\begin{pmatrix} \chi_{11} & \chi_{12} & \dots \\ \chi_{21} & \chi_{22} & \dots \\ \vdots & \vdots & \ddots \end{pmatrix}$$

# Spin-resolved linear response

conventional

→

spin-resolved

$$\chi_{IJ} = \frac{dn^I}{dv^J}$$

→

$$\chi_{IJ}^{\sigma\sigma'} = \frac{dn^{I\sigma}}{dv^{J\sigma'}}$$

$$\begin{pmatrix} \chi_{11} & \chi_{12} & \dots \\ \chi_{21} & \chi_{22} & \dots \\ \vdots & \vdots & \ddots \end{pmatrix}$$

→

$$\begin{pmatrix} \chi_{11}^{\uparrow\uparrow} & \chi_{11}^{\uparrow\downarrow} & \chi_{12}^{\uparrow\uparrow} & \chi_{12}^{\uparrow\downarrow} & \dots \\ \chi_{11}^{\downarrow\uparrow} & \chi_{11}^{\downarrow\downarrow} & \chi_{12}^{\downarrow\uparrow} & \chi_{12}^{\downarrow\downarrow} & \dots \\ \chi_{21}^{\uparrow\uparrow} & \chi_{21}^{\uparrow\downarrow} & \chi_{22}^{\uparrow\uparrow} & \chi_{22}^{\uparrow\downarrow} & \dots \\ \chi_{21}^{\downarrow\uparrow} & \chi_{21}^{\downarrow\downarrow} & \chi_{22}^{\downarrow\uparrow} & \chi_{22}^{\downarrow\downarrow} & \dots \\ \vdots & \vdots & \vdots & \vdots & \ddots \end{pmatrix}$$

# Spin-resolved linear response

conventional

→

spin-resolved

$$\chi_{IJ} = \frac{dn^I}{dv^J}$$

→

$$\chi_{IJ}^{\sigma\sigma'} = \frac{dn^{I\sigma}}{dv^{J\sigma'}}$$

$$\begin{pmatrix} \chi_{11} & \chi_{12} & \dots \\ \chi_{21} & \chi_{22} & \dots \\ \vdots & \vdots & \ddots \end{pmatrix}$$

→

$$\begin{pmatrix} \chi_{11}^{\uparrow\uparrow} & \chi_{11}^{\uparrow\downarrow} & \chi_{12}^{\uparrow\uparrow} & \chi_{12}^{\uparrow\downarrow} & \dots \\ \chi_{11}^{\downarrow\uparrow} & \chi_{11}^{\downarrow\downarrow} & \chi_{12}^{\downarrow\uparrow} & \chi_{12}^{\downarrow\downarrow} & \dots \\ \chi_{21}^{\uparrow\uparrow} & \chi_{21}^{\uparrow\downarrow} & \chi_{22}^{\uparrow\uparrow} & \chi_{22}^{\uparrow\downarrow} & \dots \\ \chi_{21}^{\downarrow\uparrow} & \chi_{21}^{\downarrow\downarrow} & \chi_{22}^{\downarrow\uparrow} & \chi_{22}^{\downarrow\downarrow} & \dots \\ \vdots & \vdots & \vdots & \vdots & \ddots \end{pmatrix}$$

# Spin-resolved linear response

conventional

→

spin-resolved

$$\chi_{IJ} = \frac{dn^I}{dv^J}$$

→

$$\chi_{IJ}^{\sigma\sigma'} = \frac{dn^{I\sigma}}{dv^{J\sigma'}}$$

$$\begin{pmatrix} \chi_{11} & \chi_{12} & \dots \\ \chi_{21} & \chi_{22} & \dots \\ \vdots & \vdots & \ddots \end{pmatrix}$$

→

$$\begin{pmatrix} \chi_{11}^{\uparrow\uparrow} & \chi_{11}^{\uparrow\downarrow} & \chi_{12}^{\uparrow\uparrow} & \chi_{12}^{\uparrow\downarrow} & \dots \\ \chi_{11}^{\downarrow\uparrow} & \chi_{11}^{\downarrow\downarrow} & \chi_{12}^{\downarrow\uparrow} & \chi_{12}^{\downarrow\downarrow} & \dots \\ \chi_{21}^{\uparrow\uparrow} & \chi_{21}^{\uparrow\downarrow} & \chi_{22}^{\uparrow\uparrow} & \chi_{22}^{\uparrow\downarrow} & \dots \\ \chi_{21}^{\downarrow\uparrow} & \chi_{21}^{\downarrow\downarrow} & \chi_{22}^{\downarrow\uparrow} & \chi_{22}^{\downarrow\downarrow} & \dots \\ \vdots & \vdots & \vdots & \vdots & \ddots \end{pmatrix}$$

$$U^I = [\chi_0^{-1} - \chi^{-1}]_{II}$$

# Spin-resolved linear response

conventional

→

spin-resolved

$$\chi_{IJ} = \frac{dn^I}{dv^J}$$

→

$$\chi_{IJ}^{\sigma\sigma'} = \frac{dn^{I\sigma}}{dv^{J\sigma'}}$$

$$\begin{pmatrix} \chi_{11} & \chi_{12} & \dots \\ \chi_{21} & \chi_{22} & \dots \\ \vdots & \vdots & \ddots \end{pmatrix}$$

→

$$\begin{pmatrix} \chi_{11}^{\uparrow\uparrow} & \chi_{11}^{\uparrow\downarrow} & \chi_{12}^{\uparrow\uparrow} & \chi_{12}^{\uparrow\downarrow} & \dots \\ \chi_{11}^{\downarrow\uparrow} & \chi_{11}^{\downarrow\downarrow} & \chi_{12}^{\downarrow\uparrow} & \chi_{12}^{\downarrow\downarrow} & \dots \\ \chi_{21}^{\uparrow\uparrow} & \chi_{21}^{\uparrow\downarrow} & \chi_{22}^{\uparrow\uparrow} & \chi_{22}^{\uparrow\downarrow} & \dots \\ \chi_{21}^{\downarrow\uparrow} & \chi_{21}^{\downarrow\downarrow} & \chi_{22}^{\downarrow\uparrow} & \chi_{22}^{\downarrow\downarrow} & \dots \\ \vdots & \vdots & \vdots & \vdots & \ddots \end{pmatrix}$$

$$U^I = [\chi_0^{-1} - \chi^{-1}]_{II}$$

→

$$f_{II}^{\sigma\sigma'} \xrightarrow{?} U^{I\sigma}$$

# Advantages of spin-resolved LR

# Advantages of spin-resolved LR

- conceptual consistency (spin-resolved functional  $\leftrightarrow$  spin-resolved linear response)

# Advantages of spin-resolved LR

- conceptual consistency (spin-resolved functional  $\leftrightarrow$  spin-resolved linear response)
- can perform unconstrained constrained linear response

# Advantages of spin-resolved LR

- conceptual consistency (spin-resolved functional  $\leftrightarrow$  spin-resolved linear response)
- can perform unconstrained constrained linear response

e.g. suppose we want to compute  $\frac{d^2 E_{\text{Hxc}}}{d(n^I)^2} \Big|_{\mu^I}$

# Advantages of spin-resolved LR

- conceptual consistency (spin-resolved functional  $\leftrightarrow$  spin-resolved linear response)
- can perform unconstrained constrained linear response

e.g. suppose we want to compute  $\frac{d^2 E_{\text{Hxc}}}{d(n^I)^2} \Big|_{\mu^I}$

This is easy with spin-resolved LR:  $\frac{d^2 E_{\text{Hxc}}}{d n^2} \Big|_{\mu} = \frac{1}{4} (f^{\uparrow\uparrow} + f^{\downarrow\downarrow} + f^{\uparrow\downarrow} + f^{\downarrow\uparrow})$

# Advantages of spin-resolved LR

- conceptual consistency (spin-resolved functional  $\leftrightarrow$  spin-resolved linear response)
- can perform unconstrained constrained linear response

e.g. suppose we want to compute  $\frac{d^2 E_{\text{Hxc}}}{d(n^I)^2} \Big|_{\mu^I}$

This is easy with spin-resolved LR:  $\frac{d^2 E_{\text{Hxc}}}{d n^2} \Big|_{\mu} = \frac{1}{4} (f^{\uparrow\uparrow} + f^{\downarrow\downarrow} + f^{\uparrow\downarrow} + f^{\downarrow\uparrow})$

- can recover the conventional linear response results

# Advantages of spin-resolved LR

- conceptual consistency (spin-resolved functional  $\leftrightarrow$  spin-resolved linear response)
- can perform unconstrained constrained linear response

e.g. suppose we want to compute  $\frac{d^2 E_{\text{Hxc}}}{d(n^I)^2} \Big|_{\mu^I}$

This is easy with spin-resolved LR:  $\frac{d^2 E_{\text{Hxc}}}{d n^2} \Big|_{\mu} = \frac{1}{4} (f^{\uparrow\uparrow} + f^{\downarrow\downarrow} + f^{\uparrow\downarrow} + f^{\downarrow\uparrow})$

- can recover the conventional linear response results
- $J$  is “free”

# Advantages of spin-resolved LR

- conceptual consistency (spin-resolved functional  $\leftrightarrow$  spin-resolved linear response)
- can perform unconstrained constrained linear response

e.g. suppose we want to compute  $\frac{d^2 E_{\text{Hxc}}}{d(n^I)^2} \Big|_{\mu^I}$

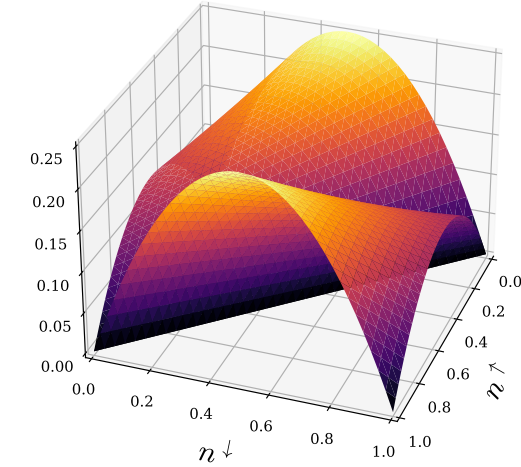
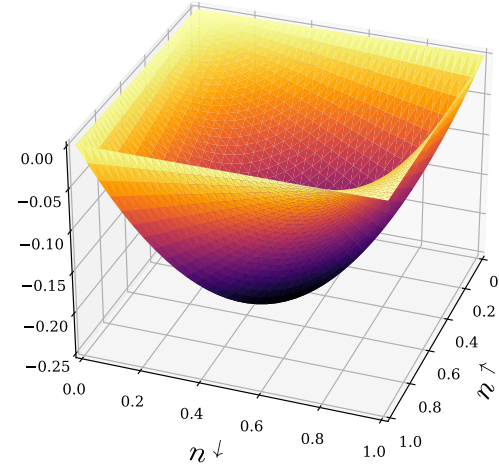
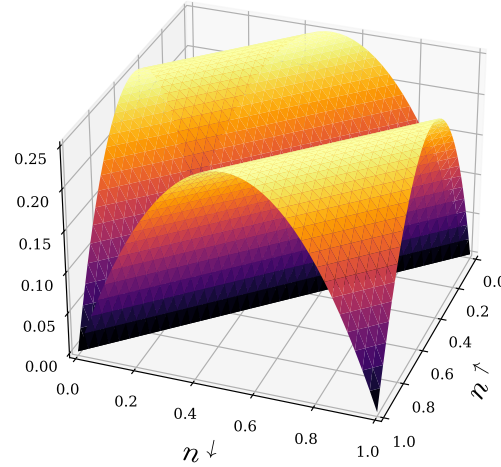
This is easy with spin-resolved LR:  $\frac{d^2 E_{\text{Hxc}}}{d n^2} \Big|_{\mu} = \frac{1}{4} (f^{\uparrow\uparrow} + f^{\downarrow\downarrow} + f^{\uparrow\downarrow} + f^{\downarrow\uparrow})$

- can recover the conventional linear response results
- $J$  is “free”
- easily implemented

# Now used in Materials Project!

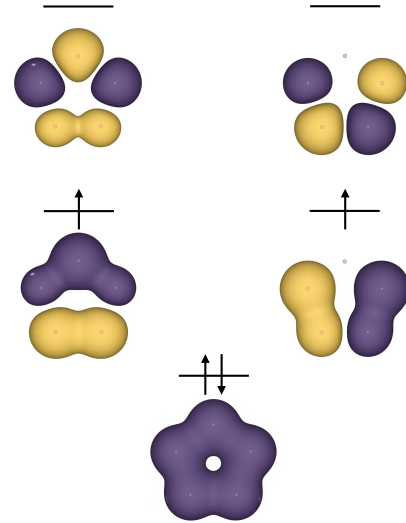
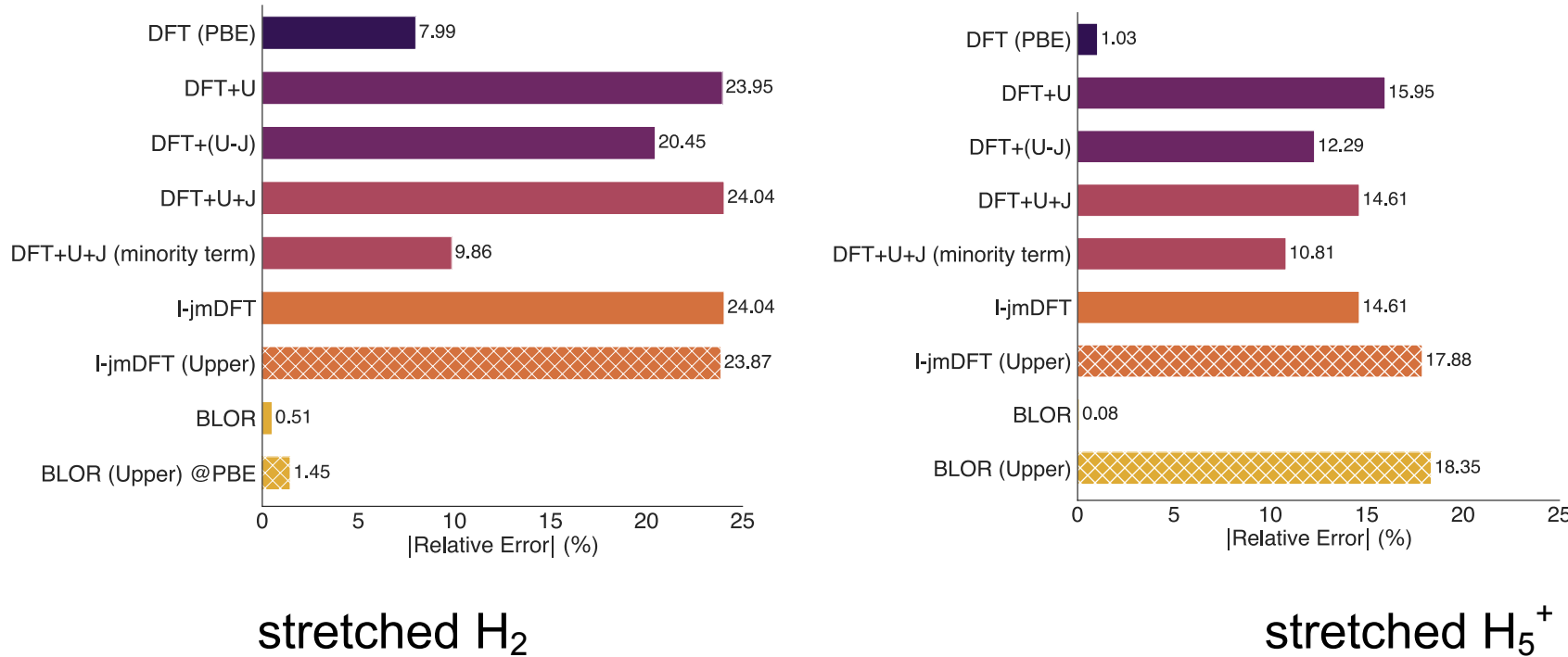


<sup>1</sup>G. C. Moore et al. *Phys. Rev. Mater.* 8, 14409 (2024)



## BLOR: a DFT+ $U$ type functional that...

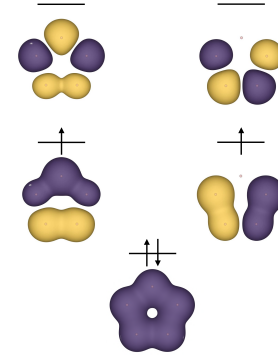
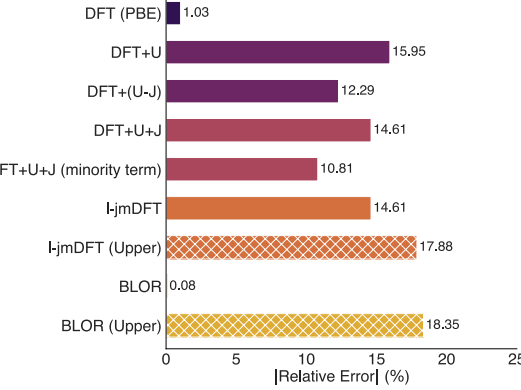
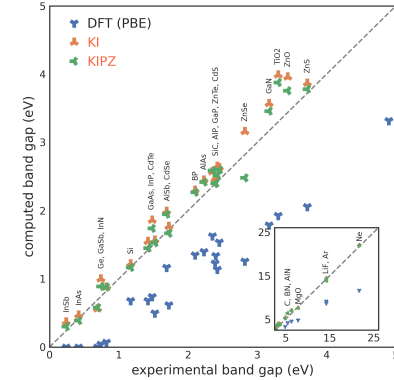
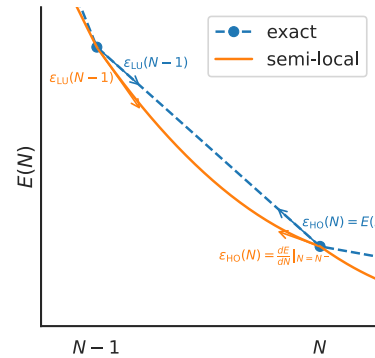
- is inspired by the intrinsic errors of approximate DFT
- relies on spin-resolved linear response
- includes a term to correct for static correlation error
- is double-counting-free



<sup>1</sup>A. C. Burgess *et al.* *Phys. Rev. Lett.* 133, 26404 (2024), A. C. Burgess *et al.* *Phys. Rev. B* 107, L121115 (2023)

# Summary

Understanding and correcting the failures of approximate DFT can yield simple but predictive functionals



# Acknowledgements



David  
O'Regan



Andrew  
Burgess



Nicola  
Colonna



Miki Bonacci



Aleksandr  
Poliukhin



Marija  
Stojkovic



Junfeng Qiao



Yannick  
Schubert

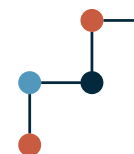


Nicola Marzari

... and many  
others!



Engineering and  
Physical Sciences  
Research Council



**Swiss National  
Science Foundation**



# Thank you!

*these slides are available at*  [\*elinscott-talks\*](https://github.com/elinscott-talks)

spare slides

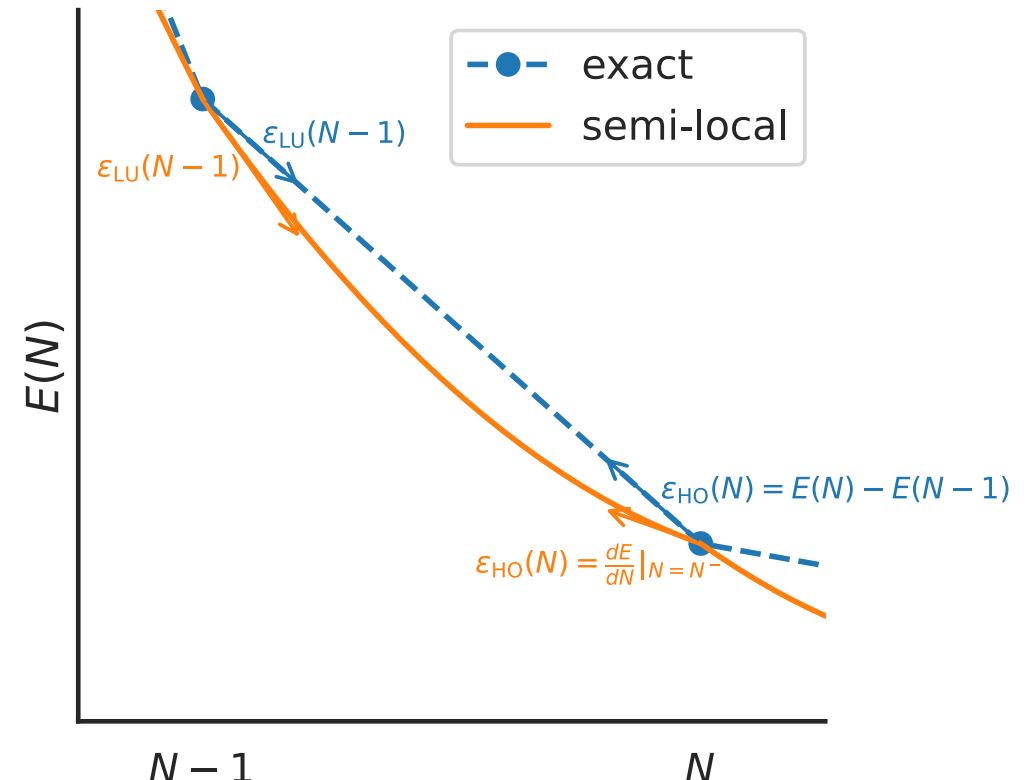
# Imposing generalised piecewise linearity

Formally, every orbital  $i$  should have an eigenenergy

$$\varepsilon_i^{\text{Koopmans}} = \langle \varphi_i | \hat{H} | \varphi_i \rangle = \frac{dE}{df_i}$$

that is

- independent of  $f_i$
- equal to  $\Delta E$  of explicit electron addition/  
removal



# Electronic screening via parameters

$$E^{\text{KI}}[\{\rho_i\}] = E^{\text{DFT}}[\rho] + \sum_i \left( - \int_0^{f_i} \langle \varphi_i | \hat{h}^{\text{DFT}}(f) | \varphi_i \rangle df + f_i \int_0^1 \langle \varphi_i | \hat{h}^{\text{DFT}}(f) | \varphi_i \rangle df \right)$$

# Electronic screening via parameters

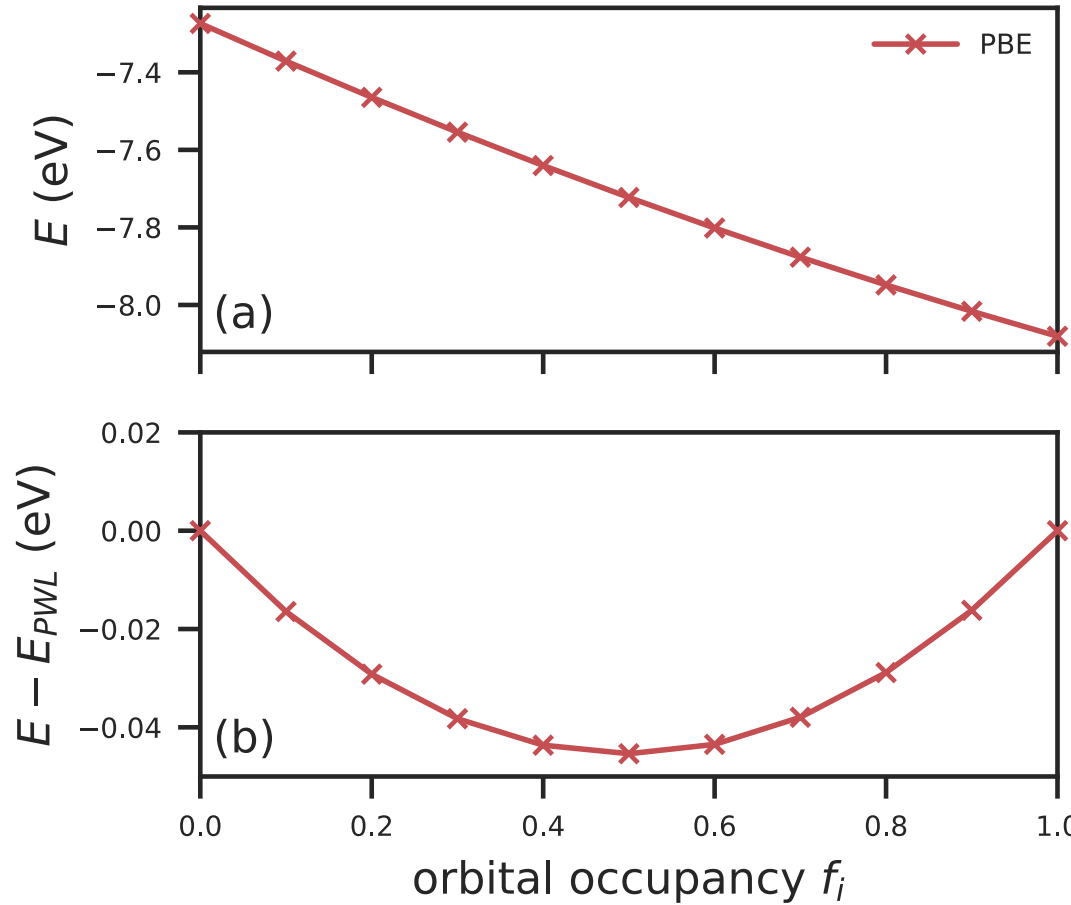
$$\begin{aligned}
 E^{\text{KI}}[\{\rho_i\}] &= E^{\text{DFT}}[\rho] + \sum_i \left( - \int_0^{f_i} \langle \varphi_i | \hat{h}^{\text{DFT}}(f) | \varphi_i \rangle df + f_i \int_0^1 \langle \varphi_i | \hat{h}^{\text{DFT}}(f) | \varphi_i \rangle df \right) \\
 &= E^{\text{DFT}}[\rho] + \sum_i \left\{ - (E^{\text{DFT}}[\rho] - E^{\text{DFT}}[\rho^{f_i \rightarrow 0}]) + f_i (E^{\text{DFT}}[\rho^{f_i \rightarrow 1}] - E^{\text{DFT}}[\rho^{f_i \rightarrow 0}]) \right\}
 \end{aligned}$$

# Electronic screening via parameters

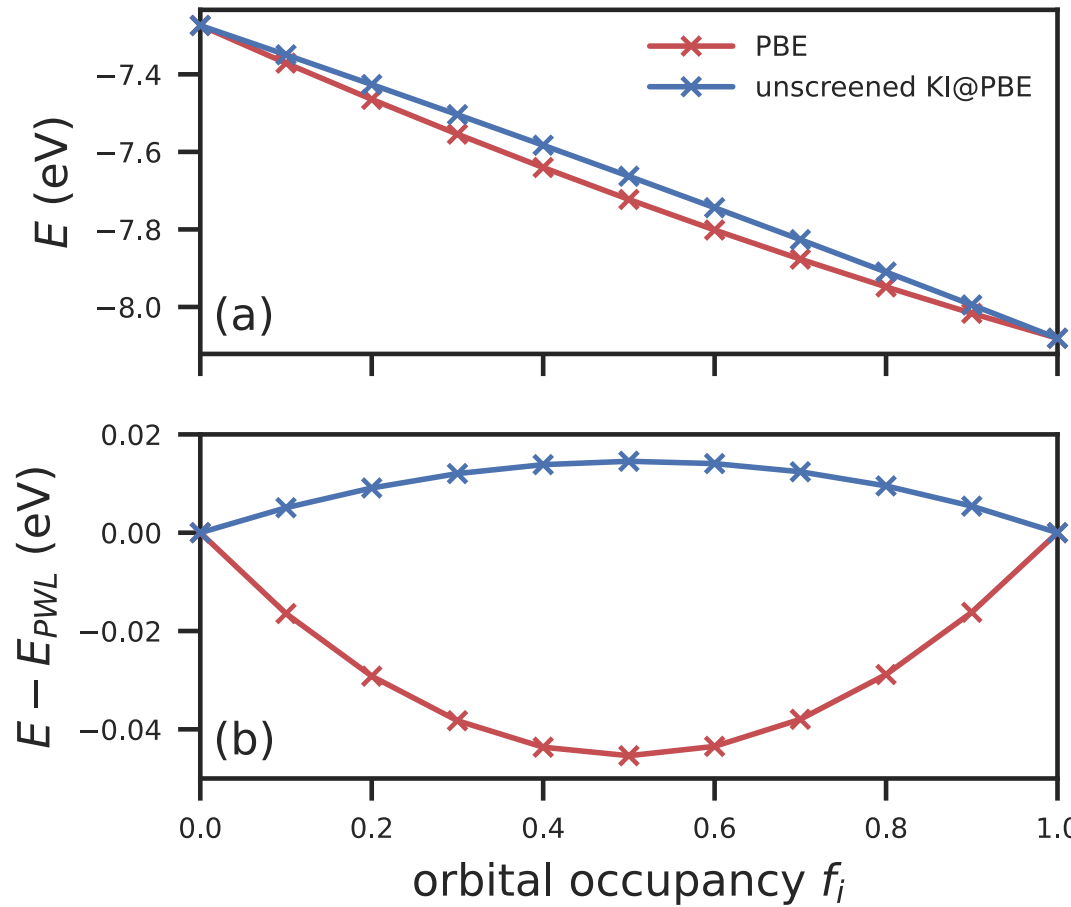
$$\begin{aligned}
 E^{\text{KI}}[\{\rho_i\}] &= E^{\text{DFT}}[\rho] + \sum_i \left( - \int_0^{f_i} \langle \varphi_i | \hat{h}^{\text{DFT}}(f) | \varphi_i \rangle df + f_i \int_0^1 \langle \varphi_i | \hat{h}^{\text{DFT}}(f) | \varphi_i \rangle df \right) \\
 &= E^{\text{DFT}}[\rho] + \sum_i \left\{ - \left( E^{\text{DFT}}[\rho] - E^{\text{DFT}}[\rho^{f_i \rightarrow 0}] \right) + f_i \left( E^{\text{DFT}}[\rho^{f_i \rightarrow 1}] - E^{\text{DFT}}[\rho^{f_i \rightarrow 0}] \right) \right\}
 \end{aligned}$$

cannot evaluate directly      cannot evaluate directly      cannot evaluate directly

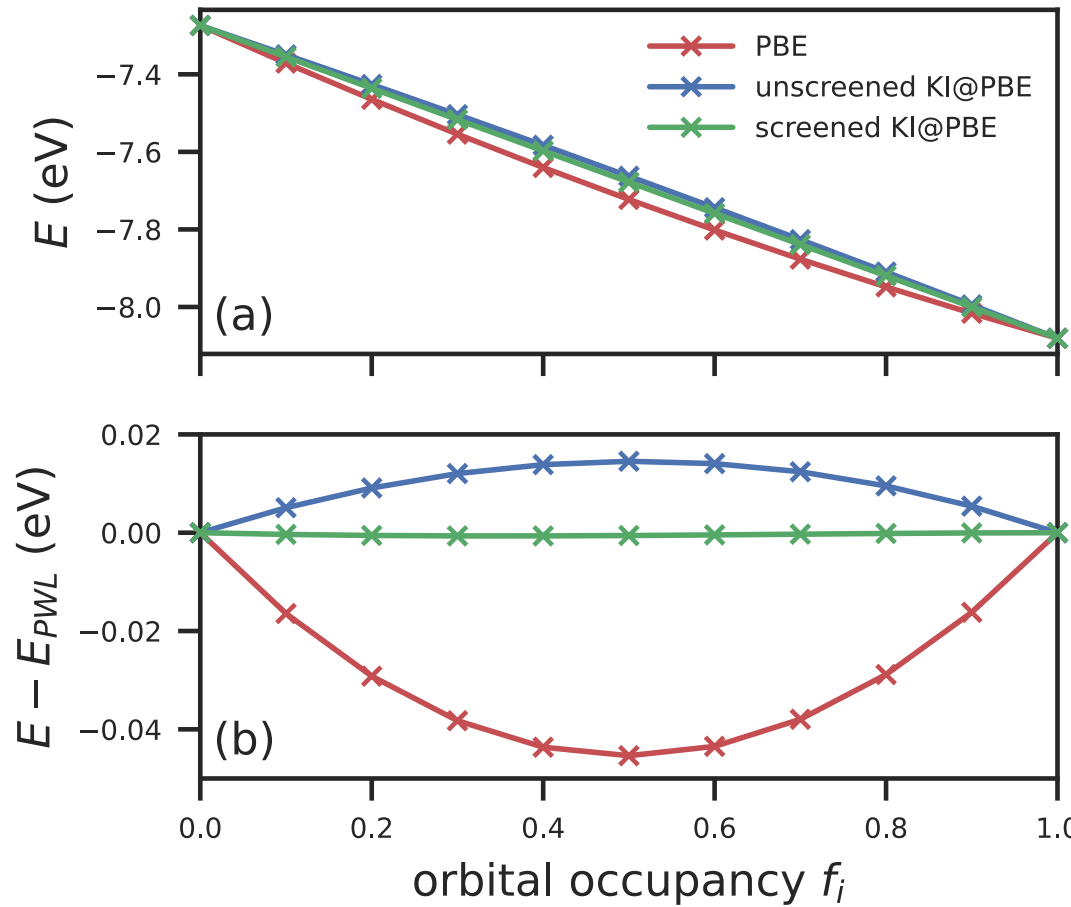
# Electronic screening via parameters



# Electronic screening via parameters



# Electronic screening via parameters



# Electronic screening via parameters

$$E_{\alpha}^{\text{KI}}[\rho, \{\rho_i\}] \approx E^{\text{DFT}}[\rho]$$

$$+ \sum_i \alpha_i \{ - (E^{\text{DFT}}[\rho] - E^{\text{DFT}}[\rho - \rho_i]) + f_i (E^{\text{DFT}}[\rho - \rho_i + n_i] - E^{\text{DFT}}[\rho - \rho_i]) \}$$

# Electronic screening via parameters

$$E_{\alpha}^{\text{KI}}[\rho, \{\rho_i\}] \approx E^{\text{DFT}}[\rho]$$

$$+ \sum_i \alpha_i \left\{ - (E^{\text{DFT}}[\rho] - E^{\text{DFT}}[\rho - \rho_i]) + f_i (E^{\text{DFT}}[\rho - \rho_i + n_i] - E^{\text{DFT}}[\rho - \rho_i]) \right\}$$

uses frozen orbitals                    uses frozen orbitals                    uses frozen orbitals

# Electronic screening via parameters

$$E_{\alpha}^{\text{KI}}[\rho, \{\rho_i\}] \approx E^{\text{DFT}}[\rho]$$

$$+ \sum_i \alpha_i \left\{ - (E^{\text{DFT}}[\rho] - E^{\text{DFT}}[\rho - \rho_i]) + f_i (E^{\text{DFT}}[\rho - \rho_i + n_i] - E^{\text{DFT}}[\rho - \rho_i]) \right\}$$

screening parameter      uses frozen orbitals      uses frozen orbitals      uses frozen orbitals

# Electronic screening via parameters

$$E_{\alpha}^{\text{KI}}[\rho, \{\rho_i\}] \approx E^{\text{DFT}}[\rho]$$

$$+ \sum_i \alpha_i \left\{ - (E^{\text{DFT}}[\rho] - E^{\text{DFT}}[\rho - \rho_i]) + f_i (E^{\text{DFT}}[\rho - \rho_i + n_i] - E^{\text{DFT}}[\rho - \rho_i]) \right\}$$

screening parameter                    uses frozen orbitals                    uses frozen orbitals                    uses frozen orbitals

which is easy to evaluate e.g.

$$H_{ij}^{\text{KI}} = \langle \varphi_j | \hat{h}^{\text{DFT}} + \alpha_i \hat{v}_i^{\text{KI}} | \varphi_i \rangle \quad \hat{v}_i^{\text{KI}} = -E_{\text{Hxc}}[\rho - n_i] + E_{\text{Hxc}}[\rho] - \int v_{\text{Hxc}}(\mathbf{r}', [\rho]) n_i d\mathbf{r}'$$

# Electronic screening via parameters

$$E_{\alpha}^{\text{KI}}[\rho, \{\rho_i\}] \approx E^{\text{DFT}}[\rho]$$

$$+ \sum_i \alpha_i \left\{ - (E^{\text{DFT}}[\rho] - E^{\text{DFT}}[\rho - \rho_i]) + f_i (E^{\text{DFT}}[\rho - \rho_i + n_i] - E^{\text{DFT}}[\rho - \rho_i]) \right\}$$

screening parameter                    uses frozen orbitals                    uses frozen orbitals                    uses frozen orbitals

which is easy to evaluate e.g.

$$H_{ij}^{\text{KI}} = \langle \varphi_j | \hat{h}^{\text{DFT}} + \alpha_i \hat{v}_i^{\text{KI}} | \varphi_i \rangle \quad \hat{v}_i^{\text{KI}} = -E_{\text{Hxc}}[\rho - n_i] + E_{\text{Hxc}}[\rho] - \int v_{\text{Hxc}}(\mathbf{r}', [\rho]) n_i d\mathbf{r}'$$

Screening parameters *not* a fitting parameter!

# Orbital-density dependence

The potential is orbital-density-dependent!

$$v_{i \in \text{occ}}^{\text{KI}} = -E_{\text{Hxc}}[\rho - n_i] + E_{\text{Hxc}}[\rho] - \int v_{\text{Hxc}}(\mathbf{r}', [\rho]) n_i d\mathbf{r}'$$

<sup>1</sup>N. L. Nguyen *et al.* *Phys. Rev. X* 8, 21051 (2018)

<sup>2</sup>N. Marzari *et al.* *Rev. Mod. Phys.* 84, 1419–1475 (2012)

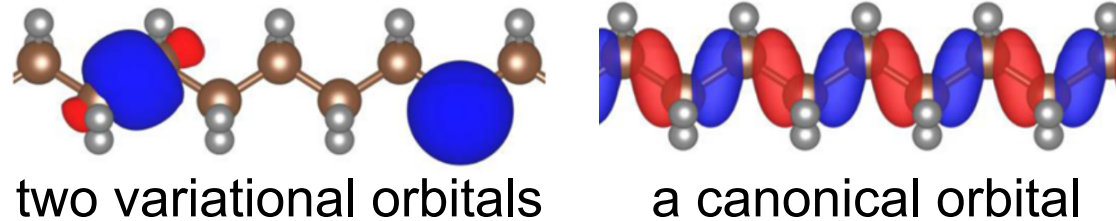
<sup>3</sup>A. Ferretti *et al.* *Phys. Rev. B* 89, 195134 (2014)

# Orbital-density dependence

The potential is orbital-density-dependent!

$$v_{i \in \text{occ}}^{\text{KI}} = -E_{\text{Hxc}}[\rho - n_i] + E_{\text{Hxc}}[\rho] - \int v_{\text{Hxc}}(\mathbf{r}', [\rho]) n_i d\mathbf{r}'$$

- loss of unitary invariance<sup>1</sup>



<sup>1</sup>N. L. Nguyen *et al.* *Phys. Rev. X* 8, 21051 (2018)

<sup>2</sup>N. Marzari *et al.* *Rev. Mod. Phys.* 84, 1419–1475 (2012)

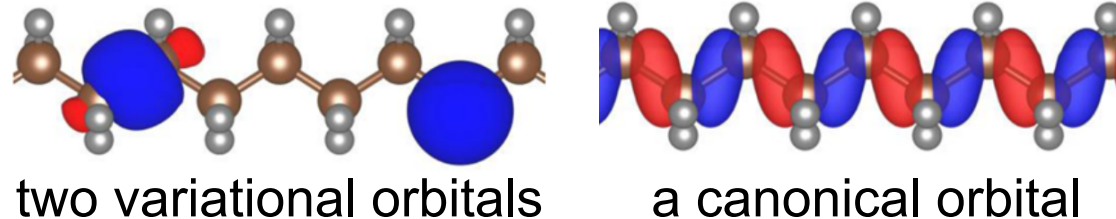
<sup>3</sup>A. Ferretti *et al.* *Phys. Rev. B* 89, 195134 (2014)

# Orbital-density dependence

The potential is orbital-density-dependent!

$$v_{i \in \text{occ}}^{\text{KI}} = -E_{\text{Hxc}}[\rho - n_i] + E_{\text{Hxc}}[\rho] - \int v_{\text{Hxc}}(\mathbf{r}', [\rho]) n_i d\mathbf{r}'$$

- loss of unitary invariance<sup>1</sup>



- we can use MLWFs<sup>2</sup>

<sup>1</sup>N. L. Nguyen *et al.* *Phys. Rev. X* 8, 21051 (2018)

<sup>2</sup>N. Marzari *et al.* *Rev. Mod. Phys.* 84, 1419–1475 (2012)

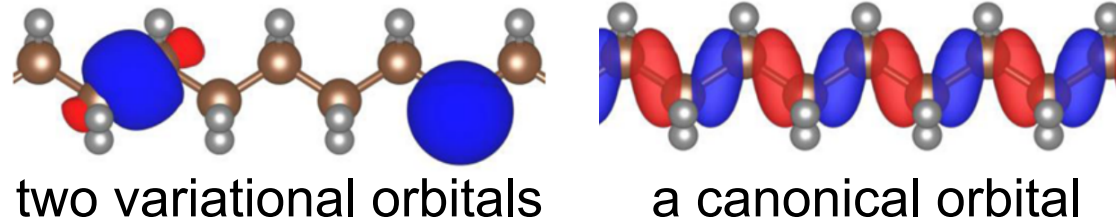
<sup>3</sup>A. Ferretti *et al.* *Phys. Rev. B* 89, 195134 (2014)

# Orbital-density dependence

The potential is orbital-density-dependent!

$$v_{i \in \text{occ}}^{\text{KI}} = -E_{\text{Hxc}}[\rho - n_i] + E_{\text{Hxc}}[\rho] - \int v_{\text{Hxc}}(\mathbf{r}', [\rho]) n_i d\mathbf{r}'$$

- loss of unitary invariance<sup>1</sup>



- we can use MLWFs<sup>2</sup>
- we know  $\hat{H}|\varphi_i\rangle$  but not  $\hat{H}$

<sup>1</sup>N. L. Nguyen *et al.* *Phys. Rev. X* 8, 21051 (2018)

<sup>2</sup>N. Marzari *et al.* *Rev. Mod. Phys.* 84, 1419–1475 (2012)

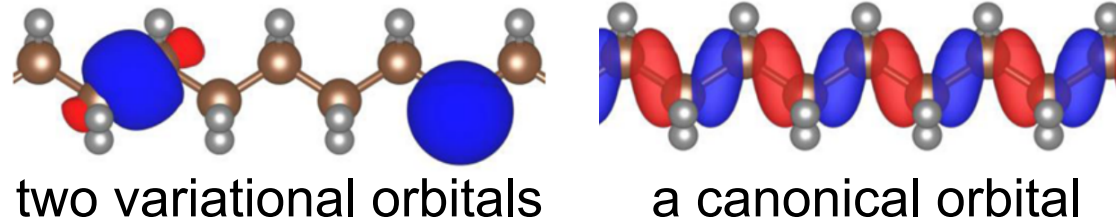
<sup>3</sup>A. Ferretti *et al.* *Phys. Rev. B* 89, 195134 (2014)

# Orbital-density dependence

The potential is orbital-density-dependent!

$$v_{i \in \text{occ}}^{\text{KI}} = -E_{\text{Hxc}}[\rho - n_i] + E_{\text{Hxc}}[\rho] - \int v_{\text{Hxc}}(\mathbf{r}', [\rho]) n_i d\mathbf{r}'$$

- loss of unitary invariance<sup>1</sup>



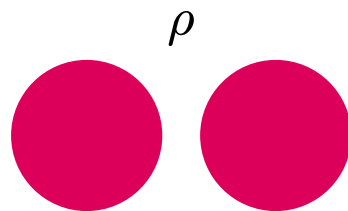
- we can use MLWFs<sup>2</sup>
- we know  $\hat{H}|\varphi_i\rangle$  but not  $\hat{H}$
- a natural generalisation of DFT towards spectral functional theory<sup>3</sup>

<sup>1</sup>N. L. Nguyen *et al.* *Phys. Rev. X* 8, 21051 (2018)

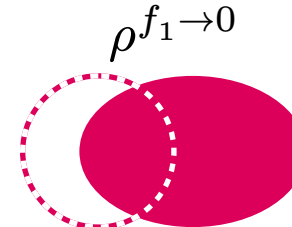
<sup>2</sup>N. Marzari *et al.* *Rev. Mod. Phys.* 84, 1419–1475 (2012)

<sup>3</sup>A. Ferretti *et al.* *Phys. Rev. B* 89, 195134 (2014)

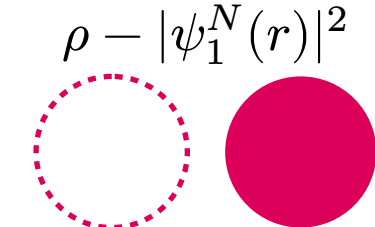
# Frozen orbital approximation



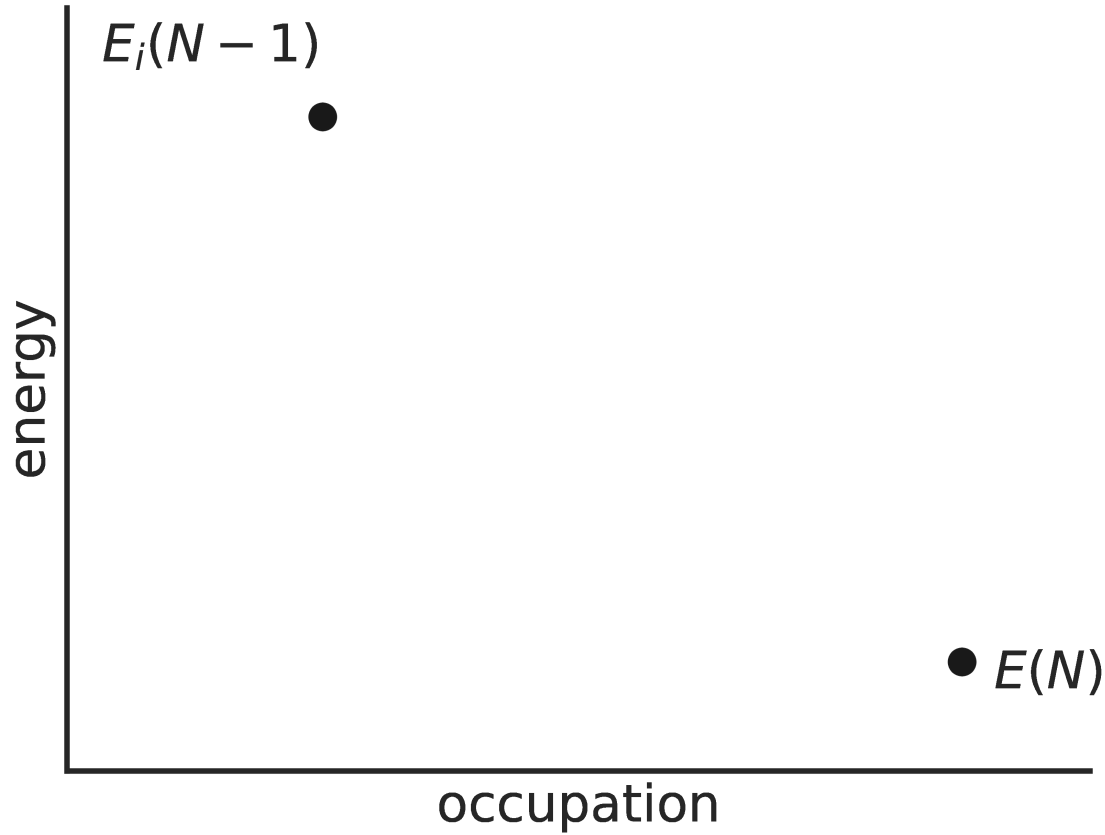
2-electron solution

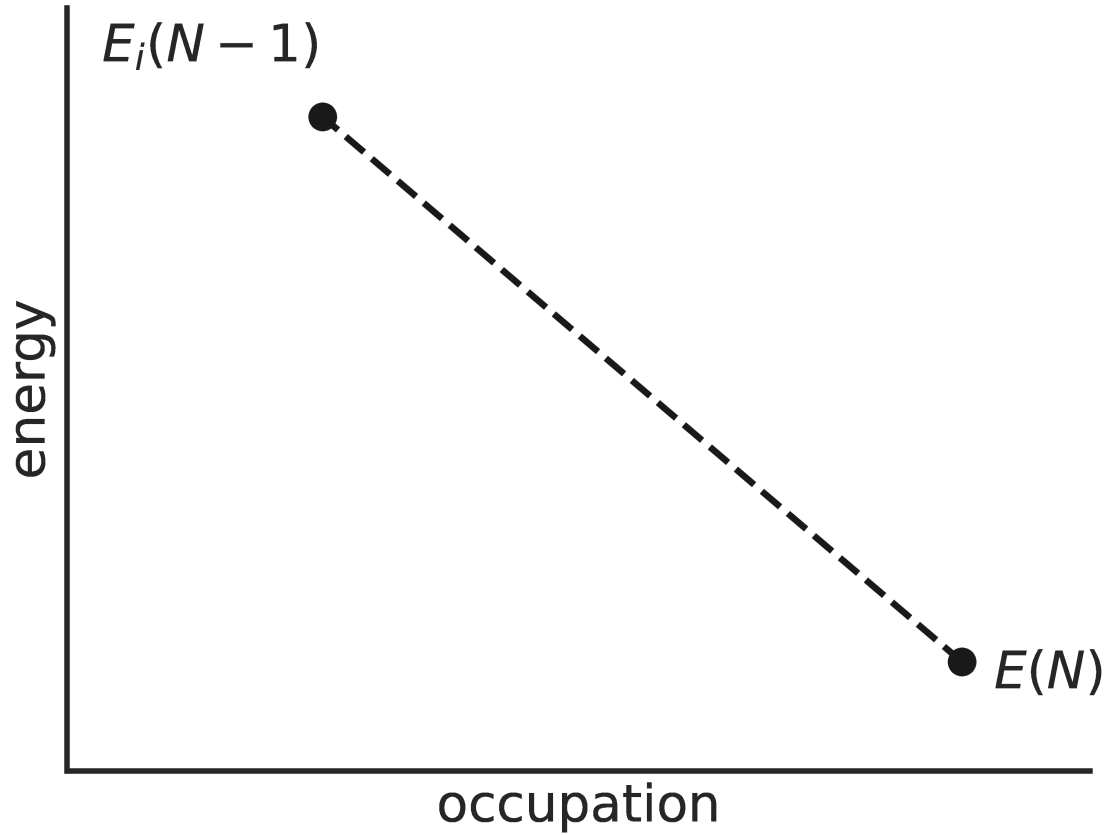


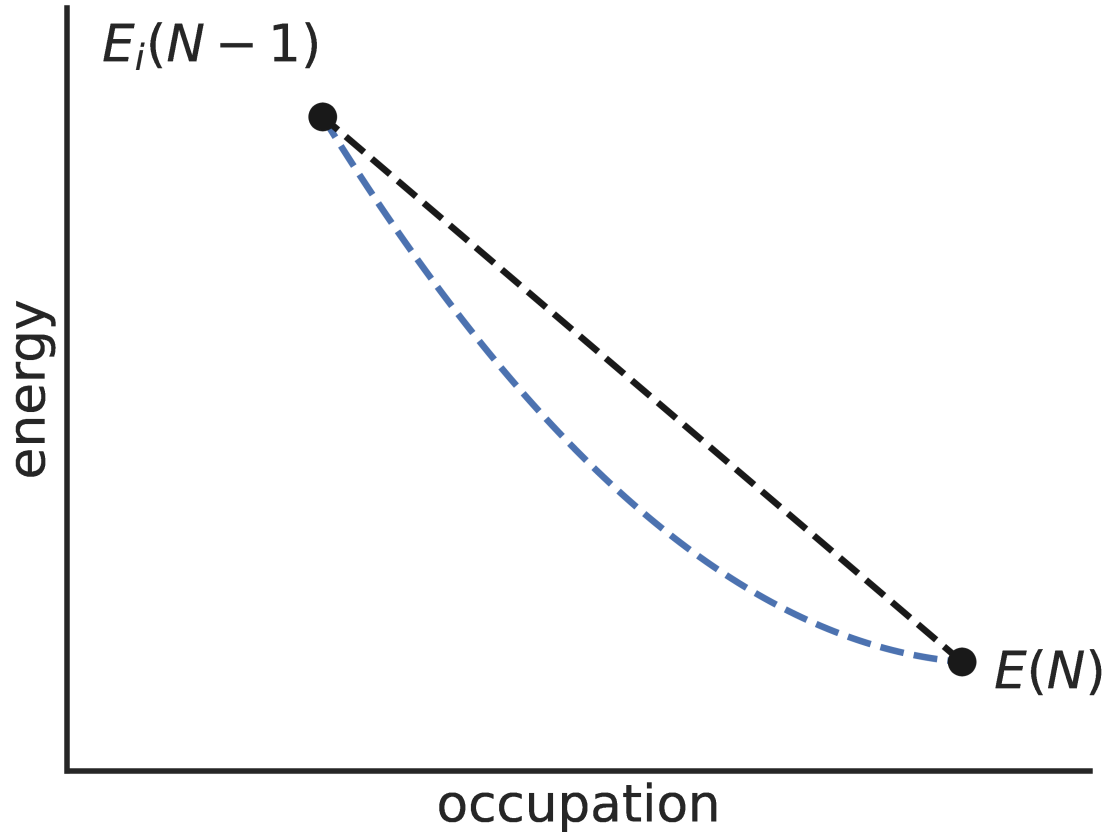
what we'd like to evaluate

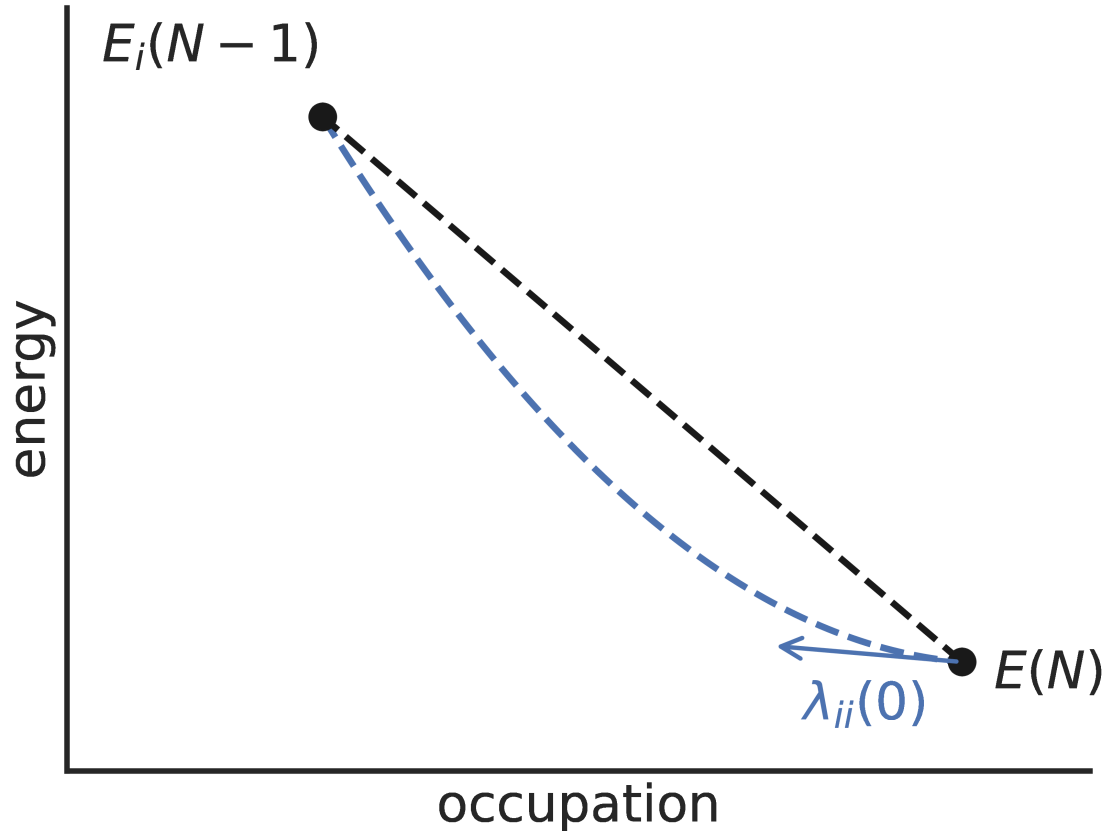


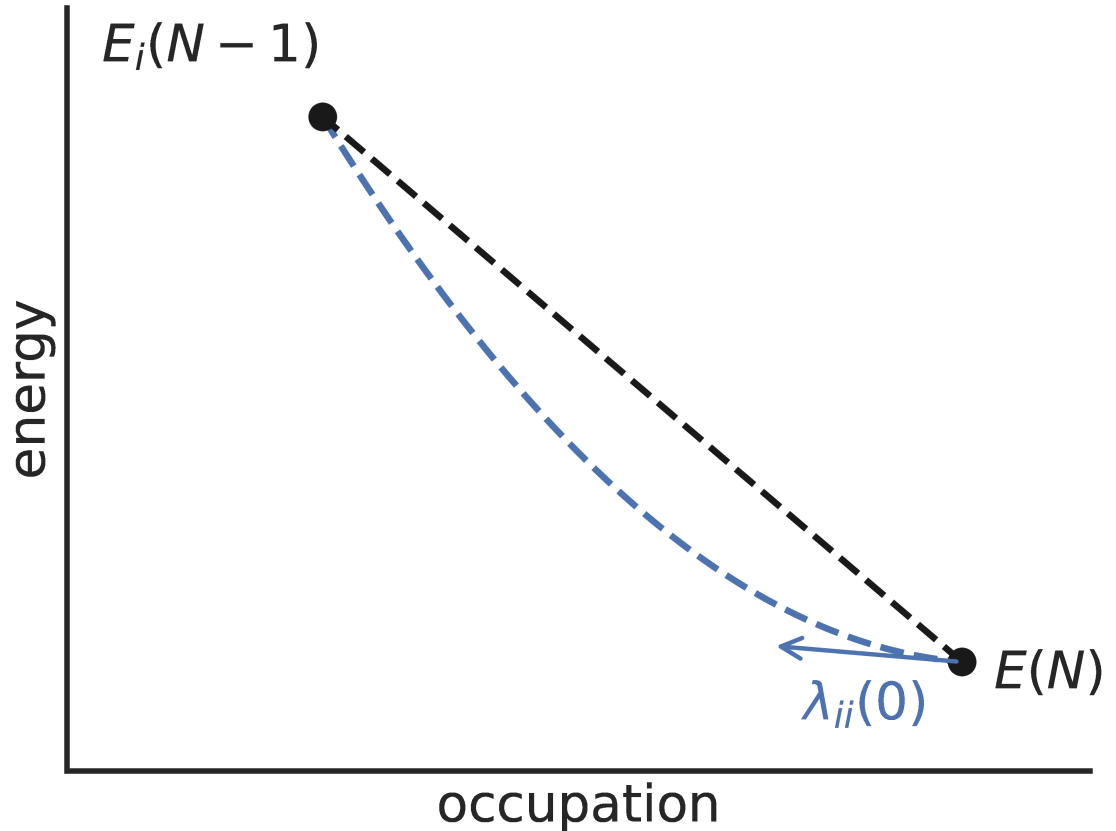
what we can quickly evaluate

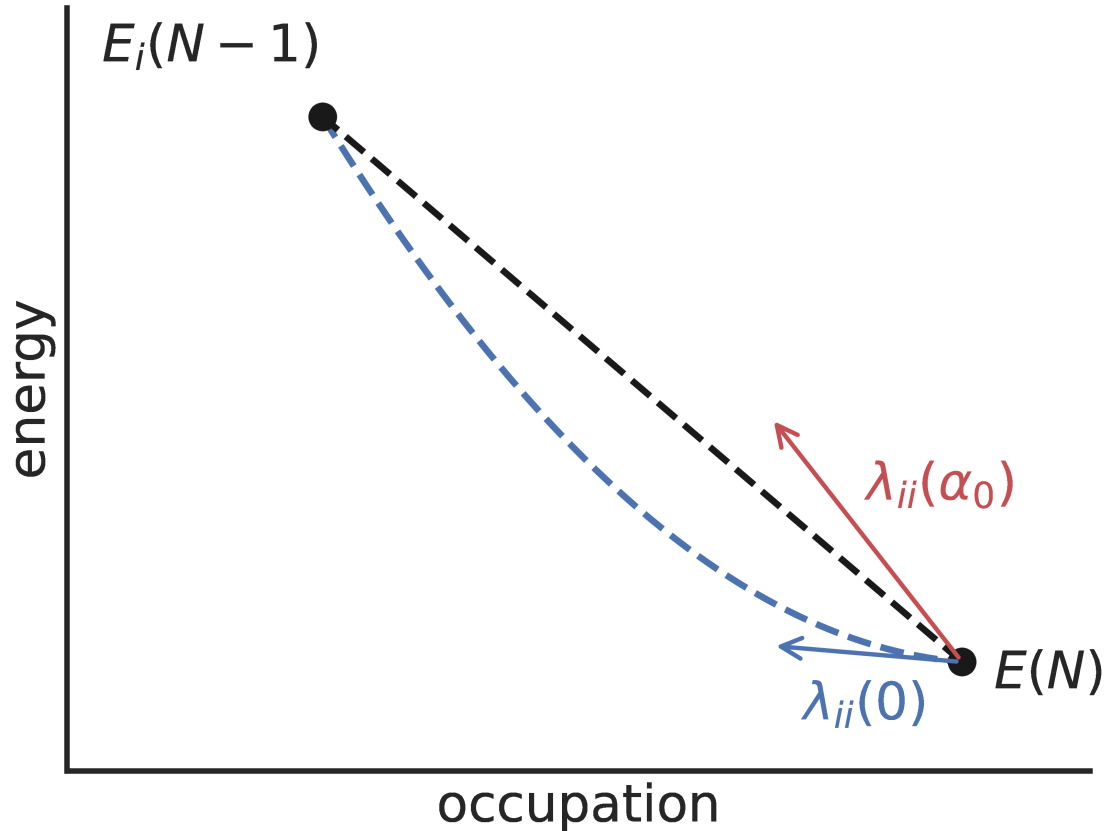


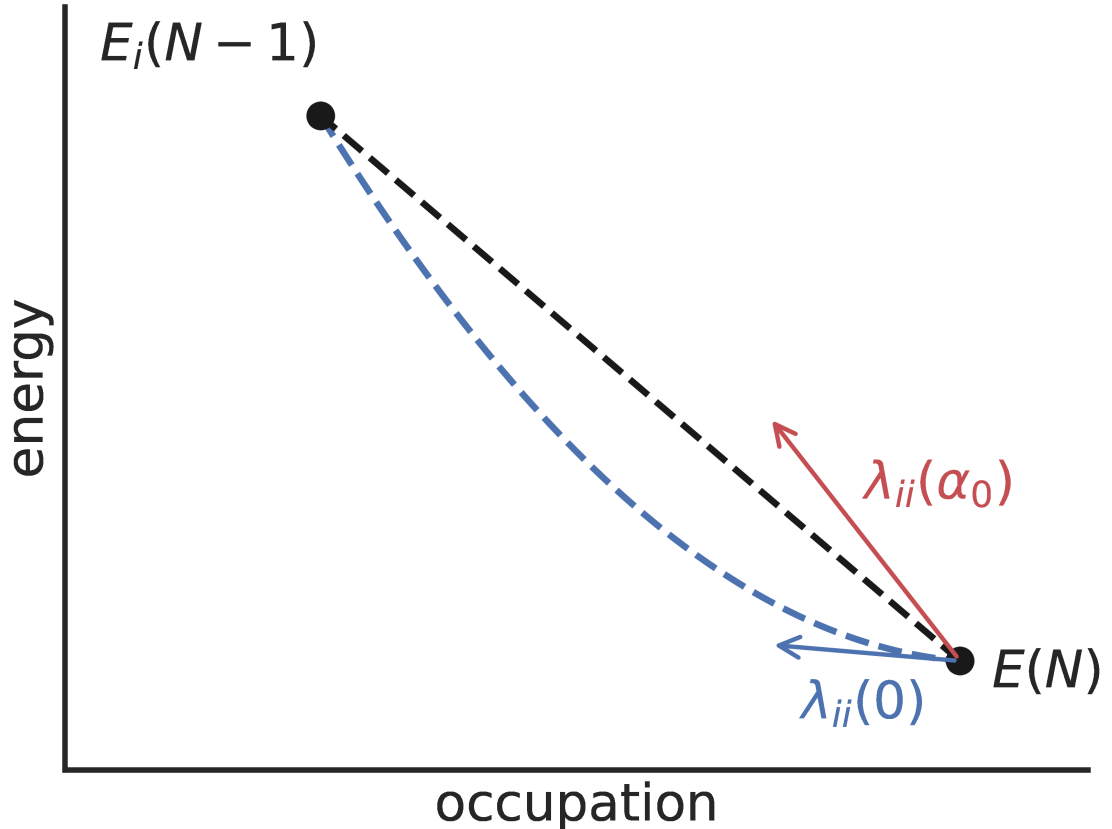








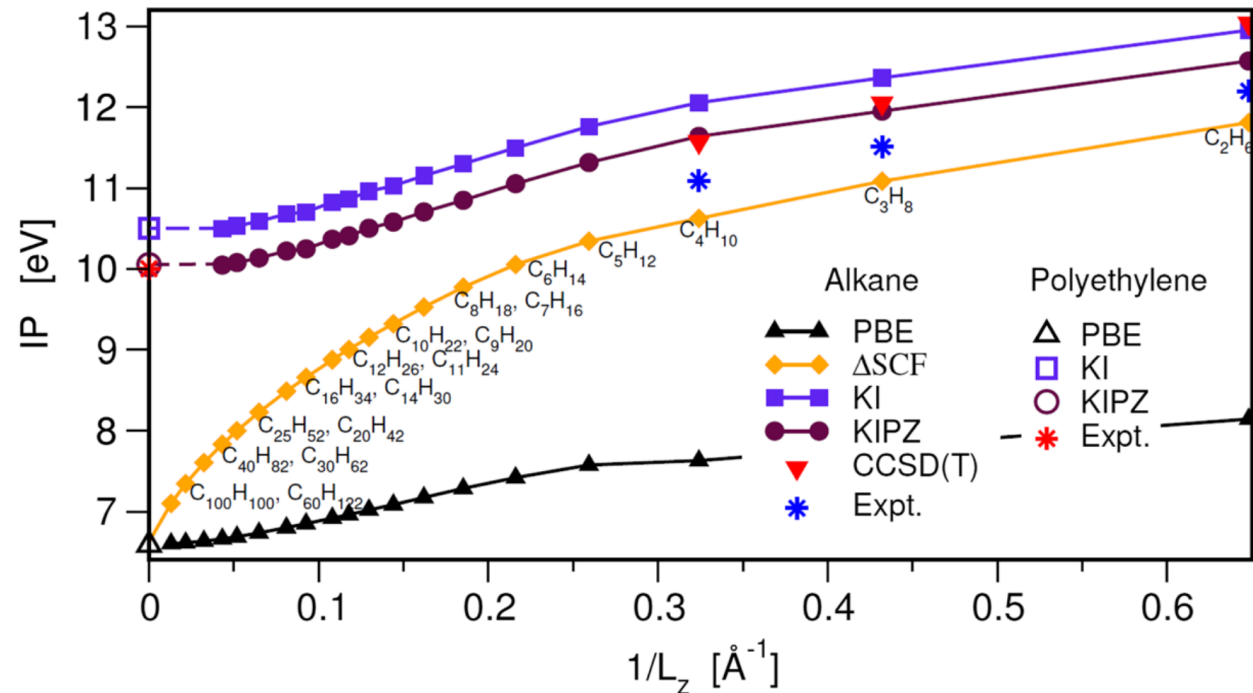




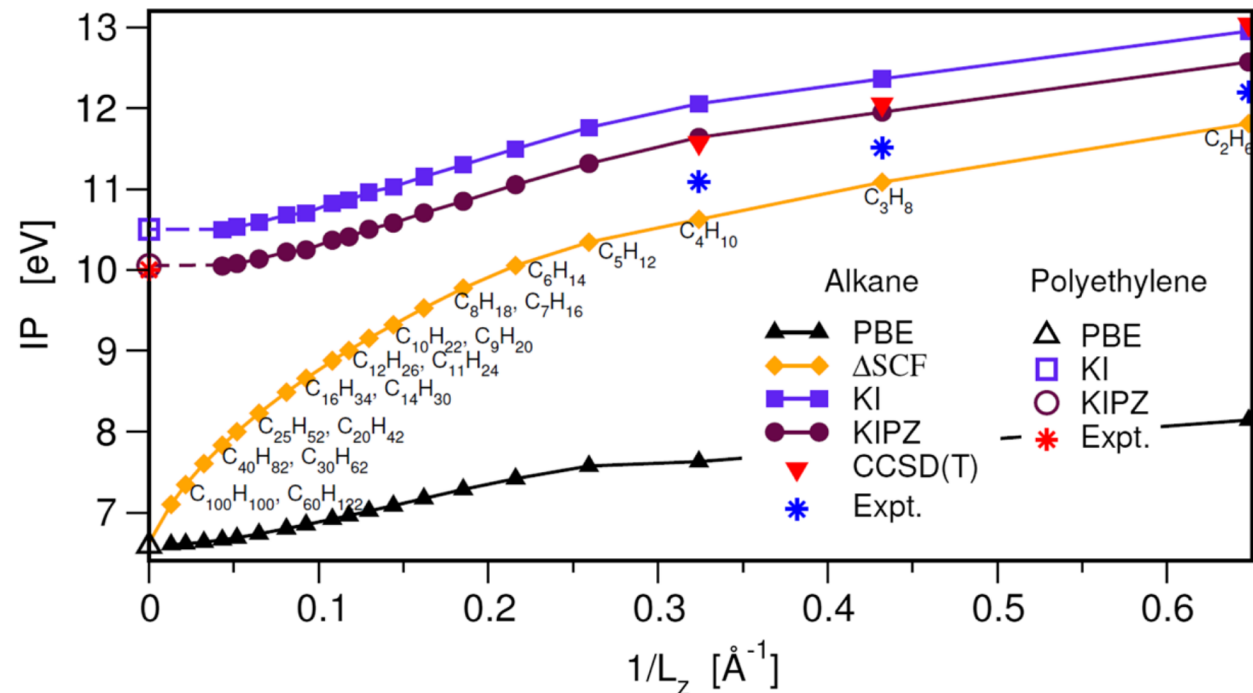
$$\alpha_i = \alpha_i^0 \frac{\Delta E_i - \lambda_{ii}(0)}{\lambda_{ii}(\alpha^0) - \lambda_{ii}(0)}$$

$$\lambda_{ii}(\alpha) = \langle \varphi_i | \hat{h}^{\text{DFT}} + \alpha \hat{v}_i^{\text{KI}} | \varphi_i \rangle$$

# Issues with extended systems



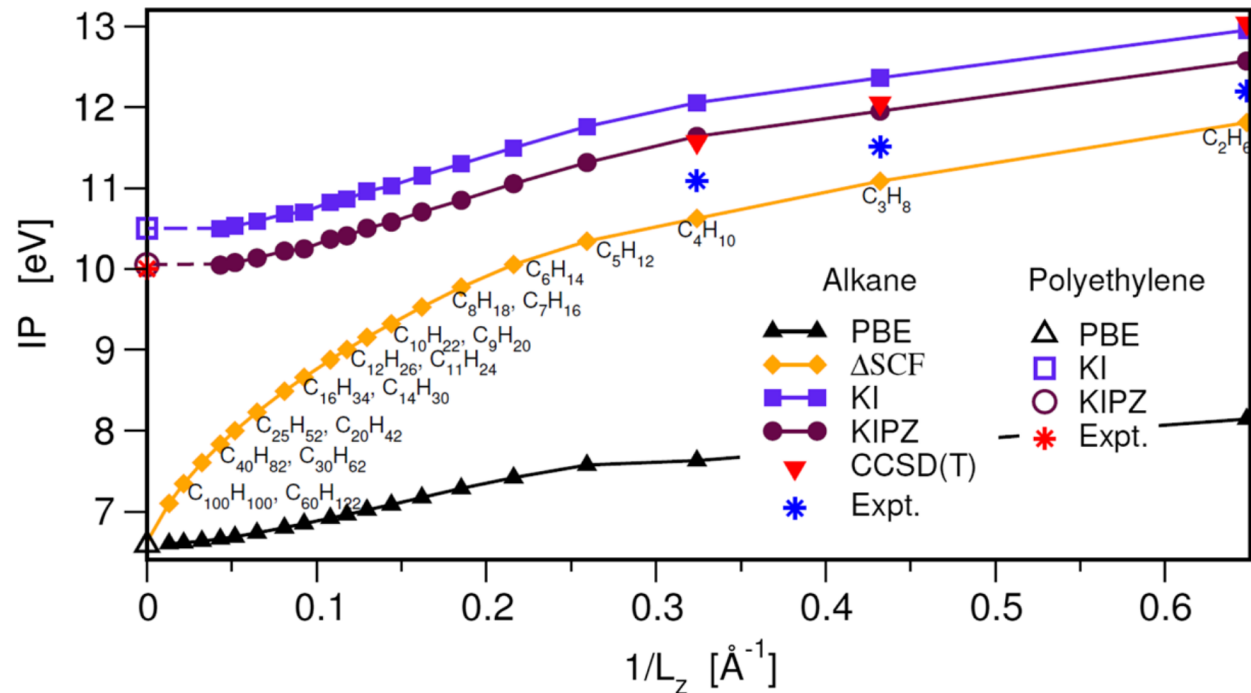
# Issues with extended systems



Two options: 1. use a more advanced functional

<sup>1</sup>N. L. Nguyen *et al.* Phys. Rev. X 8, 21051 (2018)

# Issues with extended systems

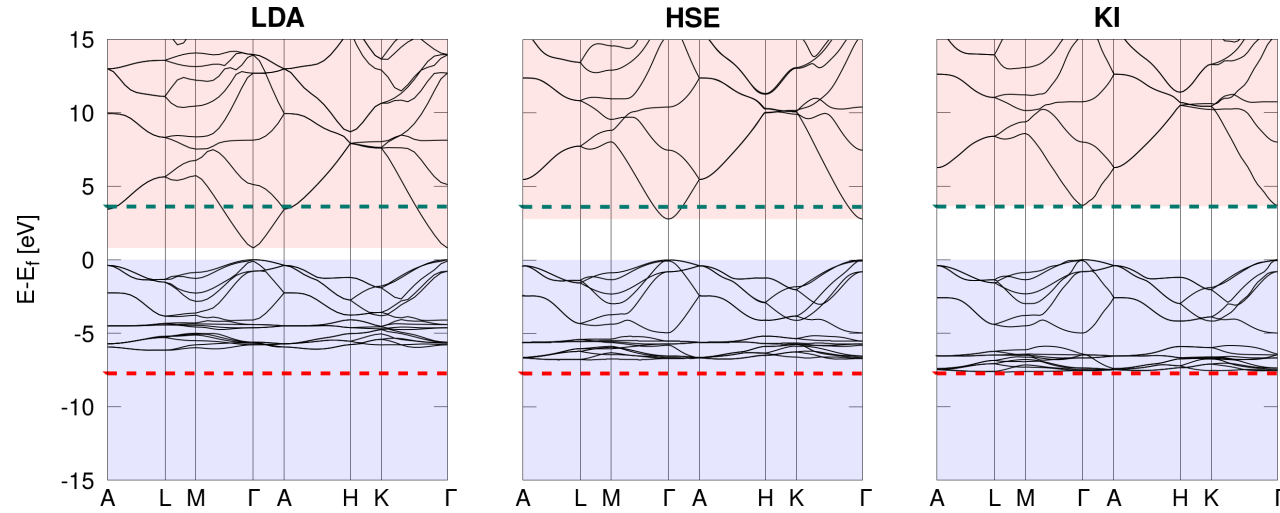


Two options: 1. use a more advanced functional, or 2. stay in the “safe” region

<sup>1</sup>N. L. Nguyen *et al.* Phys. Rev. X 8, 21051 (2018)

# Issues with extended systems

ZnO<sup>1</sup>

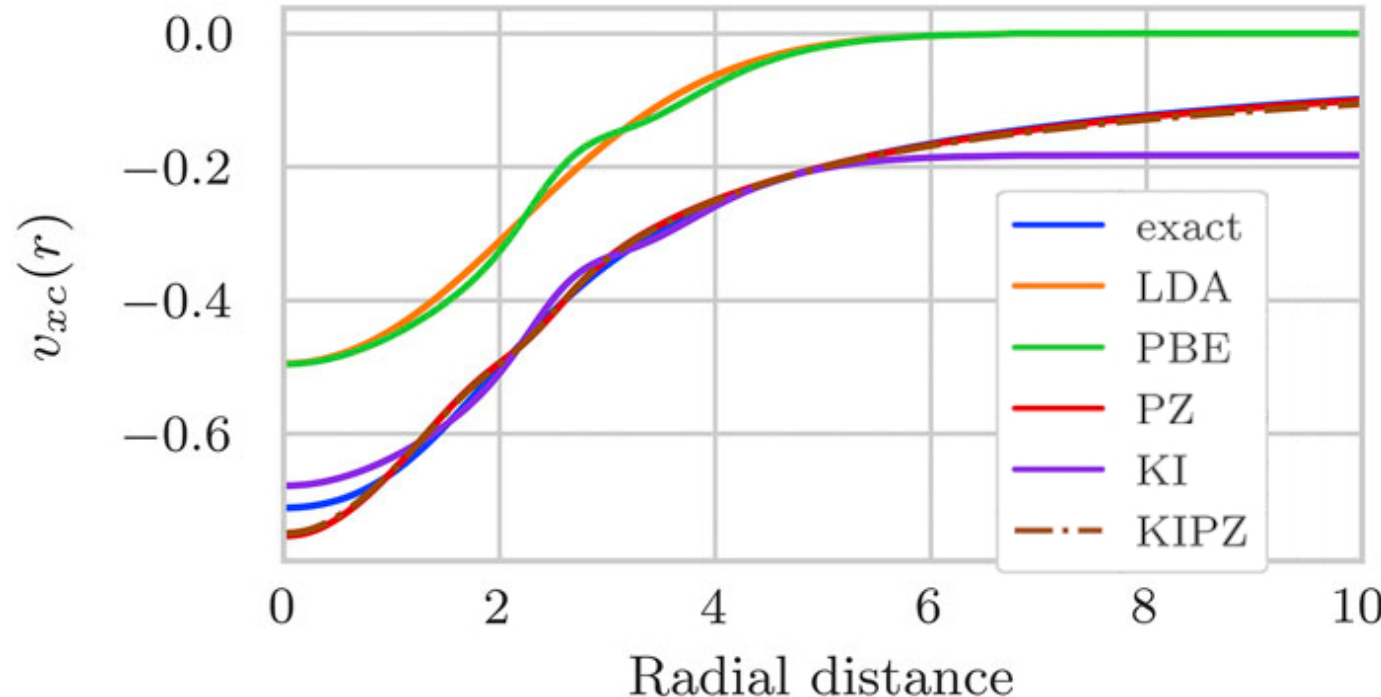


	LDA	HSE	$GW_0$	$scG\tilde{W}$	KI	exp
$E_{gap}$	0.79	2.79	3.0	3.2	<b>3.68</b>	3.60
$\langle \varepsilon_d \rangle$	-5.1	-6.1	-6.4	-6.7	<b>-6.93</b>	-7.5 to -8.81
$\Delta$	4.15				<b>4.99</b>	5.3

<sup>1</sup>N. Colonna et al. *J. Chem. Theory Comput.* 18, 5435 (2022)

# Model systems

## Hooke's atom<sup>1</sup>



<sup>1</sup>Y. Schubert *et al.* *J. Chem. Phys.* 158, 144113 (2023)

# Non-collinear spin

# Non-collinear spin

$$\rho_i(\mathbf{r})$$

<sup>1</sup>A. Marrazzo *et al.* *Phys. Rev. Res.* 6, 33085 (2024)

# Non-collinear spin

$$\rho_i(\mathbf{r}) \rightarrow \rho_i(\mathbf{r}) = (\rho_i(\mathbf{r}), m_i^x(\mathbf{r}), m_i^y(\mathbf{r}), m_i^z(\mathbf{r}))$$

<sup>1</sup>A. Marrazzo *et al.* *Phys. Rev. Res.* 6, 33085 (2024)

# Non-collinear spin

$$\rho_i(\mathbf{r}) \rightarrow \rho_i(\mathbf{r}) = (\rho_i(\mathbf{r}), m_i^x(\mathbf{r}), m_i^y(\mathbf{r}), m_i^z(\mathbf{r}))$$

e.g. for the corrective potential

$$v_i^{\text{qKI}} = -\frac{1}{2} \int d\mathbf{r} d\mathbf{r}' \rho_i(\mathbf{r}) f_{\text{Hxc}}(\mathbf{r}, \mathbf{r}') \rho_i(\mathbf{r}') + (1 - f_i) \int d\mathbf{r}' f_{\text{Hxc}}(\mathbf{r}, \mathbf{r}') \rho_i(\mathbf{r}')$$

<sup>1</sup>A. Marrazzo *et al.* *Phys. Rev. Res.* 6, 33085 (2024)

# Non-collinear spin

$$\rho_i(\mathbf{r}) \rightarrow \boldsymbol{\rho}_i(\mathbf{r}) = (\rho_i(\mathbf{r}), m_i^x(\mathbf{r}), m_i^y(\mathbf{r}), m_i^z(\mathbf{r}))$$

e.g. for the corrective potential

$$v_i^{\text{qKI}} = -\frac{1}{2} \int d\mathbf{r} d\mathbf{r}' \rho_i(\mathbf{r}) f_{\text{Hxc}}(\mathbf{r}, \mathbf{r}') \rho_i(\mathbf{r}') + (1 - f_i) \int d\mathbf{r}' f_{\text{Hxc}}(\mathbf{r}, \mathbf{r}') \rho_i(\mathbf{r}')$$

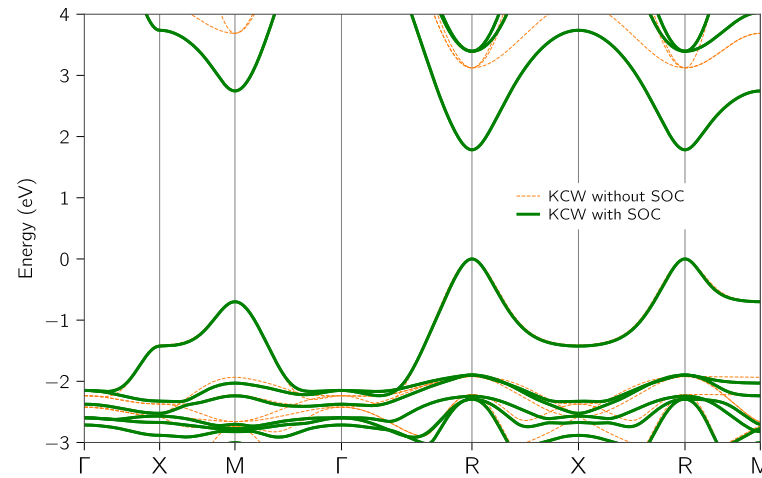
↓

$$v_i^{\text{qKI}} = -\frac{1}{2} \int d\mathbf{r} d\mathbf{r}' \boldsymbol{\rho}_i(\mathbf{r}) \mathbb{F}_{\text{Hxc}}(\mathbf{r}, \mathbf{r}') \boldsymbol{\rho}_i(\mathbf{r}') \sigma_0 + (1 - f_i) \sum_{\alpha} \int d\mathbf{r}' [\mathbb{F}_{\text{Hxc}}(\mathbf{r}, \mathbf{r}') \boldsymbol{\rho}_i(\mathbf{r}')]_{\alpha} \sigma_{\alpha}$$

<sup>1</sup>A. Marrazzo *et al.* *Phys. Rev. Res.* 6, 33085 (2024)

# Non-collinear spin

CsPbBr<sub>3</sub>



	LDA	HSE	$G_0W_0$	scG $\tilde{W}$	KI	exp
<b>with SOC</b>	0.18	0.78	0.94	1.53	<b>1.78</b>	1.85
without SOC	1.40	2.09	2.56	3.15	3.12	

<sup>1</sup>A. Marrazzo *et al.* *Phys. Rev. Res.* 6, 33085 (2024)

# Caveats

# Limitations

- only valid for systems with  $E_{\text{gap}} > 0$

# Limitations

- only valid for systems with  $E_{\text{gap}} > 0$
- empty state localisation in the bulk limit

# Limitations

- only valid for systems with  $E_{\text{gap}} > 0$
- empty state localisation in the bulk limit
- can break crystal point group symmetry

# Resonance with other efforts

- Wannier transition state method of Anisimov and Kozhevnikov<sup>1</sup>
- Optimally-tuned range-separated hybrid functionals of Kronik, Pasquarello, and others<sup>2</sup>
- Ensemble DFT of Kraisler and Kronik<sup>3</sup>
- Koopmans-Wannier method of Wang and co-workers<sup>4</sup>
- Dielectric-dependent hybrid functionals of Galli and co-workers<sup>5</sup>
- Scaling corrections of Yang and co-workers<sup>6</sup>

<sup>1</sup>V. I. Anisimov *et al.* *Phys. Rev. B* 72, 75125 (2005)

<sup>2</sup>L. Kronik *et al.* *J. Chem. Theory Comput.* 8, 1515–1531 (2012), D. Wing *et al.* *Proc. Natl. Acad. Sci.* 118, e2104556118 (2021)

<sup>3</sup>E. Kraisler *et al.* *Phys. Rev. Lett.* 110, 126403 (2013)

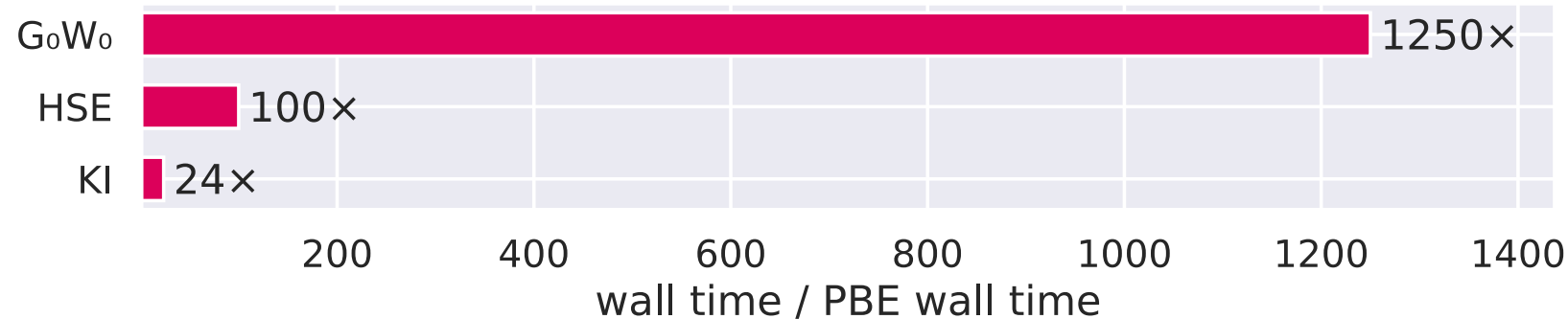
<sup>4</sup>J. Ma *et al.* *Sci. Rep.* 6, 24924 (2016)

<sup>5</sup>J. H. Skone *et al.* *Phys. Rev. B* 93, 235106 (2016)

<sup>6</sup>C. Li *et al.* *Natl. Sci. Rev.* 5, 203–215 (2018)

# Computational cost and scaling

# Computational cost and scaling



# Computational cost and scaling

The vast majority of the computational cost: determining screening parameters

$$\alpha_i = \frac{\langle n_i | \varepsilon^{-1} f_{\text{Hxc}} | n_i \rangle}{\langle n_i | f_{\text{Hxc}} | n_i \rangle}$$

<sup>1</sup>N. L. Nguyen *et al.* *Phys. Rev. X* 8, 21051 (2018), R. De Gennaro *et al.* *Phys. Rev. B* 106, 35106 (2022)

<sup>2</sup>N. Colonna *et al.* *J. Chem. Theory Comput.* 18, 5435 (2022), N. Colonna *et al.* *J. Chem. Theory Comput.* 14, 2549 (2018)

# Computational cost and scaling

The vast majority of the computational cost: determining screening parameters

$$\alpha_i = \frac{\langle n_i | \varepsilon^{-1} f_{\text{Hxc}} | n_i \rangle}{\langle n_i | f_{\text{Hxc}} | n_i \rangle}$$

- a local measure of screening of electronic interactions

<sup>1</sup>N. L. Nguyen *et al.* *Phys. Rev. X* 8, 21051 (2018), R. De Gennaro *et al.* *Phys. Rev. B* 106, 35106 (2022)

<sup>2</sup>N. Colonna *et al.* *J. Chem. Theory Comput.* 18, 5435 (2022), N. Colonna *et al.* *J. Chem. Theory Comput.* 14, 2549 (2018)

# Computational cost and scaling

The vast majority of the computational cost: determining screening parameters

$$\alpha_i = \frac{\langle n_i | \varepsilon^{-1} f_{\text{Hxc}} | n_i \rangle}{\langle n_i | f_{\text{Hxc}} | n_i \rangle}$$

- a local measure of screening of electronic interactions
- one screening parameter per orbital
- must be computed *ab initio* via...

<sup>1</sup>N. L. Nguyen *et al.* *Phys. Rev. X* 8, 21051 (2018), R. De Gennaro *et al.* *Phys. Rev. B* 106, 35106 (2022)

<sup>2</sup>N. Colonna *et al.* *J. Chem. Theory Comput.* 18, 5435 (2022), N. Colonna *et al.* *J. Chem. Theory Comput.* 14, 2549 (2018)

# Computational cost and scaling

The vast majority of the computational cost: determining screening parameters

$$\alpha_i = \frac{\langle n_i | \varepsilon^{-1} f_{\text{Hxc}} | n_i \rangle}{\langle n_i | f_{\text{Hxc}} | n_i \rangle}$$

- a local measure of screening of electronic interactions
- one screening parameter per orbital
- must be computed *ab initio* via...
  - ΔSCF<sup>1</sup>: embarrassingly parallel steps which each cost  $\mathcal{O}(N_{\text{SC}}^3) \sim \mathcal{O}(N_{\mathbf{k}}^3 N^3)$

<sup>1</sup>N. L. Nguyen *et al.* *Phys. Rev. X* 8, 21051 (2018), R. De Gennaro *et al.* *Phys. Rev. B* 106, 35106 (2022)

<sup>2</sup>N. Colonna *et al.* *J. Chem. Theory Comput.* 18, 5435 (2022), N. Colonna *et al.* *J. Chem. Theory Comput.* 14, 2549 (2018)

# Computational cost and scaling

The vast majority of the computational cost: determining screening parameters

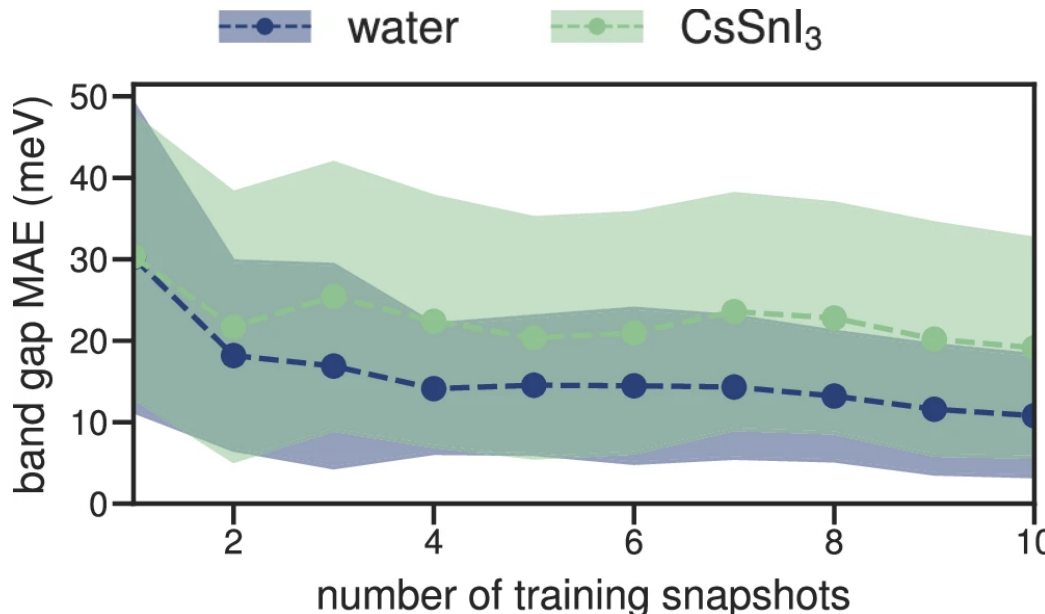
$$\alpha_i = \frac{\langle n_i | \varepsilon^{-1} f_{\text{Hxc}} | n_i \rangle}{\langle n_i | f_{\text{Hxc}} | n_i \rangle}$$

- a local measure of screening of electronic interactions
- one screening parameter per orbital
- must be computed *ab initio* via...
  - ΔSCF<sup>1</sup>: embarrassingly parallel steps which each cost  $\mathcal{O}(N_{\text{SC}}^3) \sim \mathcal{O}(N_{\mathbf{k}}^3 N^3)$
  - DFPT<sup>2</sup>:  $\mathcal{O}(N_{\mathbf{k}}^2 N^3)$

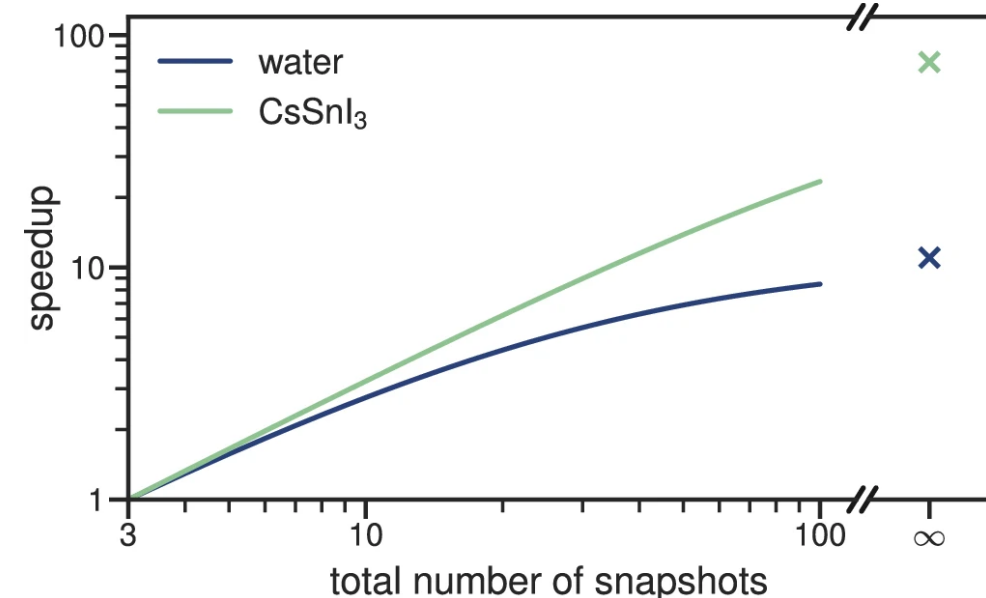
<sup>1</sup>N. L. Nguyen *et al.* *Phys. Rev. X* 8, 21051 (2018), R. De Gennaro *et al.* *Phys. Rev. B* 106, 35106 (2022)

<sup>2</sup>N. Colonna *et al.* *J. Chem. Theory Comput.* 18, 5435 (2022), N. Colonna *et al.* *J. Chem. Theory Comput.* 14, 2549 (2018)

# Machine-learned electronic screening



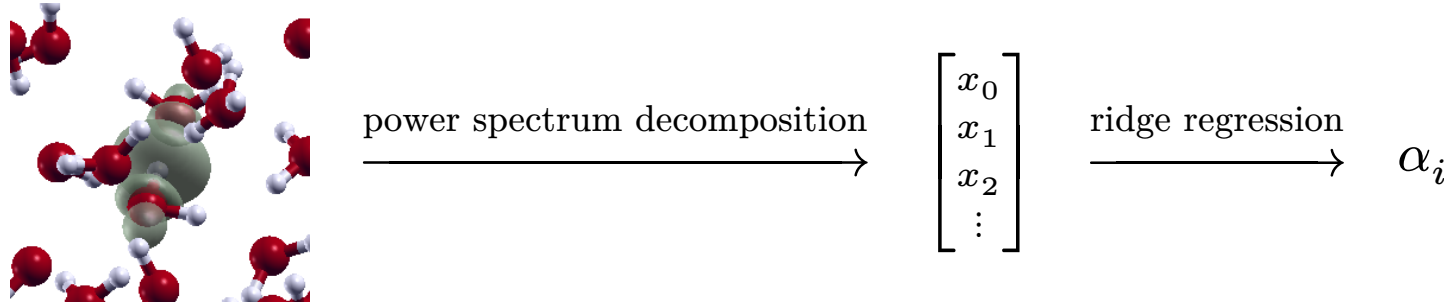
**accurate** to within  $\mathcal{O}(10 \text{ meV})$  cf. typical  
band gap accuracy of  $\mathcal{O}(100 \text{ meV})$



**speedup** of  $\mathcal{O}(10)$  to  $\mathcal{O}(100)$

<sup>1</sup>Y. Schubert *et al.* *npj Comput Mater* 10, 1–12 (2024)

# Machine-learned electronic screening

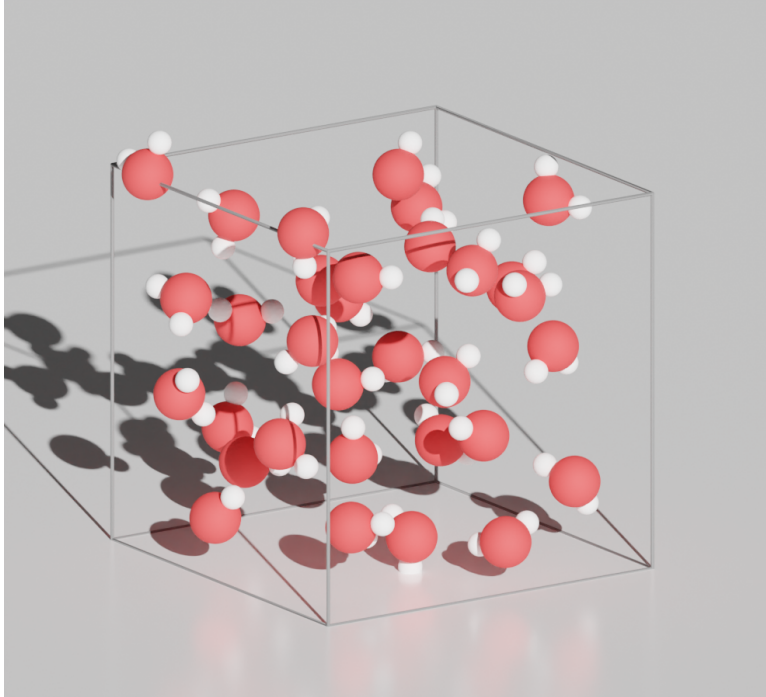


$$c_{nlm,k}^i = \int d\mathbf{r} g_{nl}(r) Y_{lm}(\theta, \varphi) n^i(\mathbf{r} - \mathbf{R}^i)$$

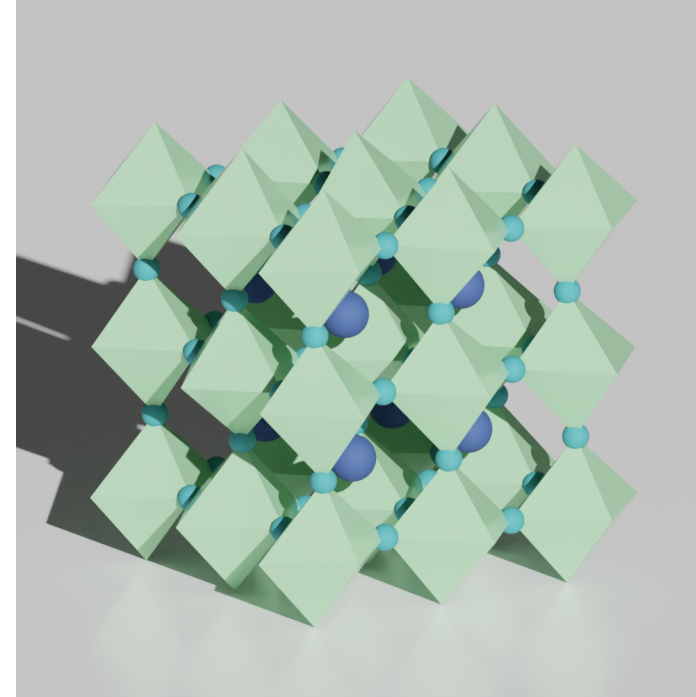
$$p_{n_1 n_2 l, k_1 k_2}^i = \pi \sqrt{\frac{8}{2l+1}} \sum_m c_{n_1 lm, k_1}^{i*} c_{n_2 lm, k_2}^i$$

<sup>1</sup>Y. Schubert *et al.* *npj Comput Mater* 10, 1–12 (2024)

# Machine-learned electronic screening



water

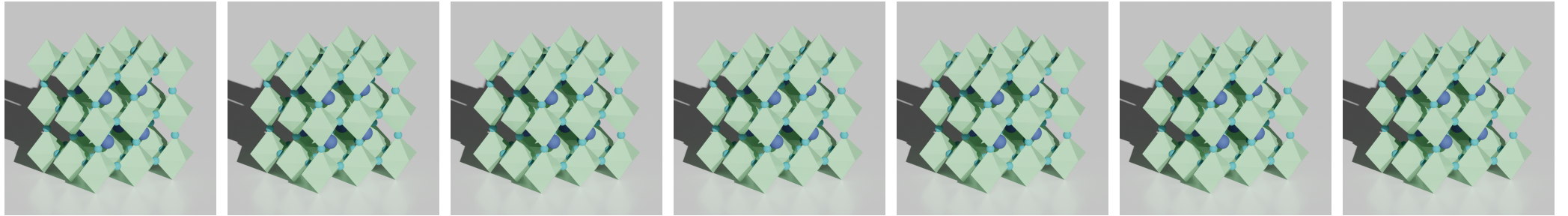


$\text{CsSnI}_3$

<sup>1</sup>Y. Schubert *et al.* *npj Comput Mater* 10, 1–12 (2024)

# Machine-learned electronic screening

The use-case

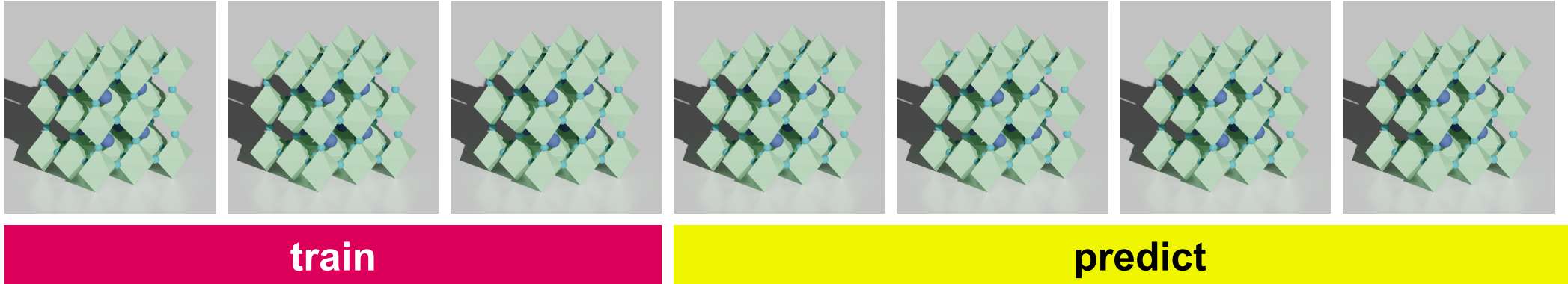


train

predict

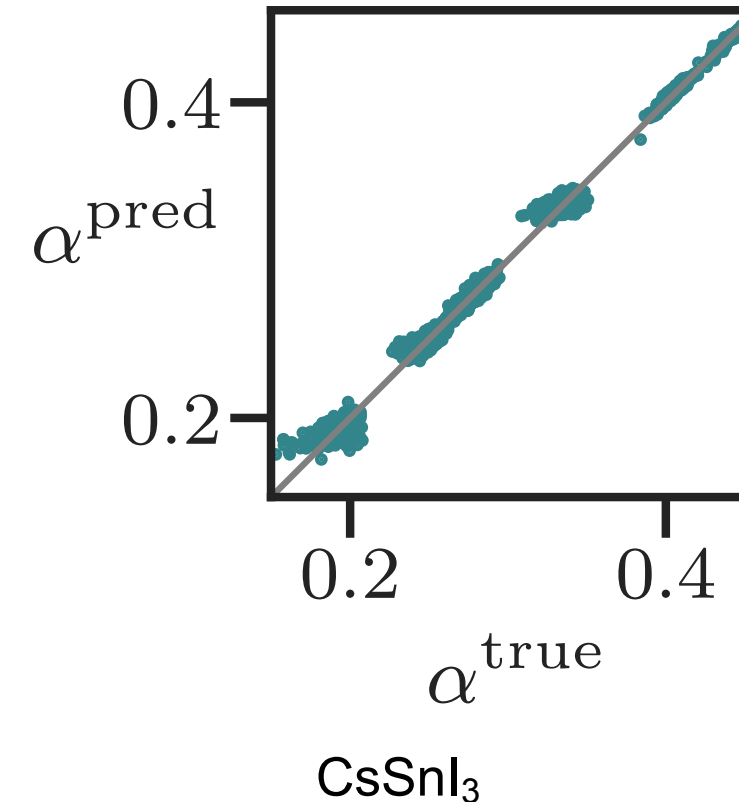
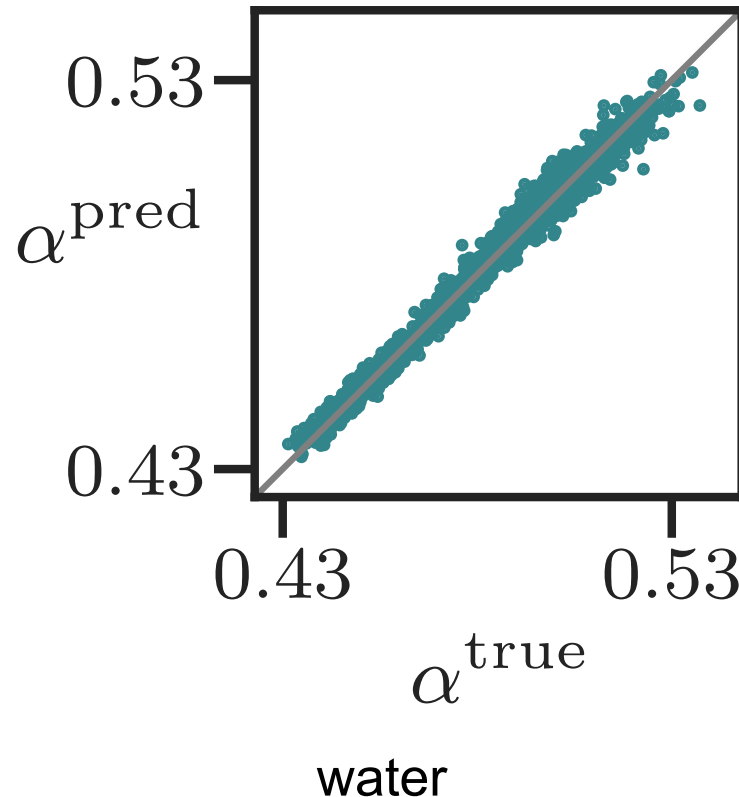
# Machine-learned electronic screening

The use-case



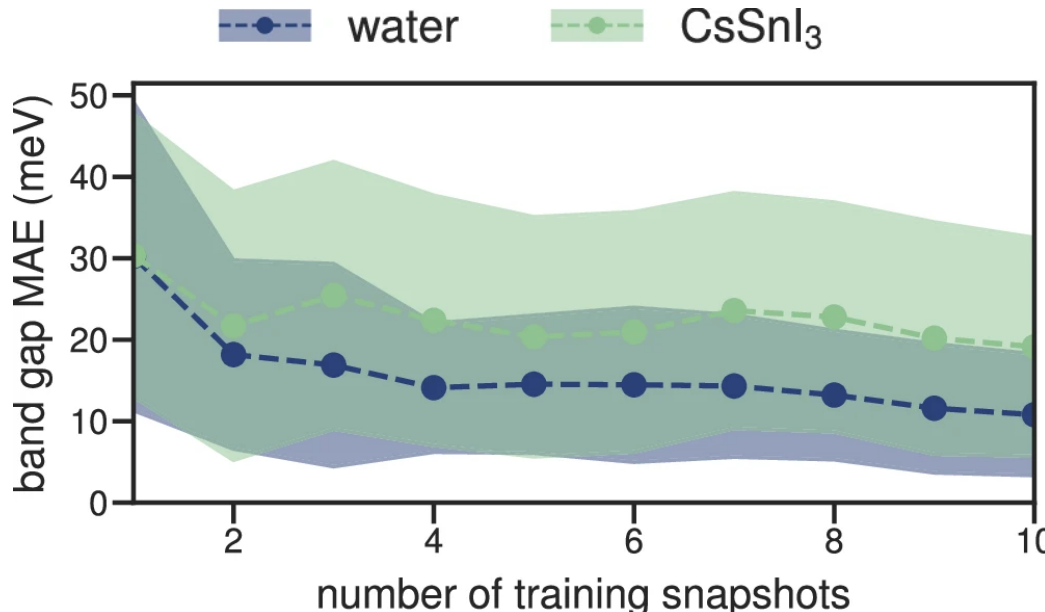
N.B. not a general model

# Machine-learned electronic screening

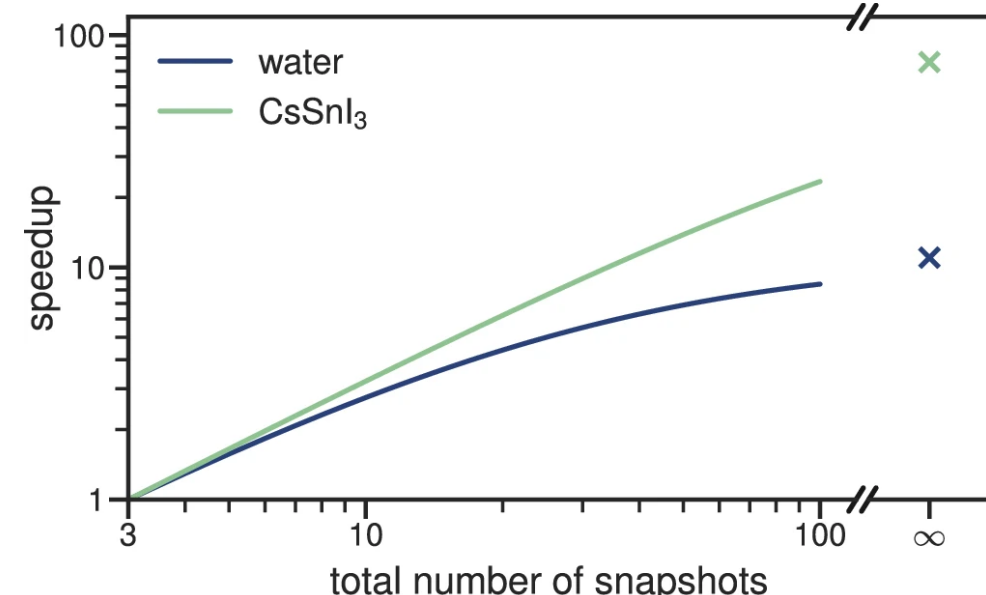


<sup>1</sup>Y. Schubert *et al.* *npj Comput Mater* 10, 1–12 (2024)

# Machine-learned electronic screening



**accurate** to within  $\mathcal{O}(10 \text{ meV})$  cf. typical  
band gap accuracy of  $\mathcal{O}(100 \text{ meV})$



**speedup** of  $\mathcal{O}(10)$  to  $\mathcal{O}(100)$

<sup>1</sup>Y. Schubert *et al.* *npj Comput Mater* 10, 1–12 (2024)

# Taking advantage of symmetries

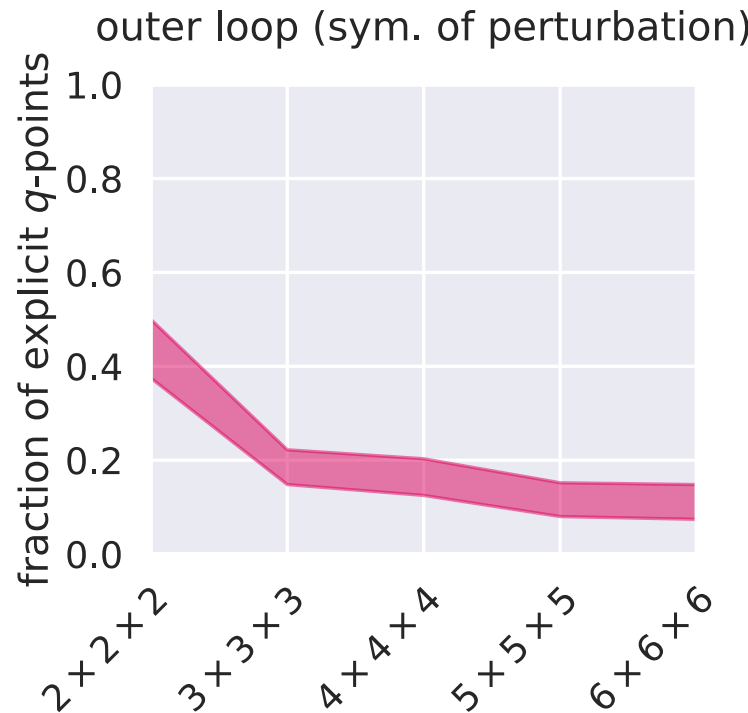
To compute screening parameters via DFPT...

```

1:function CalculateAlpha( $n$ )
2:   for  $q \in \text{BZ}$  do
3:     for  $k \in \text{BZ}$  do
4:       ▷ Linear system  $Ax = b$  to obtain  $\Delta\psi_{\mathbf{k}+\mathbf{q},v}(\mathbf{r})$ 
5:     end
6:      $\Delta\rho_q^{0n} \leftarrow \sum_{\mathbf{k}\mathbf{v}} \psi_{\mathbf{k}\mathbf{v}}^*(\mathbf{r}) \Delta\psi_{\mathbf{k}+\mathbf{q},v}(\mathbf{r}) + c.c.$ 
7:      $\Pi_{0n,\mathbf{q}}^{(r)} \leftarrow \langle \Delta\rho_q^{0n} | f_{\text{Hxc}} | \rho_{\mathbf{q}}^{0n} \rangle$ 
8:      $\Pi_{0n,\mathbf{q}}^{(u)} \leftarrow \langle \rho_{\mathbf{q}}^{0n} | f_{\text{Hxc}} | \rho_{\mathbf{q}}^{0n} \rangle$ 
9:   end
10:  return  $1 + \sum_{\mathbf{q}} \Pi_{0n,\mathbf{q}}^{(r)} / \sum_{\mathbf{q}} \Pi_{0n,\mathbf{q}}^{(u)}$ 
11end

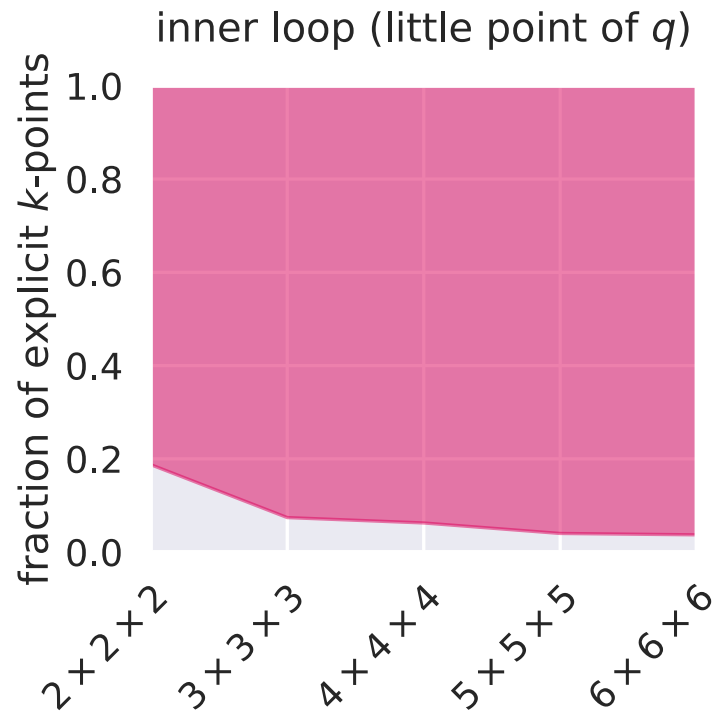
```

# Taking advantage of symmetries



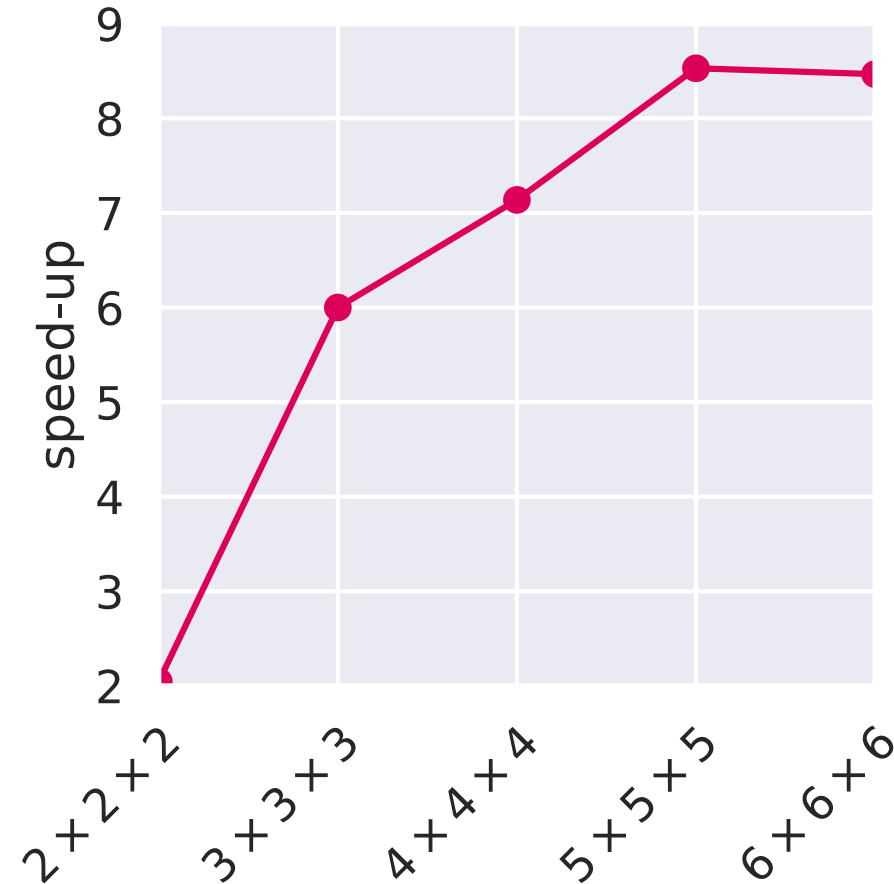
$q \in \text{BZ} \rightarrow q \in \text{IBZ}(n)$  (the symmetry of the perturbation; lower than that of the primitive cell)

# Taking advantage of symmetries



$k \in \text{BZ} \rightarrow k \in \text{IBZ}(q)$  (can only use symmetries that leave  $q$  invariant)

# Taking advantage of symmetries



# Automated Wannierisation

```
{  
  "workflow": {  
    "functional": "ki",  
    "method": "dfpt",  
    "init_orbitals": "mlwfs",  
    "pseudo_library": "PseudoDojo/0.4/LDA/SR/standard/upf",  
    "block_wannierization_threshold": 5.0,  
    "orbital_groups_spread_tol": 0.05  
  },  
  "atoms": {  
    "cell_parameters": {  
      "periodic": true,  
      "ibrav": 2,  
      "celldms": {"1": 10.68374}  
    },  
    "atomic_positions": {  
      "units": "crystal",  
      "positions": [[{"Ga": 0.00, 0.00, 0.00},  
                    {"As": 0.25, 0.25, 0.25}]]  
    }  
  },  
},
```

```

    "kpoints": {
        "grid": [6, 6, 6]
    },
    "calculator_parameters": {
        "ecutwfc": 60.0,
        "w90": {
            "projections": [
                [{"site": "As", "ang_mtm": "d"}, {"site": "Ga", "ang_mtm": "d"}, {"site": "As", "ang_mtm": "sp3"}], [{"site": "Ga", "ang_mtm": "sp3"}]
            ],
            "dis_froz_max": 14.6,
            "dis_win_max": 18.6
        },
        "ui": {
            "smooth_int_factor": 2
        }
    }
}

```

# Automated Wannierisation

Koopmans functionals rely heavily on Wannier functions...

- to initialise the minimising orbitals, or
- in place of the minimising orbitals entirely

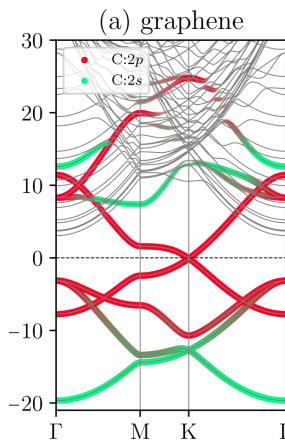
<sup>1</sup>J. Qiao *et al.* *npj Comput Mater* 9, 208 (2023)

<sup>2</sup>J. Qiao *et al.* *npj Comput Mater* 9, 206 (2023)

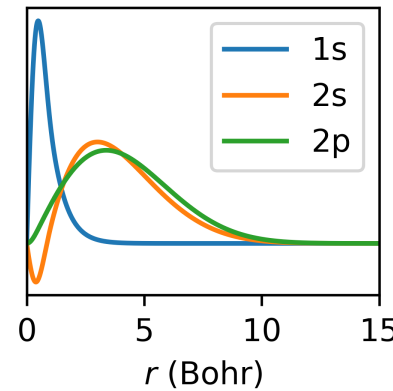
# Automated Wannierisation

Koopmans functionals rely heavily on Wannier functions...

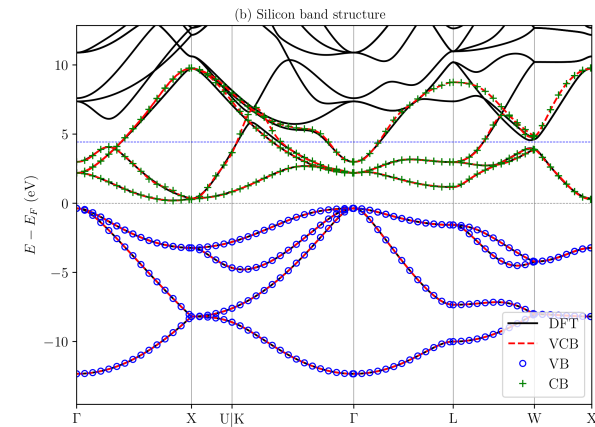
- to initialise the minimising orbitals, or
- in place of the minimising orbitals entirely



projectability-based  
disentanglement<sup>1</sup>



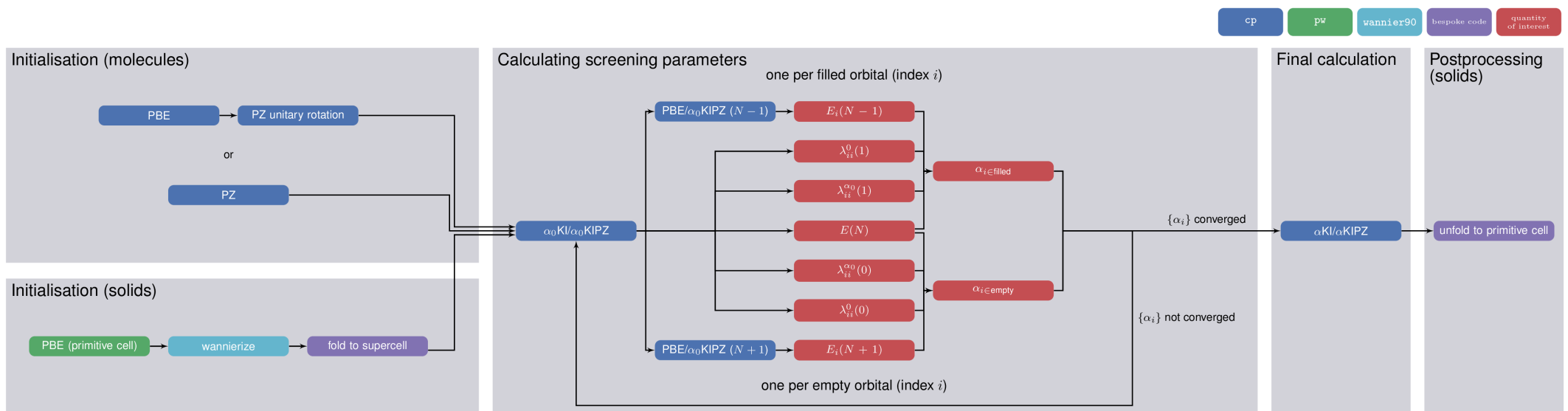
use PAOs found in  
pseudopotentials



parallel transport to separate  
manifolds<sup>2</sup>

<sup>1</sup>J. Qiao *et al.* *npj Comput Mater* 9, 208 (2023)

<sup>2</sup>J. Qiao *et al.* *npj Comput Mater* 9, 206 (2023)



# koopmans 🤝 AiiDA

<sup>1</sup>S. P. Huber *et al.* *Sci Data* 7, 300 (2020)



```
$ koopmans run tio2.json
```

<sup>1</sup>S. P. Huber *et al.* *Sci Data* 7, 300 (2020)



```
$ koopmans run tio2.json → $ koopmans run --engine=aiida tio2.json
```

remote compute, parallel step execution, provenance-tracking, (requires configuration,  
WIP...)

<sup>1</sup>S. P. Huber *et al.* *Sci Data* 7, 300 (2020)

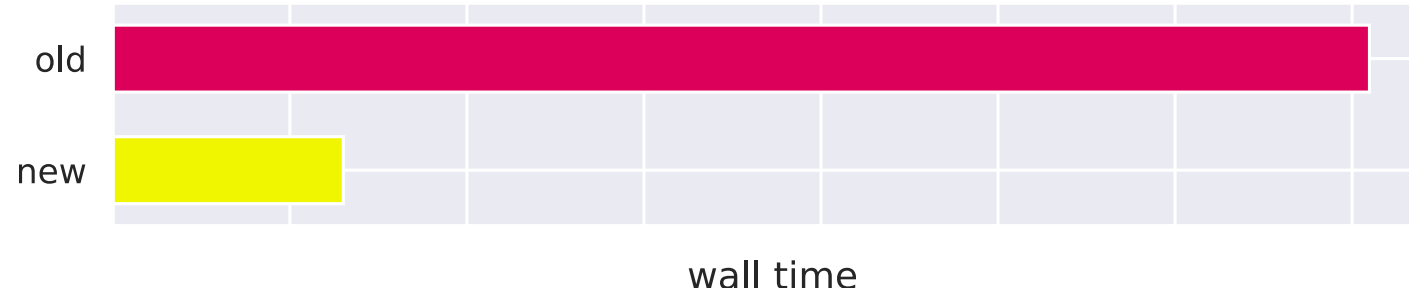
# koopmans

# AiiDA

```
$ koopmans run tio2.json → $ koopmans run --engine=aiida tio2.json
```

remote compute, parallel step execution, provenance-tracking, (requires configuration,  
WIP...)



<sup>1</sup>S. P. Huber *et al.* *Sci Data* 7, 300 (2020)

# Connections with approx. self-energies

Orbital-density functional theory:

$$(h + \alpha_i v_i^{KI}) |\psi_i\rangle = \lambda_i |\psi_i\rangle$$

$v_i^{KI}(\mathbf{r})$  is real, local, and state-dependent

<sup>1</sup>N. Colonna *et al.* *J. Chem. Theory Comput.* 15, 1905 (2019), A. Ferretti *et al.* *Phys. Rev. B* 89, 195134 (2014)

# Connections with approx. self-energies

Orbital-density functional theory:

$$(h + \alpha_i v_i^{KI}) |\psi_i\rangle = \lambda_i |\psi_i\rangle$$

$v_i^{KI}(\mathbf{r})$  is real, local, and state-dependent

cf. Green's function theory:

$$(h + \Sigma_i) |\psi_i\rangle = z_i |\psi_i\rangle$$

$\Sigma_i(\mathbf{r}, \mathbf{r}')$  is complex, non-local, and state-dependent

<sup>1</sup>N. Colonna *et al.* *J. Chem. Theory Comput.* 15, 1905 (2019), A. Ferretti *et al.* *Phys. Rev. B* 89, 195134 (2014)

# Connections with approx. self-energies

Hartree-Fock self-energy in localized representation

$$\begin{aligned}\Sigma_x(\mathbf{r}, \mathbf{r}') &= -\sum_{k\sigma}^{\text{occ}} \psi_{k\sigma}(\mathbf{r}) f_H(\mathbf{r}, \mathbf{r}') \psi_{k\sigma}^*(\mathbf{r}') \\ &\implies \langle \varphi_{i\sigma} | \Sigma_x | \varphi_{j\sigma'} \rangle \approx -\langle \varphi_{i\sigma} | v_H[n_{i\sigma}] | \varphi_{i\sigma} \rangle \delta_{ij} \delta_{\sigma\sigma'}\end{aligned}$$

Unscreened KIPZ@ Hartree ( $v_{\text{xc}} \rightarrow 0$ ;  $f_{\text{Hxc}} \rightarrow f_H$ ;  $\varepsilon^{-1} \rightarrow 1$ )

$$\langle \varphi_{i\sigma} | v_{j\sigma', \text{xc}}^{\text{KIPZ}} | \varphi_{j\sigma'} \rangle \approx \left\{ \left( \frac{1}{2} - f_{i\sigma} \right) \langle n_{i\sigma} | f_H | n_{i\sigma} \rangle - E_H[n_{i\sigma}] \right\} \approx -\langle \varphi_{i\sigma} | v_H[n_{i\sigma}] | \varphi_{i\sigma} \rangle \delta_{ij} \delta_{\sigma\sigma'}$$

# Connections with approx. self-energies

Screened exchange plus Coulomb hole (COHSEX)

$$\Sigma_{\text{xc}}^{\text{SEX}}(s, s') = - \sum_{k\sigma}^{\text{occ}} \psi_{k\sigma}(\mathbf{r}) \psi_{k\sigma}^*(\mathbf{r}) W(\mathbf{r}, \mathbf{r}')$$

$$\Sigma_{\text{xc}}^{\text{COH}}(s, s') = \frac{1}{2} \delta(s, s') \{W(\mathbf{r}, \mathbf{r}') - f_H(\mathbf{r}, \mathbf{r}')\}$$

$$\Rightarrow \langle \varphi_{i\sigma} | \Sigma_{\text{xc}}^{\text{COHSEX}} | \varphi_{j\sigma'} \rangle \approx \left\{ \left( \frac{1}{2} - f_{i\sigma} \right) \langle n_{i\sigma} | W | n_{i\sigma} \rangle - E_H[n_{i\sigma}] \right\} \delta_{ij} \delta_{\sigma\sigma'}$$

KIPZ@ Hartree with RPA screening ( $v_{\text{xc}} \rightarrow 0$ ;  $f_{\text{Hxc}} \rightarrow f_H$ ;  $\varepsilon^{-1} \rightarrow \text{RPA}$ )

$$\langle \varphi_{i\sigma} | v_{j\sigma', \text{xc}}^{\text{KIPZ}} | \varphi_{j\sigma'} \rangle \approx \left\{ \left( \frac{1}{2} - f_{i\sigma} \right) \langle n_{i\sigma} | W | n_{i\sigma} \rangle - E_H[n_{i\sigma}] \right\} \delta_{ij} \delta_{\sigma\sigma'}$$

# Connections with approx. self-energies

Static  $GW\Gamma_{xc}$  — local (DFT-based) vertex corrections<sup>1</sup>

$$\Sigma_{\text{xc}(1,2)}^{GW\Gamma_{\text{xc}}} = iG(1,2)W_{t-e}(1,2)$$

$$W_{t-e} = (1 - f_{\text{Hxc}}\chi_0)^{-1}f_H$$

$$\Rightarrow \langle \varphi_{i\sigma} | \Sigma_{\text{xc}}^{GW\Gamma_{\text{xc}}} | \varphi_{j\sigma'} \rangle \approx \left\{ \left( \frac{1}{2} - f_{i\sigma} \right) \langle n_{i\sigma} | W_{t-e} | n_{i\sigma} \rangle - E_H[n_{i\sigma}] \right\} \delta_{ij} \delta_{\sigma\sigma'}$$

KIPZ@ DFT ( $v_{\text{xc}} \rightarrow \text{DFT}$ ;  $f_{\text{Hxc}} \rightarrow \text{DFT}$ ;  $\varepsilon^{-1} \rightarrow \text{DFT}$ )

$$\langle \varphi_{i\sigma} | v_{j\sigma',\text{xc}}^{\text{KIPZ}} | \varphi_{j\sigma'} \rangle \approx \left\{ \langle \varphi_{i\sigma} | v_{\sigma,\text{xc}}^{\text{DFT}} | \varphi_{i\sigma} \rangle + \left( \frac{1}{2} - f_{i\sigma} \right) \langle n_{i\sigma} | \varepsilon_{t-e}^{-1} f_{\text{Hxc}} | n_{i\sigma} \rangle - E_H[n_{i\sigma}] \right\} \delta_{ij} \delta_{\sigma\sigma'}$$

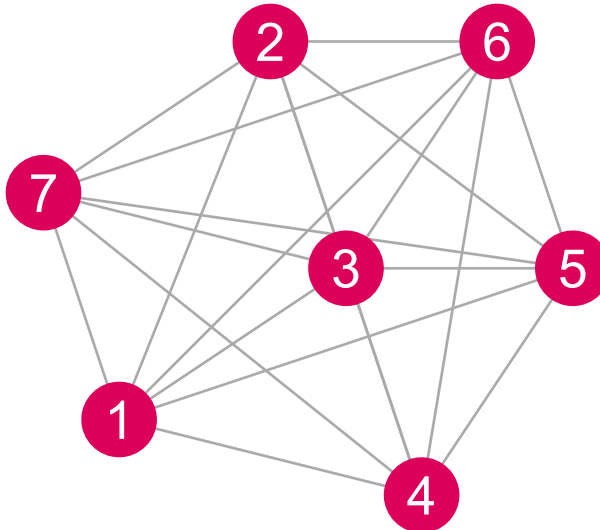
<sup>1</sup>M. S. Hybertsen *et al.* *Phys. Rev. B* 35, 5585–5601 (1987), R. Del Sole *et al.* *Phys. Rev. B* 49, 8024–8028 (1994)

# Open questions

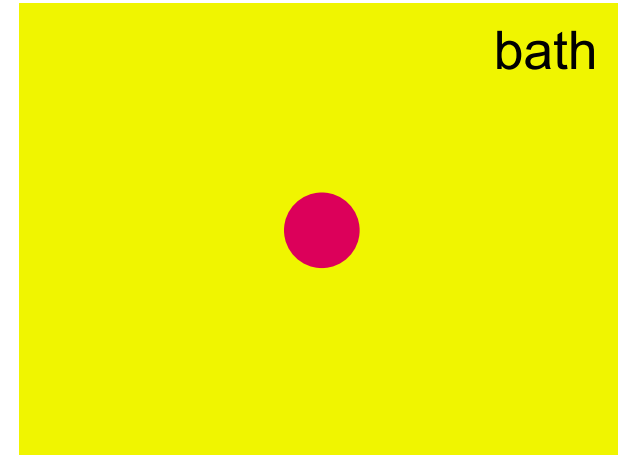
- why does correcting *local* charged excitations correct the description of delocalized excitations?
- is there a good metric for selecting variational orbitals (*i.e.* the subspace with respect to which we enforce piecewise linearity)?
- are off-diagonal corrections appropriate? What form should they take?
- how to extend to metallic systems?
- can we provide a formal basis for the Koopmans correction?
  - GKS
  - spectral functional theory<sup>1</sup>
  - ensemble DFT
  - RDMFT

<sup>1</sup>A. Ferretti *et al.* *Phys. Rev. B* 89, 195134 (2014)

# What is screening $U$ ?



all sites included in response matrix  
bare  $U$



only one site included in response matrix  
fully-screened  $U$

# What is screening $U$ ?

fully-screened	$\begin{pmatrix} \chi_{11}^{\uparrow\uparrow} & & & \\ & \chi_{11}^{\downarrow\downarrow} & & \\ & & \chi_{22}^{\uparrow\uparrow} & \\ & & & \chi_{22}^{\downarrow\downarrow} \\ & & & \ddots \end{pmatrix}$	$U^{I\sigma} = \frac{1}{(\chi_0)_{II}^{\sigma\sigma}} - \frac{1}{\chi_{II}^{\sigma\sigma}}$
not screened by opposite spin	$\begin{pmatrix} \chi_{11}^{\uparrow\uparrow} & \chi_{11}^{\uparrow\downarrow} & & & \\ & \chi_{11}^{\downarrow\uparrow} & \chi_{11}^{\downarrow\downarrow} & & \\ & & \chi_{22}^{\uparrow\uparrow} & \chi_{22}^{\uparrow\downarrow} & \\ & & \chi_{22}^{\downarrow\uparrow} & \chi_{22}^{\downarrow\downarrow} & \\ & & & \ddots & \end{pmatrix}$	$f_I^{\sigma\sigma'} = [(\chi_0)_{II}^{\sigma\sigma}]^{-1} - [\chi_{II}^{\sigma\sigma}]^{-1}$ $f_I^{\sigma\sigma'} \xrightarrow{???} U^I \text{ or } U^{I\sigma}$
also not screened by other Hubbard sites	$\begin{pmatrix} \chi_{11}^{\uparrow\uparrow} & \chi_{11}^{\uparrow\downarrow} & \chi_{12}^{\uparrow\uparrow} & \chi_{12}^{\uparrow\downarrow} & \dots \\ \chi_{11}^{\downarrow\uparrow} & \chi_{11}^{\downarrow\downarrow} & \chi_{12}^{\downarrow\uparrow} & \chi_{12}^{\downarrow\downarrow} & \dots \\ \chi_{21}^{\uparrow\uparrow} & \chi_{21}^{\uparrow\downarrow} & \chi_{22}^{\uparrow\uparrow} & \chi_{22}^{\uparrow\downarrow} & \dots \\ \chi_{21}^{\downarrow\uparrow} & \chi_{21}^{\downarrow\downarrow} & \chi_{22}^{\downarrow\uparrow} & \chi_{22}^{\downarrow\downarrow} & \dots \\ \vdots & \vdots & \vdots & \vdots & \ddots \end{pmatrix}$	$f_{IJ}^{\sigma\sigma'} = \dots$ $\text{(left as an exercise to the reader)}$

# 1. Conceptual consistency

spin-resolved linear response  $\leftrightarrow$  spin-resolved DFT+ $U$  functional

<sup>1</sup>A. C. Burgess *et al.* *Phys. Rev. B* 107, L121115 (2023)

spin-resolved linear response  $\leftrightarrow$  spin-resolved DFT+ $U$  functional

... we didn't explore DFT+ $U^\sigma$ ; instead see BLOR<sup>1</sup>)

<sup>1</sup>A. C. Burgess *et al.* *Phys. Rev. B* 107, L121115 (2023)

## 2. Unconstrained constrained linear response

# Unconstrained constrained linear response

Suppose we want to compute  $\frac{d^2 E_{\text{Hxc}}}{d(n^I)^2} \Big|_{\mu^I}$

# Unconstrained constrained linear response

Suppose we want to compute  $\frac{d^2 E_{\text{Hxc}}}{d(n^I)^2} \Big|_{\mu^I}$

This is easy with spin-resolved LR:

# Unconstrained constrained linear response

Suppose we want to compute  $\frac{d^2 E_{\text{Hxc}}}{d(n^I)^2} \Big|_{\mu^I}$

This is easy with spin-resolved LR:

$$\frac{d^2 E_{\text{Hxc}}}{d(n^I)^2} = \frac{1}{2} \frac{dv_{\text{Hxc}}^\uparrow + dv_{\text{Hxc}}^\downarrow}{d(n^\uparrow + n^\downarrow)} = \frac{1}{2} \frac{f^{\uparrow\uparrow}dn^\uparrow + f^{\uparrow\downarrow}dn^\downarrow + f^{\downarrow\uparrow}dn^\uparrow + f^{\downarrow\downarrow}dn^\downarrow}{dn^\uparrow + dn^\downarrow}$$

# Unconstrained constrained linear response

Suppose we want to compute  $\frac{d^2 E_{\text{Hxc}}}{d(n^I)^2} \Big|_{\mu^I}$

This is easy with spin-resolved LR:

$$\frac{d^2 E_{\text{Hxc}}}{d(n^I)^2} = \frac{1}{2} \frac{dv_{\text{Hxc}}^\uparrow + dv_{\text{Hxc}}^\downarrow}{d(n^\uparrow + n^\downarrow)} = \frac{1}{2} \frac{f^{\uparrow\uparrow}dn^\uparrow + f^{\uparrow\downarrow}dn^\downarrow + f^{\downarrow\uparrow}dn^\uparrow + f^{\downarrow\downarrow}dn^\downarrow}{dn^\uparrow + dn^\downarrow}$$

“Impose” the constraint by setting  $dn^\uparrow = dn^\downarrow$  to get...

$$\frac{d^2 E_{\text{Hxc}}}{dn^2} \Big|_{\mu} = \frac{1}{4} (f^{\uparrow\uparrow} + f^{\downarrow\downarrow} + f^{\uparrow\downarrow} + f^{\downarrow\uparrow})$$

# Unconstrained constrained linear response

Suppose we want to compute  $\frac{d^2 E_{\text{Hxc}}}{d(n^I)^2} \Big|_{\mu^I}$

This is easy with spin-resolved LR:

$$\frac{d^2 E_{\text{Hxc}}}{d(n^I)^2} = \frac{1}{2} \frac{dv_{\text{Hxc}}^\uparrow + dv_{\text{Hxc}}^\downarrow}{d(n^\uparrow + n^\downarrow)} = \frac{1}{2} \frac{f^{\uparrow\uparrow}dn^\uparrow + f^{\uparrow\downarrow}dn^\downarrow + f^{\downarrow\uparrow}dn^\uparrow + f^{\downarrow\downarrow}dn^\downarrow}{dn^\uparrow + dn^\downarrow}$$

“Impose” the constraint by setting  $dn^\uparrow = dn^\downarrow$  to get...

$$\frac{d^2 E_{\text{Hxc}}}{dn^2} \Big|_{\mu} = \frac{1}{4} (f^{\uparrow\uparrow} + f^{\downarrow\downarrow} + f^{\uparrow\downarrow} + f^{\downarrow\uparrow})$$

This simple average is one choice (of many) for  $M : f_I^{\sigma\sigma'} \rightarrow U^I$

**3. We can recover conventional linear response**

# Conventional linear response

For conventional LR,  $dv^{I\uparrow} = dv^{I\downarrow} = dv$

# Conventional linear response

For conventional LR,  $dv^{I\uparrow} = dv^{I\downarrow} = dv$ , in which case:

$$dn = \sum_{\sigma} dn^{\sigma} = \sum_{\sigma\sigma'} \chi^{\sigma\sigma'} dv^{\sigma'} = \sum_{\sigma\sigma'} \chi^{\sigma\sigma'} dv \implies \chi_{\text{conv}} = \frac{dn}{dv} = \sum_{\sigma\sigma'} \chi^{\sigma\sigma'}$$

# Conventional linear response

For conventional LR,  $dv^{I\uparrow} = dv^{I\downarrow} = dv$ , in which case:

$$dn = \sum_{\sigma} dn^{\sigma} = \sum_{\sigma\sigma'} \chi^{\sigma\sigma'} dv^{\sigma'} = \sum_{\sigma\sigma'} \chi^{\sigma\sigma'} dv \implies \chi_{\text{conv}} = \frac{dn}{dv} = \sum_{\sigma\sigma'} \chi^{\sigma\sigma'}$$

Likewise,

$$(\varepsilon^{-1})_{\text{conv}} = \dots = \frac{1}{2} \sum_{\sigma\sigma'} (f\chi)^{\sigma\sigma'}$$

# Conventional linear response

For conventional LR,  $dv^{I\uparrow} = dv^{I\downarrow} = dv$ , in which case:

$$dn = \sum_{\sigma} dn^{\sigma} = \sum_{\sigma\sigma'} \chi^{\sigma\sigma'} dv^{\sigma'} = \sum_{\sigma\sigma'} \chi^{\sigma\sigma'} dv \implies \chi_{\text{conv}} = \frac{dn}{dv} = \sum_{\sigma\sigma'} \chi^{\sigma\sigma'}$$

Likewise,

$$(\varepsilon^{-1})_{\text{conv}} = \dots = \frac{1}{2} \sum_{\sigma\sigma'} (f\chi)^{\sigma\sigma'}$$

And thus

$$U = (\varepsilon^{-1} - 1) \chi^{-1} = \frac{1}{2} \frac{\sum_{\sigma\sigma'} (f\chi)^{\sigma\sigma'}}{\sum_{\sigma\sigma'} \chi^{\sigma\sigma'}}$$

**4.  $J$  is free**

As defined by

$$J = -\frac{1}{2} \frac{dv_{\text{Hxc}}^{\uparrow} - dv_{\text{Hxc}}^{\downarrow}}{d(n^{\uparrow} - n^{\downarrow})} = -\frac{1}{4} \frac{(f^{\uparrow\uparrow} - f^{\downarrow\uparrow})dn^{\uparrow} - (f^{\downarrow\downarrow} - f^{\uparrow\downarrow})dn^{\downarrow}}{d(n^{\uparrow} - n^{\downarrow})}$$

Different ways to define  $J$ :

As defined by

$$J = -\frac{1}{2} \frac{dv_{\text{Hxc}}^{\uparrow} - dv_{\text{Hxc}}^{\downarrow}}{d(n^{\uparrow} - n^{\downarrow})} = -\frac{1}{4} \frac{(f^{\uparrow\uparrow} - f^{\downarrow\uparrow})dn^{\uparrow} - (f^{\downarrow\downarrow} - f^{\uparrow\downarrow})dn^{\downarrow}}{d(n^{\uparrow} - n^{\downarrow})}$$

Different ways to define  $J$ :

1. while keeping  $n = n^{\uparrow} + n^{\downarrow}$  fixed:

$$J = -\frac{1}{4}(f^{\uparrow\uparrow} - f^{\downarrow\uparrow} - f^{\uparrow\downarrow} + f^{\downarrow\downarrow})$$

As defined by

$$J = -\frac{1}{2} \frac{dv_{\text{Hxc}}^{\uparrow} - dv_{\text{Hxc}}^{\downarrow}}{d(n^{\uparrow} - n^{\downarrow})} = -\frac{1}{4} \frac{(f^{\uparrow\uparrow} - f^{\downarrow\uparrow})dn^{\uparrow} - (f^{\downarrow\downarrow} - f^{\uparrow\downarrow})dn^{\downarrow}}{d(n^{\uparrow} - n^{\downarrow})}$$

Different ways to define  $J$ :

1. while keeping  $n = n^{\uparrow} + n^{\downarrow}$  fixed:

$$J = -\frac{1}{4}(f^{\uparrow\uparrow} - f^{\downarrow\uparrow} - f^{\uparrow\downarrow} + f^{\downarrow\downarrow})$$

2. for a perturbation where  $dv^{\uparrow} = -dv^{\downarrow}$

## **5. Easy to implement**

# References

# References

- N. L. Nguyen, G. Borghi, A. Ferretti, I. Dabo & N. Marzari. First-Principles Photoemission Spectroscopy and Orbital Tomography in Molecules from Koopmans-Compliant Functionals. *Phys. Rev. Lett.* 114, 166405 (2015).
- M. Puppin *et al.* Evidence of Large Polarons in Photoemission Band Mapping of the Perovskite Semiconductor CsPbBr<sub>3</sub>. *Phys. Rev. Lett.* 124, 206402 (2020).
- G. Onida, L. Reining & A. Rubio. Electronic excitations: density-functional versus many-body Green's-function approaches. *Rev. Mod. Phys.* 74, 601 (2002).
- I. Dabo *et al.* Koopmans' condition for density-functional theory. *Phys. Rev. B* 82, 115121 (2010).
- J. P. Perdew, R. G. Parr, M. Levy & J. L. Balduz. Density-functional theory for fractional particle number: derivative discontinuities of the energy. *Phys. Rev. Lett.* 49, 1691–1694 (1982).
- W. Yang, Y. Zhang & P. W. Ayers. Degenerate ground states and a fractional number of electrons in density and reduced density matrix functional theory. *Phys. Rev. Lett.* 84, 5172–5175 (2000).
- A. C. Burgess, E. Linscott & D. D. O'Regan. The convexity condition of density-functional theory. *J. Chem. Phys.* 159, 211102 (2023).
- A. C. Burgess, E. Linscott & D. D. O'Regan. Tilted-Plane Structure of the Energy of Finite Quantum Systems. *Phys. Rev. Lett.* 133, 26404 (2024).
- N. Colonna, N. L. Nguyen, A. Ferretti & N. Marzari. Koopmans-compliant functionals and potentials and their application to the GW100 test set. *J. Chem. Theory Comput.* 15, 1905 (2019).
- N. L. Nguyen, N. Colonna, A. Ferretti & N. Marzari. Koopmans-compliant spectral functionals for extended systems. *Phys. Rev. X* 8, 21051 (2018).
- M. Stojkovic, E. Linscott & N. Marzari. Predicting the suitability of photocatalysts for water splitting using Koopmans spectral functionals: The case of TiO<sub>2</sub> polymorphs. (2024) doi:10.48550/arXiv.2412.17488.

# References



- E. B. Linscott *et al.* koopmans: An open-source package for accurately and efficiently predicting spectral properties with Koopmans functionals. *J. Chem. Theory Comput.* 19, 7097 (2023).
- E. B. Linscott, D. J. Cole, M. C. Payne & D. D. O'Regan. Role of spin in the calculation of Hubbard  $\text{\textbackslash mkbibemph\{U\}}$  and Hund's  $\text{\textbackslash mkbibemph\{J\}}$  parameters from first principles. *Phys. Rev. B* 98, 235157 (2018).
- C. Rödl, F. Fuchs, J. Furthmüller & F. Bechstedt. Quasiparticle band structures of the antiferromagnetic transition-metal oxides MnO, FeO, CoO, and NiO. *Phys. Rev. B* 79, 235114 (2009).
- R. G. Parr & W. Yang. *Density-Functional Theory of Atoms and Molecules*. (Oxford University Press, Oxford, 1989).
- A. G. Petukhov, I. I. Mazin, L. Chioncel & A. I. Lichtenstein. Correlated metals and the LDA+\$U\$ method. *Phys. Rev. B* 67, 153106 (2003).
- M. Cococcioni & S. de Gironcoli. Linear response approach to the calculation of the effective interaction parameters in the LDA+\$U\$ method. *Phys. Rev. B* 71, 35105 (2005).
- G. C. Moore *et al.* High-throughput determination of Hubbard  $\text{\textbackslash mkbibemph\{U\}}$  and Hund  $\text{\textbackslash mkbibemph\{J\}}$  values for transition metal oxides via the linear response formalism. *Phys. Rev. Mater.* 8, 14409 (2024).
- A. C. Burgess, E. Linscott & D. D. O'Regan.  $\text{\textbackslash mathrm\{vphantom\}DFT\text{\textbackslash vphantom\{}+U\$}$ -type functional derived to explicitly address the flat plane condition. *Phys. Rev. B* 107, L121115 (2023).
- N. Marzari, A. A. Mostofi, J. R. Yates, I. Souza & D. Vanderbilt. Maximally localized Wannier functions: Theory and applications. *Rev. Mod. Phys.* 84, 1419–1475 (2012).
- A. Ferretti, I. Dabo, M. Cococcioni & N. Marzari. Bridging density-functional and many-body perturbation theory: orbital-density dependence in electronic-structure functionals. *Phys. Rev. B* 89, 195134 (2014).

# References



- N. Colonna, R. De Gennaro, E. Linscott & N. Marzari. Koopmans spectral functionals in periodic boundary conditions. *J. Chem. Theory Comput.* 18, 5435 (2022).
- Y. Schubert, N. Marzari & E. Linscott. Testing Koopmans spectral functionals on the analytically solvable Hooke's atom. *J. Chem. Phys.* 158, 144113 (2023).
- A. Marrazzo & N. Colonna. Spin-dependent interactions in orbital-density-dependent functionals: Noncollinear Koopmans spectral functionals. *Phys. Rev. Res.* 6, 33085 (2024).
- V. I. Anisimov & A. V. Kozhevnikov. Transition state method and Wannier functions. *Phys. Rev. B* 72, 75125 (2005).
- L. Kronik, T. Stein, S. Refaelly-Abramson & R. Baer. Excitation Gaps of Finite-Sized Systems from Optimally Tuned Range-Separated Hybrid Functionals. *J. Chem. Theory Comput.* 8, 1515–1531 (2012).
- D. Wing *et al.* Band gaps of crystalline solids from Wannier-localization-based optimal tuning of a screened range-separated hybrid functional. *Proc. Natl. Acad. Sci.* 118, e2104556118 (2021).
- E. Kraisler & L. Kronik. Piecewise Linearity of Approximate Density Functionals Revisited: Implications for Frontier Orbital Energies. *Phys. Rev. Lett.* 110, 126403 (2013).
- J. Ma & L.-W. Wang. Using Wannier functions to improve solid band gap predictions in density functional theory. *Sci. Rep.* 6, 24924 (2016).
- J. H. Skone, M. Govoni & G. Galli. Nonempirical range-separated hybrid functionals for solids and molecules. *Phys. Rev. B* 93, 235106 (2016).
- C. Li, X. Zheng, N. Q. Su & W. Yang. Localized orbital scaling correction for systematic elimination of delocalization error in density functional approximations. *Natl. Sci. Rev.* 5, 203–215 (2018).
- R. De Gennaro, N. Colonna, E. Linscott & N. Marzari. Bloch's theorem in orbital-density-dependent functionals: Band structures from Koopmans spectral functionals. *Phys. Rev. B* 106, 35106 (2022).

# References

- N. Colonna, N. L. Nguyen, A. Ferretti & N. Marzari. Screening in Orbital-Density-Dependent Functionals. *J. Chem. Theory Comput.* 14, 2549 (2018).
- Y. Schubert, S. Luber, N. Marzari & E. Linscott. Predicting electronic screening for fast Koopmans spectral functional calculations. *npj Comput Mater* 10, 1–12 (2024).
- J. Qiao, G. Pizzi & N. Marzari. Projectability disentanglement for accurate and automated electronic-structure Hamiltonians. *npj Comput Mater* 9, 208 (2023).
- J. Qiao, G. Pizzi & N. Marzari. Automated mixing of maximally localized Wannier functions into target manifolds. *npj Comput Mater* 9, 206 (2023).
- S. P. Huber *et al.* AiiDA 1.0, a scalable computational infrastructure for automated reproducible workflows and data provenance. *Sci Data* 7, 300 (2020).
- M. S. Hybertsen & S. G. Louie. Ab initio static dielectric matrices from the density-functional approach. I. Formulation and application to semiconductors and insulators. *Phys. Rev. B* 35, 5585–5601 (1987).
- R. Del Sole, L. Reining & R. W. Godby. GW\ensuremath{\Gamma} approximation for electron self-energies in semiconductors and insulators. *Phys. Rev. B* 49, 8024–8028 (1994).